

**Atrazine-Induced Changes in Rodent Hepatic Enzymes
and Adrenal Morphology**

by

Arthur Dudley Zimmerman

A thesis submitted to the Graduate Faculty of
Auburn University
in partial fulfillment of the
requirements for the Degree of
Master of Science

Auburn, Alabama
May 7, 2013

Keywords: atrazine, liver, glutathione-s-transferase,
cytochrome P-450, adrenal gland, ACTH

Copyright 2013 by Arthur Dudley Zimmerman

Approved by

Chad Foradori, Chair, Assistant Professor of Anatomy, Physiology and Pharmacology
Robert Judd, Associate Professor of Anatomy, Physiology and Pharmacology
Robert Kemppainen, Professor of Anatomy, Physiology and Pharmacology
Satyanarayana Pondugula, Assistant Professor of Anatomy, Physiology and Pharmacology

Abstract

Atrazine (ATR) is one of the most commonly used herbicides worldwide. It is a broad-spectrum herbicide used to control both pre- and post-emergence broadleaf and grassy weeds. ATR's effects on the hypothalamic-pituitary-gonadal (HPG) axis are the most widely studied, and recent evidence suggests that some of these effects might be mediated by alterations in adrenal gland steroidogenesis and secretion. Furthermore, studies have revealed attenuated effects on the HPG axis after repeated ATR exposure, suggesting an upregulation in the metabolism of atrazine. Our objective was to characterize the effects of ATR exposure on glutathione-*s*-transferase (GST)-mediated hepatic phase II xenobiotic metabolism components as well as the regulation of hepatic phase I cytochrome P450 (CYP) enzymes. We also examined the effects of ATR on adrenal gland morphology, enzymatic immunoreactivity and expression as well as circulating levels of corticosterone (CORT) and aldosterone. Adult ovariectomized (OVX) rats were gavaged daily with vehicle or various doses of ATR for 1, 2, 3 and 4 or 4, 8 and 14 days. In a subsequent study, rats were treated with vehicle, ATR (100 mg/kg) or restraint stressed, and adrenal morphology and hormone secretions were again examined. Findings indicate that ATR treatment results in increased GST-mediated metabolism and upregulated CYP enzyme expression. Furthermore, ATR leads to changes in adrenal gland morphology, enzyme expression and hormone secretions that mimic the effects of restraint stress.

Acknowledgments

This thesis would not be possible without my advisor, Dr. Chad D. Foradori, and I am grateful for his continual support, guidance and encouragement. I would also like to thank my committee members, Dr. Robert Judd, Dr. Robert Kemppainen and Dr. Satyanarayana Pondugula for their supervision and help along the way. I want to also thank my fiancée, Chelsea, and my family for their love and support.

Table of Contents

Abstract.....	ii
Acknowledgments.....	iii
List of Tables	v
List of Figures.....	vi
List of Abbreviations	viii
Chapter I: Review of Literature (Part 1)	1
Atrazine.....	1
Hypothalamic-Pituitary-Gonadal (HPG) Axis.....	2
Xenobiotic Metabolism.....	8
Conclusions and Objectives.....	20
Chapter II: Changes in hepatic phase I and phase II biotransformation enzyme expression and substrate availability following atrazine exposure	21
Chapter III: Changes in hepatic phase I and phase II biotransformation enzyme expression and substrate availability following long-term atrazine exposure	43
Chapter IV: Review of Literature (Part 2)	66
Hypothalamic-Pituitary-Adrenal (HPA) Axis	66
Conclusions and Objectives.....	75
Chapter V: Changes in adrenal gland morphology and enzymatic expression in the rodent following atrazine exposure or restraint stress	77
Chapter VI: Conclusions	115
References.....	119

List of Tables

Table 1. Hepatic GST expression levels following 1, 2, 3 and 4 days of 100 mg/kg of ATR ...	41
Table 2. Hepatic CYP expression levels following 1, 2, 3 and 4 days of 100 mg/kg of ATR ...	42
Table 3. Hepatic GST expression levels following 4, 8 and 14 days of 6.5, 50 or 100 mg/kg of ATR	64
Table 4. Hepatic CYP expression levels following 4, 8 and 14 days of 6.5, 50 or 100 mg/kg of ATR	65
Table 5. Average total number of cells per region of interest (ROI) in each adrenal cortical layer following 1, 2, 3 and 4 days of 100 mg/kg of ATR	112
Table 6. Average total number of cells per region of interest (ROI) in each adrenal cortical layer following 4, 8 and 14 days of 6.5, 50 or 100 mg/kg of ATR.....	113
Table 7. Total number of Ki67 positive cells per region of interest (ROI) in each adrenal cortical layer following 4 and 14 days of 100 mg/kg of ATR or restraint stress.....	114

List of Figures

Figure 1. Chemical structure of ATR	1
Figure 2. Metabolism of ATR into major chlorinated metabolites.....	14
Figure 3. Hepatic mRNA expression levels for GSTa3, GSTm1, GSTp1 and mGST2 following 1, 2, 3 and 4 days of 100 mg/kg of ATR.....	38
Figure 4. Hepatic GSH levels, cytosolic GST activity and microsomal GST activity following 1, 2, 3 and 4 days of 100 mg/kg of ATR.....	39
Figure 5. Hepatic mRNA expression for Cyp2b2, Cyp2e1, Cyp26b1, Cyp17a1, Cyp3a18 and Cyp3a23/3a1 following 4 days of 100 mg/kg of ATR.....	40
Figure 6. Hepatic mRNA expression levels for GSTa3, GSTa4, GSTm2, GSTo1, GSTp1 and mGST1 following 4, 8 and 14 days of 6.5, 50 or 100 mg/kg of ATR	60
Figure 7. Hepatic GSH levels, cytosolic GST activity and microsomal GST activity following 4, 8 and 14 days of 6.5, 50 or 100 mg/kg of ATR.....	61
Figure 8. Hepatic GST omega protein levels following 4, 8 and 14 days of 6.5, 50 or 100 mg/kg of ATR.....	62
Figure 9. Hepatic mRNA expression levels for Cyp1a2, Cyp2b2, Cyp2d2, Cyp2e1, Cyp4f6 and Cyp3a23/3a1 following 4, 8 and 14 days of 6.5, 50 or 100 mg/kg of ATR.....	63
Figure 10. Steroidogenesis in rat adrenal cortex.....	71
Figure 11. Individual adrenal cortical layer and overall cortical thickness following 1, 2, 3 and 4 days of 100 mg/kg of ATR.....	98
Figure 12. Individual adrenal cortical layer thickness relative to body weight following 1, 2, 3 and 4 days of 100 mg/kg of ATR.....	99
Figure 13. Aldosterone synthase immunoreactivity following 1, 2, 3 and 4 days of 100 mg/kg of ATR.....	100

Figure 14. Percent right adrenal weight relative to total body weight following 1, 2, 3 and 4 days of 100 mg/kg of ATR or 4, 8 and 14 days of 6.5, 50 or 100 mg/kg of ATR.	101
Figure 15. Percent pituitary weight relative to total body weight following 1, 2, 3 and 4 days of 100 mg/kg of ATR or 4, 8 and 14 days of 6.5, 50 or 100 mg/kg of ATR	102
Figure 16. Adrenal mRNA expression levels for aldosterone synthase, 11 β - hydroxylase and AT ₁ R following 4 days of 100 mg/kg of ATR.....	103
Figure 17. Individual adrenal cortical layer and overall cortical thickness following 4, 8 and 14 days of 6.5, 50 or 100 mg/kg of ATR	104
Figure 18. Individual adrenal cortical layer thickness relative to body weight following 4, 8 and 14 days of 6.5, 50 or 100 mg/kg of ATR	105
Figure 19. Aldosterone synthase immunoreactivity following 4, 8 and 14 days of 6.5, 50 or 100 mg/kg of ATR.....	106
Figure 20. Individual adrenal cortical layer and overall cortical thickness following 4 and 14 days of 100 mg/kg of ATR or restraint stress	107
Figure 21. Individual adrenal cortical layer thickness relative to body weight following 4 and 14 days of 100 mg/kg of ATR or restraint stress	108
Figure 22. Aldosterone synthase immunoreactivity following 4 days of 100 mg/kg of ATR or restraint stress	109
Figure 23. Plasma CORT and aldosterone levels following 4 and 14 days of 100 mg/kg of ATR or restraint stress.....	110
Figure 24. Fluorescein immunohistochemical staining following 4 days of 100 mg/kg or ATR or restraint stress.....	111

List of Abbreviations

ACE	Angiotensin I-converting enzyme
ACTH	Adrenocorticotrophic hormone
ADX	Adrenalectomy
Ang I	Angiotensin I
Ang II	Angiotensin II
ANP	Atrial natriuretic peptide
AP	Alkaline phosphatase
ATR	Atrazine
AT ₁ R	Ang II type 1 receptors
AT1R _A	Ang II type 1 A receptors
AT1R _B	Ang II type 1 B receptors
atRA	All-trans-retinoic acid
AU	Area under the curve
cAMP	Cyclic adenosine monophosphate
CBC	Carboxymethylcellulose
CO	Carbon monoxide
CORT	Corticosterone
CRH	Corticotrophic-releasing hormone
cGST	Cytosolic glutathione- <i>s</i> -transferase

CYP	Cytochrome P450
DACT	Diaminochlorotriazine
DHEA	Dehydroepiandrosterone
DEA	Desethyl-atrazine
DIA	Desisopropyl-atrazine
EB	17 β -estradiol-benzoate
EB+P	17 β -estradiol-benzoate + progesterone
EGFP	Enhanced green fluorescent protein
ER	Endoplasmic reticulum
EROD	7-ethoxy-resorufin <i>O</i> -deethylase
E2	Estradiol
FAD	Flavin adenine dinucleotide
FMN	Flavin mononucleotide
FSH	Follicle-stimulating hormone
GAPDH	Glyceraldehyde 3-phosphate dehydrogenase
GH	Growth hormone
GnRH	Gonadotropin-releasing hormone
GnRHR	Gonadotropin-releasing hormone receptor
GR	Glucocorticoid receptor
GSH	Glutathione
GST	Glutathione- <i>s</i> -transferase
GSTa	Glutathione- <i>s</i> -transferase alpha
GSTa1	Glutathione- <i>s</i> -transferase alpha 1

GSTm	Glutathione- <i>s</i> -transferase mu
GSTm1	Glutathione- <i>s</i> -transferase mu 1
GSTo	Glutathione- <i>s</i> -transferase omega
GSTp	Glutathione- <i>s</i> -transferase pi
GST1	Glutathione- <i>s</i> -transferase 1
HPA	Hypothalamic-pituitary-adrenal
HPG	Hypothalamic-pituitary-gonadal
LH	Luteinizing-hormone
MAPEG	Membrane-associated proteins in eicosanoid and glutathione metabolism
mGST	Microsomal glutathione- <i>s</i> -transferase
mRNA	Messenger ribonucleic acid
OVX	Ovariectomized
P	Progesterone
PBPK	Physiologically based pharmacokinetic
PCR	Polymerase-chain reaction
PR	Progesterone Receptor
PROD	7-pentoxo-resorufin <i>O</i> -demethylation
PVN	Paraventricular nucleus
P450 _{scc}	Side-chain cleaving enzyme
RAS	Renin-angiotensin system
RT-PCR	Reverse-transcriptase polymerase-chain reaction
SD	Sprague-Dawley
ST	Sulfotransferases

StAR	Steroidogenic acute regulatory
UGT	UDP-glucuronyltransferase
U.S.	United States
zF	Zona fasciculata
zG	Zona glomerulosa
zR	Zona reticularis

Chapter I

Review of the Literature (Part 1)

Atrazine

Atrazine (2-chloro-4-ethylamino-6-isopropylamino-s-triazine; ATR) is one of the most commonly used herbicides in the United States (U.S.) and across the world, with approximately 80 million pounds applied each year in the U.S. alone [1]. It is used to stop both pre- and post-emergence broadleaf and grassy weeds, and has been used on over 50 different crops including corn, sorghum and sugarcane [1]. ATR belongs to the chloro-s-triazine (triazine) family of herbicides, and is prepared from cyanuric chloride followed by subsequent treatment with ethylamine and isopropyl amine (**Figure 1**).

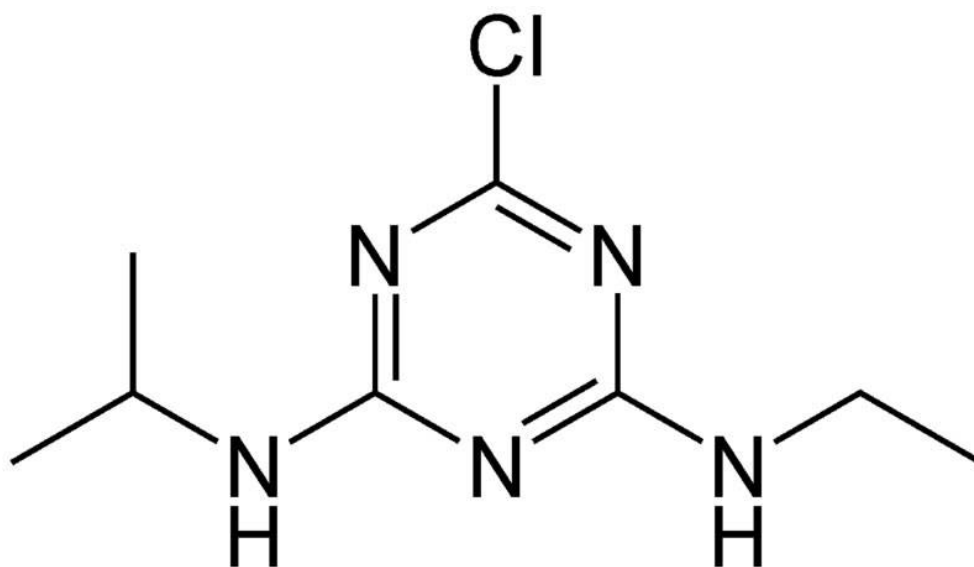


Figure 1: Chemical structure of atrazine.

Its principal mode of action is the inhibition of the Hill's reaction during photosynthesis [2]. The Hill's reaction occurs when the hydrogens of water photoreduce an electron acceptor, followed by the evolution of oxygen [3]. ATR prevents this electron transfer at the reducing site of the photosystem complex II in the chloroplasts by binding to the plastoquinone-binding protein [2, 4]. This results in the breakdown of the electron transport process, and leads to plant death due to starvation and oxidative damage. The plastoquinone-binding protein is not found in animal species, giving ATR a specific target in weeds that does not cross react with animal species.

With a half-life of approximately 60 days in topsoil, and substantially longer in subsurface soils and ground water, ATR is the most common herbicide found in surface and drinking water [5]. Applicators, farmers and their families commonly have high levels of ATR and its metabolites in their saliva and urine [6, 7]. In humans, triazines influence endocrine responses, but it appears their potential impact is primarily on reproduction and development and is not related to carcinogenesis [8]. In rats, the effects of ATR exposure on the hypothalamic-pituitary-gonadal (HPG) axis are the most sensitive and reproducible studies.

Hypothalamic-Pituitary-Gonadal (HPG) Axis

Gonadotropin-releasing hormone (GnRH) is a linear, decapeptide neurohormone synthesized and secreted in pulsatile manner from neurons in the preoptic area and hypothalamus. GnRH travels down the GnRH neuron axon to the median eminence, where it is secreted into the hypophyseal portal system and carried to the adenohypophysis (anterior pituitary) by the hypophyseal portal blood. GnRH binds to and activates gonadotropin-releasing hormone receptor, a seven-transmembrane G-protein coupled receptor on gonadotrophs. Binding of GnRH activates an

internal cascade that results in the synthesis and secretion of the gonadotropins luteinizing-hormone (LH) and follicle-stimulating hormone (FSH). LH and FSH are released into general circulation and carried to the gonads where they regulate gonadal function including testosterone production in males and estradiol (E2) and progesterone (P) production in females. These sex hormones are transported through general circulation to the hypothalamus or anterior pituitary where, in a primarily negative feedback manner, they regulate the secretion of GnRH, LH or FSH.

GnRH pulsatile release leads to a synchronized pulsatile secretion of LH from gonadotrophs with a relative amplitude and pulse frequency [9]. In both males and females, pulsatile GnRH and LH release is required for normal steroidogenesis in the gonads and reproductive function [10-12]. When normal GnRH/LH pulsatile secretion is disrupted, gonadotrophs become nonresponsive and reproductive function is lost [13-15].

In females, LH secretion is bimodal. In addition to pulsatile LH release, females also have a preovulatory LH surge, which is required for normal ovulation. Around the time of ovulation, E2 and progesterone (P) levels rise and become activators of GnRH secretion through positive feedback at the level of the hypothalamus [16, 17]. This leads to a surge of GnRH which travels through the hypophyseal portal system to the anterior pituitary, resulting in a surge of LH secretion [18].

Effects of ATR on Hormone-Induced LH Surge

ATR treatment has been shown to disrupt the hormone-induced surge of LH [19]. Young adult female Wistar rats (60-90 days old) were ovariectomized and administered a gavage of vehicle (CBC) or 50, 100 or 200 mg/kg/b.w. of ATR for 4 consecutive days. Using a previously validated method [20], these animals were primed with 17 β -estradiol-benzoate (EB) and progesterone (P) to effectively induce a preovulatory-like surge of LH. Animals treated with ATR inhibited the EB+P induced LH surge at 50, 100 and 200 mg/kg/b.w. of ATR compared to the control group. Furthermore, all ATR-treated groups showed lower peak amplitude in the surge of LH as well as a reduced area under the curve (AUC).

There is also evidence that ATR inhibits the hormone-induced LH surge without altering estrogen receptor activation [21]. In this study, adult female Sprague-Dawley (SD) rats were ovariectomized and treated with vehicle (CBC) or 30, 100 or 300 mg/kg/b.w. of ATR in 0.5% CBC for 5 consecutive days. Rats were primed with EB+P to induce a surge of LH, and plasma LH levels were determined. As previously reported, ATR-treated rats showed a reduced peak hormone-induced LH surge level in a dose-dependent manner, and ATR treatment did not affect estrogen receptor activation. This suggests that alterations in the hormone-induced LH surge following ATR treatment might originate from changes in GnRH secretion at the level of the hypothalamus.

Effects of ATR on Pulsatile LH Release

ATR exposure prolongs the estrous cycle [22, 23], induces characteristics of premature reproductive aging [24, 25] and increases the prevalence of infertility [26-29]. ATR and its

metabolites have also been shown to delay the onset of puberty in both male and female rats [28, 30] as well as lower the level of plasma testosterone [27, 29, 31]. Research has shown that these effects might be mediated through an ATR-induced disruption of normal, pulsatile LH secretion [32]. An increasing nocturnal release of LH is associated with the onset of puberty [33-36], and the cyclic release of LH is associated with normal testosterone release from the testis [37, 38].

In a recent study [32], young adult female Wistar rats (60-90 days old) were ovariectomized and gavaged once daily for four consecutive days with vehicle (1% carboxymethylcellulose (CBC) sodium salt) or 50, 100 or 200 mg/kg/b.w. of ATR in CBC. Animals treated with 200 mg/kg/b.w. of ATR showed a significant reduction in LH pulse frequency along with increased pulse amplitude compared to control animals. Furthermore, this pulsatile LH release was altered without changing pituitary sensitivity to a GnRH receptor agonist, suggesting ATR might affect GnRH secretion as well.

Effects of ATR on GnRH Neuronal Activation and Secretion

Changes in LH secretion are directly linked to alterations in GnRH release without variations in pituitary sensitivity to GnRH [39-41], and ATR treatment has been shown to affect the percentage of activated GnRH neurons [19]. Young adult female Wistar rats (60-90 days old) with enhanced green fluorescent protein (eGFP)-GnRH neurons were ovariectomized and then administered a gavage of vehicle (CBC) or 50, 100 or 200 mg/kg/b.w. of ATR for 4 consecutive days. These animals were also EB+P primed to effectively induce a preovulatory-like surge of LH as previously described [20]. Animals treated with 100 or 200 mg/kg/b.w. of ATR showed a reduced percentage of GnRH neurons immunoreactive for cFos compared to animals treated with

vehicle or 50 mg/kg/b.w. of ATR. cFos is an immediate, early gene that is a marker for neuronal activation. cFOS is often expressed when neurons are activated, and studies have demonstrated that GnRH neurons express cFOS during a hormone-induced surge of LH [20, 42, 43]. A high correlation exists between the amplitude of the LH surge and the number of GnRH neurons immunoreactive for cFOS, suggesting cFOS is a reliable marker for GnRH neuronal activation. From this study, it can be concluded that ATR treatment leads to a reduced activation of GnRH neurons, and therefore, could cause a potential reduction in GnRH secretion.

Foradori et al. (2013) examined just that by measuring GnRH release, messenger RNA levels and protein levels in ATR-treated animals [44]. Young adult female Wistar rats were ovariectomized and then treated with vehicle (CBC) or 200 mg/kg/b.w. of ATR via gavage for four consecutive days. Following the final day of treatment, GnRH levels were measured from *ex vivo* hypothalamic implants. ATR-treated animals showed a reduced GnRH pulse frequency and increased pulse amplitude compared to control groups. Furthermore, animals treated with 50, 100 or 200 mg/kg/b.w. of ATR showed no changes in GnRH gene expression or peptide levels, suggesting that ATR inhibits GnRH pulsatile secretions without altering GnRH messenger ribonucleic acid (mRNA) levels and protein synthesis.

Interestingly, Foradori et al. (2009) showed that acute effects of ATR exposure on the hormone-induced surge of LH and GnRH neuronal activation are transient [19]. Young adult female Wistar rats (60-90 days old) with eGFP-GnRH neurons were ovariectomized and then administered a gavage of vehicle (CBC) or 200 mg/kg/b.w. of ATR for 4 consecutive days. Animals were EB+P primed to effectively induce a preovulatory-like surge of LH on the final

day of ATR treatment, two days after withdrawal from treatment or four days after withdrawal from treatment.

As previously shown, ATR treatment inhibited the hormone-induced LH surge compared to control on the final day of treatment [19]. Two days after withdrawal from treatment, ATR-treated animals had significantly lower LH levels compared to control animals. However, LH levels measured two days after withdrawal from ATR treatment were significantly higher than LH levels measured on the final day of ATR treatment. Furthermore, four days after ATR withdrawal, peak LH levels were not significantly different compared to control animals.

The effects of acute ATR exposure on GnRH neuronal activation showed a similar withdrawal effect. ATR treatment led to a reduced percentage of cFOS immunoreactive GnRH neurons on the final day of ATR treatment compared to control. Two days after ATR treatment withdrawal, the percentage of GnRH neurons immunoreactive with cFOS were still significantly lower in ATR-treated animals when compared to control, but these levels were higher than ATR-treated animals on the final day of treatment. Four days after withdrawal from ATR treatment, the percentage of cFOS immunoreactive GnRH neurons was not significantly different from the control group. These findings suggest that the effects of ATR on GnRH neuronal activation and secretion were more pharmacological in nature. ATR had to be present at high enough concentrations to affect reproductive output, but as these concentrations subsided (1-2 days), so did the disruptive effects. These findings, along with the lack of ATR's effect on GnRH cell number, mRNA or protein levels, suggest ATR is not neurotoxic to neurons responsible for neuroendocrine control of reproduction.

Therefore, the effects of ATR treatment on reproduction might not only be due to dosage, time from treatment but also metabolism. Increased ATR metabolism could result in a more efficient expulsion of ATR and its metabolites, dampening the effects of ATR after prolonged exposure. However, there are currently no published studies that have examined the long-term effects of atrazine exposure on LH secretion in rats.

Xenobiotic Metabolism

ATR is readily absorbed from the gastrointestinal tract and is mainly distributed to the liver and kidneys [45-47]. Previous studies have examined both phase I and phase II biotransformation components after ATR exposure.

Phase I Xenobiotic Metabolism

In 1959, R.T. Williams established the terms phase I and phase II biotransformation to describe the biphasic nature of mammalian metabolism [48]. Phase I metabolism involves several enzyme systems, however, the predominant enzyme system in phase I metabolism are the cytochrome P450 (CYP) enzymes. The primary role of CYP enzymes is to biochemically modify xenobiotic compounds in order to detoxify and/or bioactivate these compounds. Xenobiotic compounds are chemicals that are foreign to the body such as drugs, carcinogens or herbicides. CYP enzymes perform a variety of reactions that include monooxygenation, *N*- and *O*-dealkylation, aliphatic and aromatic hydroxylation, *N*- and *S*-oxidation and deamination. Many of the CYP enzyme isoforms are in the hepatic endoplasmic reticulum (ER), and catalyze a large number of reactions with a seemingly unlimited number of xenobiotic compounds. NADPH-cytochrome P450 reductase is a flavoprotein containing both flavin adenine dinucleotide (FAD) and flavin

mononucleotide (FMN), and is the electron donor for the CYP enzymes on the liver ER. Most of the environmental chemicals produced today are potential CYP enzyme substrates.

CYP Enzyme Classes

CYP enzymes were discovered in 1958 while Martin Klingenberg was studying rat liver microsomes. He reported his observation of a carbon monoxide (CO)-binding pigment that was characterized by an absorbance spectra at 450 nm [49]. However, the term CYP was not ascribed until 1962 when evidence was provided that this CO-binding pigment was a hemoprotein [50]. CYP enzymes are named with an Arabic numeral designating the family number, followed by a letter for the subfamily and a final numeral to denote the individual gene product. As of 2009, 57 functional CYP genes had been identified in humans. Furthermore, over 11,000 individual CYP enzymes have been identified across all species of organisms [51].

CYP1, CYP2 and CYP3 enzyme classes are known to be involved in the majority of drug biotransformations and some steroid metabolism [52]. However, there is limited information about the specific role of many of these CYP enzymes due to the seemingly unlimited number of substrates modified by these specific CYP enzymes. CYP1A2 is induced by cigarette smoking [53] or the ingestion of charbroiled foods [54], and is known to metabolize a number of drugs including theophylline, caffeine, imipramine, paracetamol and phenacitin [55]. CYP2E1 is responsible for the metabolism of small organic compounds such as alcohol and carbon tetrachloride as well as the halogenated anaesthetic agents halothane, enflurane, diethyl ether, trichloroethylene, chloroform, isoflurane and methoxyflurane [56]. It is also responsible for the breakdown of many low molecular weight toxins, carcinogens and environmental chemicals

including benzene, styrene, acetone, vinyl chloride and N-nitrosamines. In the rat, CYP2D1 is inducible by 3-methylcholanthrene and phenobarbital [57]. Members of the CYP3A subfamily are the most abundant CYP enzymes found in the liver of humans and account for close to 30% of all hepatic CYP proteins. Specifically, in humans, CYP3A4 is the most abundant CYP enzyme present in the liver. In the rat, CYP2C enzymes are the most abundant CYP enzymes in the liver, and are responsible for the hydroxylations of steroids, a role that is performed by the CYP3A enzyme subfamily in humans [57].

Many CYP enzymes are involved in various biosynthetic pathways. CYP4F enzymes mediate the omega-hydroxylation of leukotriene B₄, a potent mediator of inflammation. CYP11A1 is known as the side-chain cleaving enzyme, and catalyzes the conversion of cholesterol to pregnenolone, the first reaction in the process of steroidogenesis. CYP17A1 has 17-alpha-hydroxylase and 17,20-lyase activities, and catalyzes the conversion of pregnenolone to dehydroepiandrosterone (DHEA) [58]. CYP27A1, also known as sterol 27-hydroxylase, has broad substrate specificity and performs the 27-hydroxylation of cholesterol. CYP26A1, CYP26B1 and CYP26C1 are all-trans-retinoic acid (atRA) hydrolyses, and regulate the cellular concentrations of atRA via oxidative metabolism [59].

CYP7A1 is a cholesterol 7-alpha-hydroxylase, and catalyzes the rate-limiting step in the synthesis of bile acid [60, 61]. CYP7B1 is also expressed in the liver, and is essential for the inactivation of oxysterols and their subsequent conversion into bile salts [62]. CYP8B1 has sterol 12-alpha-hydroxylase activity, and is also important in the synthesis of the bile acids [63]. CYP8B1 controls the ratio of cholic acid over chenodeoxycholic acid in bile. CYP7B1 is a

steroid-hydroxylating enzyme that is involved in the metabolism of several physiological steroids [64, 65], and has been associated with endocrine signaling, neuronal viability, and cholesterol homeostasis [65-67].

Phase II Xenobiotic Metabolism

Various conjugates of xenobiotic compounds were first discovered and characterized in the mid- to late 1800's [68, 69]. Phase II xenobiotic metabolism components typically follow and work synergistically with the phase I components to metabolize, detoxify and/or bioactivate xenobiotic compounds [70]. However, not all phase II biotransformation substrates require activation by CYP enzymes.

The most common phase II biotransformation enzymes are the transferase enzymes, and the most common phase II biotransformation schemes include glucuronidation, sulfation, methylation and glutathione (GSH) conjugation. Specific phase II biotransformation enzyme families include UDP-glucuronosyltransferases (UGTs), sulfotransferases (STs), methyltransferases and glutathione-*s*-transferases (GSTs). The metabolic products of phase II conjugations are generally excreted more easily than the parent compounds because they are more lipophilic. Furthermore, the metabolic conjugates from phase II biotransformation of xenobiotic compounds are noticeably less toxic than the products of the phase I reactions and/or parent compounds.

*Glutathione-*s*-transferases (GSTs)*

GST enzyme isoforms can be found in almost every living organism including microbes, insects, plants, fish and mammals [71]. Research has discovered more than 20 distinct GST enzymes in

humans alone [72, 73]. Most of the GST enzymes have the capability to catalyze the conjugation of reduced GSH with compounds containing an electrophilic center through the formation of a thioether bond [74]. This bond is formed between the sulfur atom of reduced GSH and the substrate. The inserted GSH molecule gives the compound a 'marker' that allows it to be removed from the cell during phase III of xenobiotic metabolism [75]. Many GST isoforms can also catalyze other GSH-dependent reactions, such as the reduction of organic hydroperoxides [76]. GST enzymes also possess non-catalytic functions related to the sequestering of carcinogens or modulation of signal transduction pathways [77-79].

There are actually two distinct superfamilies of GST enzymes. The first superfamily functions as a cytosolic dimeric enzyme, known as cytosolic GST (cGST) [51, 80, 81]. cGSTs have been assigned to at least eight classes based on their degree of sequence identity: alpha, mu, kappa, omega, pi, sigma, theta and zeta [70, 81-83]. The second GST superfamily is microsomal GST (mGST), also known as membrane-associated proteins in eicosanoid and glutathione metabolism (MAPEG) [84]. cGSTs are typically involved in the metabolism of xenobiotic compounds [71], while mGSTs are usually involved in the biosynthesis of leukotrienes and prostanoids [84]. Individual GST enzymes have been characterized to metabolize a spectrum of electrophilic compounds with overlapping substrates between specific GST isoforms [70]. However, evidence also shows that most of the GST isoforms possess unique catalytic features, giving each isoform the capability to detoxify specific xenobiotic compounds.

There is evidence in the rat that cGST class alpha, mu and theta are expressed in the liver, while cGST class pi is only present in liver hepatocytes following treatment with a carcinogen [70, 85].

Furthermore, there are sexual dimorphisms in the secretion of growth hormone (GH) between male and female rats, which leads to hepatic differences in the expression of both alpha and mu GST classes [86].

ATR Metabolites

ATR metabolism occurs within both non-mammalian and mammalian species, as well as in the environment. Metabolism of ATR in plants and biotransformation in the environment has been shown to produce hydroxyatrazine as well as the chlorinated metabolites desisopropyl-atrazine (DIA), desethyl-atrazine (DEA) and diaminochlorotriazine (DACT) [87-89]. In both humans and other animals, mercapturated forms of the chlorinated metabolites have been identified as well [90-92]. Furthermore, a physiologically based pharmacokinetic (PBPK) model shows that ATR is rapidly absorbed and metabolized into its subsequent metabolites [93].

Fifteen minutes after an oral gavage of 75 mg/kg of body weight of ATR, all three chlorinated metabolites are present in significantly higher plasma concentrations than ATR (**Figure 2**).

Further *in vivo* studies have revealed that after one gavage of 50 mg/kg/b.w. of ATR, ATR is quickly broken down into its subsequent metabolites and expelled from the body approximately 12 hours after gavage [94]. DEA and DIA are expelled approximately 20-24 hours after gavage, while DACT levels still remains high after 24 hours. Although levels of DACT remain high, DACT does not induce the effects on the neuroendocrine axis examined after DIA, DEA or ATR exposure [21, 95, 96].

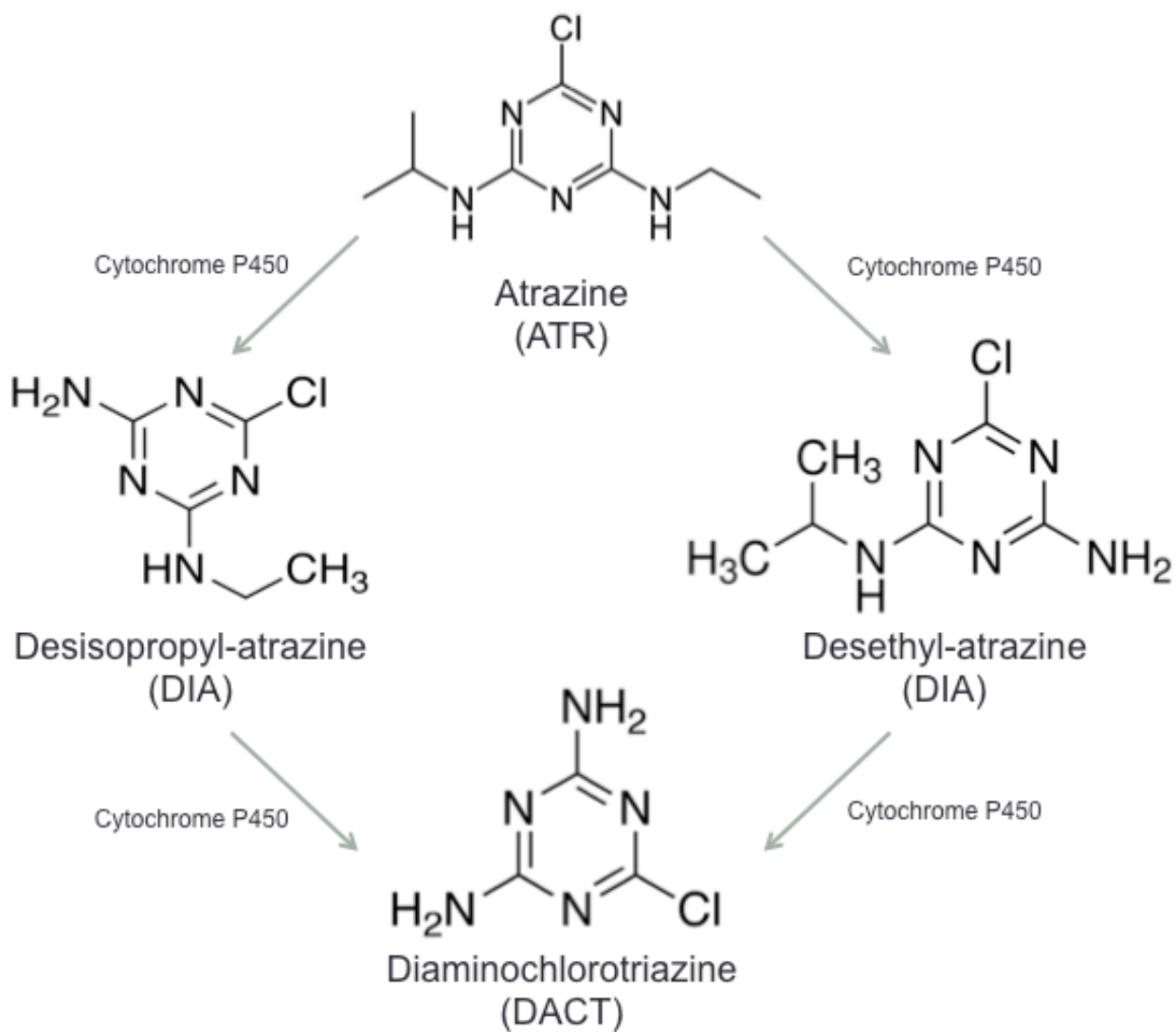


Figure 2: Metabolism of ATR into major chlorinated metabolites.

Furthermore, peak ATR levels are reduced after repeated gavages, which suggests quicker breakdown of ATR into its metabolites due to an increase in expression of liver xenobiotic metabolism components.

Phase I Metabolism of ATR in the Liver

Phase I hepatic xenobiotic biotransformation components play an important role in the initial metabolism of ATR in rats [97, 98], but the specific CYP enzymes responsible have not been well elucidated. An *in vitro* study using rat liver microsomes showed that the dominant phase I metabolic reactions by CYP enzymes are *N*-monodealkylation and isopropylhydroxylation monooxygenase reactions [97-99]. In these studies, the metabolites of ATR were formed after incubation of ATR with a NADPH-generating system and liver microsomes *in vitro*, which indicates that the metabolism of ATR is mediated via CYP enzymes [97, 98].

Using liver microsomes from both male and female SD rats (8 weeks old), Hanioka et al (1998) examined the role of CYP1A1, CYP1A2, CYP2B1, CYP2C11, CYP2E1, CYP3A2, CYP4A1 and CYP2D1 in the metabolism of ATR [100]. ATR metabolism was determined measuring the rate of formation of DIA, DEA and hydroxyatrazine [98]. Anti-rat CYP2B1 antibody inhibited the formation of ATR metabolites in female rats by 32-42%, and anti-rat CYP2E1 antibody inhibited ATR biotransformation by 37-47%. Furthermore, anti-rat CYP2C11 and CYP2D1 antibodies also inhibited ATR biotransformation, while anti-rat CYP1A2, CYP3A2 and CYP4A1 antibodies had no effect on ATR metabolite formation. Immunoblots were used to examine the protein levels of each CYP enzyme, however, results found no correlation between the rate of formation of ATR metabolites and specific CYP enzyme protein levels.

An additional *ex vivo* study examined the role of CYP enzymes in ATR metabolism in liver microsomes from male Wistar rats (8 weeks old) [101]. Animals were treated for 3 days with various doses of ATR via intraperitoneal injection, and the protein levels of CYP1A1/2, CYP2B1/2, CYP2C11/6, CYP2E1, CYP3A1/2 and CYP4A1/2 were measured. ATR induced a 1.7 fold increased in protein level for CYP2B1/2, and there was no significant differences in the protein levels of CYP2C11/6, CYP2E1, CYP3A1/2 and CYP4A1/2 due to ATR treatment. They also looked at catalytic and kinetic analyses, and found that ATR significantly inhibited CYP2C11 activity. The results of this study suggest that CYP2B1/2 might be the primary CYP enzyme involved in ATR metabolism.

CYP isoforms and their inducibility in the metabolic pathway of ATR have also been examined using rat liver microsomes from male SD rats (8 weeks old) [99]. Hepatic CYP1A1/2, CYP2B1/2, CYP2C11/6, CYP2E1, CYP3A1/2 and CYP4A1/2/3 were studied using anti-rat antibodies. The study concluded that the *N*-monodealkylation of ATR was induced by both CYP1A1/2 and CYP2B1/2, while the isopropylhydroxylation was induced only by CYP2B1/2. This study also suggests that CYP2B1/2 is the predominant CYP enzyme involved in the phase I biotransformation of ATR, while CYP1A1/2 might only play a minor role.

Using immunoblots in male Fisher rats (6 weeks old), ATR exposure has been shown to significantly increase the level of hepatic CYP1A2, while only slightly increasing the level of CYP2B after one day of ATR treatment [102]. Hepatic CYP3A remained unchanged after ATR exposure, and CYP1A1 was below the detection level of their assay. Unlike previous reports, Islam et al. (2002) indicates that CYP1A2 might actually play the predominant role in ATR

metabolism, while CYP2B has only a minor contribution in ATR breakdown. Furthermore, they also revealed that intraperitoneal injections of 10, 50, 100, 200 or 300 mg/kg/b.w. of ATR for 3 consecutive days did not induce any toxic effect on the liver, suggesting that ATR exposure leads to an increase in specific CYP enzyme isoforms not due to toxic effects on the liver.

Pogrmic-Majkic et al. (2012) examined both CYP1A1/2 and CYP2B enzymatic activity in the liver using 7-ethoxy-resorufin *O*-deethylase (EROD) and 7-pentoxo-resorufin *O*-demethylation (PROD) assays [103]. Peripubertal male Wistar rats were gavaged with 50 or 200 mg/kg/b.w. of ATR from postnatal day 23 to day 50. The higher ATR dose of 200 mg/kg/b.w. significantly increased the activity of CYP1A1/2 by 56% when compared to the control; however, no dosage of ATR increased CYP2B enzymatic activity. Although EROD and PROD assays have been used to examine the catalytic activities of CYP1A1, CYP1A2 and CYP2B, the use of anti-peptide antibodies provides a more informative evaluation of the level of specific CYP enzymes [104]. However, the results of this study were consistent with the results from a previous immunoblot study [102], signifying further that CYP1A1/2 is the predominant CYP enzyme involved in the phase I biotransformation of ATR with only a minor contribution from CYP2B.

Human H295R adrenocortical carcinoma cells have also been used to examine the activity and mRNA expression levels of CYP19 (aromatase) due to ATR exposure [105]. ATR, in a dose-dependent manner, induced CYP19 activity to a maximum of a 2.5 fold increase compared to control, and ATR treatment increased CYP19 mRNA levels by 1.5 to 2.0 fold. This suggests that ATR exposure might affect not only the protein and activity levels of the CYP enzymes, but also the regulation of CYP enzymes at a transcriptional level.

Phase II Metabolism of ATR in the Liver

Although phase I biotransformation components play the predominant role in ATR metabolism in rats, research has also shown the importance of phase II xenobiotic metabolism components. In female rats, a significant fold increase in mRNA expression of UGT has been reported in the liver [106] after ATR treatment. Conjugation of ATR to GSH by rat liver fractions is also involved in the phase II xenobiotic metabolism of ATR [107]. Moreover, GSH conjugation plays an important role in phase II-mediated biotransformation in humans [108-110], and GST pi (GSTp) in the mouse is responsible for the majority of the GSH-dependent biotransformation of ATR in the liver [111, 112]. However, most of the studies that have examined the role of phase II biotransformation components in the metabolism of ATR have characterized only a few of the specific GST isoforms.

Islam et al (2002) examined the role of GSTp and GST alpha 1 (GSTa1) in the metabolism of ATR in male Fischer rats (6 weeks old) [102]. Intraperitoneal injections of 10, 50, 100, 200 or 300 mg/kg/b.w. of ATR in rats for 3 consecutive days induced higher levels of GSTp compared to control groups, while no dosage of ATR induced an increase in GSTa1. This suggests that GSTp might play an important role in the phase II-mediated metabolism of ATR. Furthermore, using alkaline phosphatase (AP) as a membrane marker enzyme [113], this study investigated whether ATR was a specific inducer of GSTp and CYP1A2 or just a general up-regulator of membrane proteins in the liver. This test has been previously shown to be a sensitive marker of liver function due to pesticide intoxication [114]. They found that there was no induction of AP, and therefore, ATR specifically activated GSTp and CYP1A2 without causing any toxic effects at any dose examined.

The levels of GST1 using immunohistochemical staining, as well as the expression levels of GST mu 1 (GSTm1) using reverse-transcriptase polymerase-chain reaction (RT-PCR) analysis have also been examined [115]. Following 14 consecutive days of ATR treatment (400 mg/kg/b.w.) on male Wistar rats (two months old), no difference in immunostaining of GST1 or expression levels of GSTm1 between ATR-treated and control groups was found. Further analysis of these results showed a potential reduction in the expression level of GSTm1 compared to control, which indicates potential tissue degeneration due to ATR exposure. Tissue breakdown following ATR treatment has been reported [116], however, in this study, the high dose of ATR used and/or the length of treatment might have caused the reported degeneration. Indeed, Santa Maria et al. (1987) reported that subacute treatment of ATR did not induce histological changes in liver hepatocytes at 100 mg/kg/b.w. [114]. Significant histological changes were only observed in animals treated with 600 mg/kg/b.w. of ATR, with proliferation and degeneration of smooth ER, lipid accumulation, mitochondrial malformation and alterations of bile canaliculi as the most prominent alterations. Similar changes were observed following 200 and 400 mg/kg/b.w. of ATR, but to a much lesser extent compared to 600 mg/kg/b.w.

More recently, Pogrmic-Majkic et al (2012) examined the effect of ATR exposure on GST activity in both the testes and liver [103]. Peripubertal male Wistar rats were gavaged with 50 or 200 mg/kg/b.w. of ATR from postnatal day 23 to day 50. In the interstitial testicular cells, GST enzyme activity was reduced 1.4 times after 50 mg/kg/b.w. of ATR treatment and 2.5 times after 200 mg/kg/b.w. of ATR compared to the control group. In contrast, GST enzyme activity in the liver was 1.2 times higher in the 50 mg/kg/b.w. of ATR-treated group compared to the control group, and 1.3 times higher in the 200 mg/kg/b.w. of ATR-treated group.

Conclusion and Objectives

ATR exposure leads to numerous effects on the function of the HPG axis, which are duration and dose dependent. These effects change over multiple exposures, which suggests a possible upregulation in the metabolism of ATR. Both phase I and phase II xenobiotic metabolism components play a role in ATR metabolism, however, the long-term regulation of these components has not been thoroughly examined after repeated exposure to ATR. In our studies, we fully characterize both the short- and long-term effects of ATR exposure on the expression levels of the GST-mediated hepatic phase II xenobiotic metabolism components, as well the hepatic phase I xenobiotic metabolism cytochrome P450 (CYP) enzymes involved in ATR metabolism.

Chapter II

Changes in Hepatic Phase I and Phase II Biotransformation Enzyme Expression and Substrate Availability Following Atrazine Exposure

Abstract

Atrazine (2-chloro-4-ethylamino-6-isopropylamino-s-triazine; ATR) is one of the most commonly used herbicides in the United States and across the world. ATR is a broad-spectrum herbicide used to control both pre- and post-emergence broadleaf and grassy weeds. In mammals, phase I and phase II hepatic xenobiotic metabolism components are involved in ATR metabolism; however, the regulation of these components has not been thoroughly examined after ATR exposure. Adult ovariectomized Sprague-Dawley rats were gavaged daily with 1% methylcellulose vehicle or 100 mg/kg/b.w. of ATR for 1, 2, 3 or 4 consecutive days. On the afternoon of the final treatment day, livers were removed and stored at -70°C until assaying for cytochrome P450 (CYP) and glutathione-*s*-transferase (GST) mRNA expression levels, GST protein levels, total glutathione (GSH) and GST (cytosolic and microsomal) activity. We found an increase in expression levels for multiple, novel GST and CYP isoforms, cytosolic GST activity and GSH levels after 3 and 4 days of treatment. Specifically, we found an almost 24-fold increase in CYP2B2 mRNA expression, as well as a significant increase in expression for CYP2E1, CYP3A23/3A1, CYP26B1, CYP17A1 and multiple CYP4F isoforms. Hepatic expression levels for GSTa3, GSTm1, GSTm3, GSTp1 and mGST2 were elevated above control values after 3 days of ATR treatment and for a total of 11 GST isoforms following 4 days of

ATR treatment. Multiple novel hepatic phase I and phase II xenobiotic metabolism enzymes are implicated in possible ATR metabolism or overall liver adaptation in response to short-term, high-dose ATR treatment in the rat.

Introduction

Atrazine (2-chloro-4-ethylamino-6-isopropylamino-s-triazine; ATR) is one of the most commonly used herbicides worldwide, with approximately 80 million pounds applied each year in the U.S. alone [1]. It is used to stop both pre- and post-emergence broadleaf and grassy weeds, and has been used on over 50 different crops including corn, sorghum and sugarcane [1]. Its principal mode of action is to inhibit the Hill's reaction during photosynthesis [2].

ATR is readily absorbed from the gastrointestinal tract and is largely distributed to the liver and kidneys [45-47]. It is quickly broken down into its subsequent metabolites and expelled from the rat approximately 12 hours after gavage [94]. Previous studies have examined some components of both phase I and phase II biotransformation components after ATR exposure. Cytochrome P450 (CYP) enzyme-mediated phase I hepatic xenobiotic biotransformation components play an important role in the initial metabolism of ATR in rats [97, 98]. *In vitro* studies have revealed that CYP1A1/2, CYP2B1/2, CYP2C11, CYP2D1 and CYP2E1 are involved in ATR metabolism, with CYP2B1/2 being implicated as the predominant enzyme [99-101]. More recent *in vivo* studies using male rats suggest that CYP1A1/2 actually plays the predominant role in the metabolism of ATR with a minor contribution from CYP2B1/2 [102, 103]. However, these studies were limited in scope and did not examine hepatic CYP expression levels after repeated exposures and doses or *in vivo* using female rats.

Although phase I biotransformation components play the chief role in ATR metabolism in rats, phase II xenobiotic metabolism also plays a role in ATR elimination. Glutathione (GSH) conjugation is involved in the phase II-mediated xenobiotic metabolism of ATR by rat [107] and human liver fractions [108-110]. Glutathione-*s*-transferase (GST) activity has also been shown to increase in rats following ATR treatment [103] with GST pi (GSTp) in the mouse [111, 112] and rat [102] likely being responsible for the majority of the GSH-dependent conjugation of ATR in the liver. However, studies examining the role of phase II biotransformation components in the metabolism of ATR have only characterized a few of the specific GST isoforms.

Both phase I and phase II xenobiotic metabolism components play a role in ATR metabolism. However, the regulation of these components has not been thoroughly examined after repeated exposure to ATR. In the present study, we examine the effects of ATR treatment on the expression, protein levels and activity of GST hepatic phase II xenobiotic metabolism components. In addition, ATR's effects on expression of most known rat CYP enzymes were investigated. By doing so, we establish possible new players in hepatic ATR metabolism, and we can better understand the effects ATR has on liver function and perhaps its own metabolism.

Materials and Methods

Animals. All animal surgical procedures and experimental protocols were approved by the WIL Research Institutional Animal Care and Use Committee. All animal procedures were performed by WIL Research Laboratories. Adult female Sprague-Dawley (SD) rats (minimum of 12 weeks old) were individually housed in suspended wire cages on a 14h schedule (lights on 0500) with ad libitum access to food and water. All animals were ovariectomized and implanted with a 12-

14 mm long estradiol (4 mg/mL in sesame oil) silastic capsule before additional procedures were performed. All animals received a single daily dose of vehicle (1% carboxymethylcellulose sodium salt (CBC)) in deionized water (5 mL/kg) 7 days prior to the first day of treatment. Animals were administered ATR or vehicle by gavage once daily (100 mg/kg of body weight) for 1, 2, 3 or 4 consecutive days (10-15 animals per group). Following completion of the last treatment, animals were euthanized by carbon dioxide inhalation and the right lobe of the liver was collected and weighed. Tissue was flash frozen in liquid nitrogen and stored at -70°C until analyzed.

RNA Extraction. RNA extraction was performed using the Qiagen® (Valencia, CA) RNeasy® Microarray Tissue kit (73304). Tissue (40-60 mg) from the right lobe of the liver was weighed and placed in 1 mL of QIAzol® lysis reagent in a DNase/Rnase free 1.7 mL microcentrifuge tube. Tissue was homogenized for 30-40 seconds using the pellet mixer (VWR, Radnor, PA; 47747-370). Following homogenization, the homogenate was placed on the bench top at room temperature for 5 minutes to promote dissociation of the nucleoprotein complexes. Chloroform (200 µL) was added, mixed and allowed to sit at room temperature for 3 minutes. Homogenates were then centrifuged at 12,000 x g for 15 minutes at 4°C. The upper aqueous layer was transferred to a new microcentrifuge tube and mixed with 600 µL of 70% ethanol. The mixture was transferred to an Rneasy Mini spin column in a 2 mL collection tube and centrifuged at 8,000 x g for 15 seconds at room temperature. On-column Dnase Digestion was performed using the Rnase-free Dnase set (Qiagen; 79254). RNA was eluted off the spin column and collected in a 1.5 mL collection tube. Sample concentration (ng/µL) and purity (260/280 ratio) were determined using the Thermo Scientific (Pittsburgh, PA) NanoDrop ND-1000

Spectrophotometer. cDNA synthesis was performed using the Qiagen RT² First Strand Kit (330401).

Real-time PCR Analysis-GST. Real-time PCR analysis was performed using a custom Qiagen RT² Profiler PCR array. Eight liver samples were selected at random from each control and experimental group, and mRNA expression levels for 13 isoforms of GST were analyzed: GST alpha 3 (GSTa3), GST alpha 4 (GSTa4), GST kappa 1 (GSTk1), GST mu 1 (GSTm1), GST mu 2 (GSTm2), GST mu 3 (GSTm3), GST omega 1 (GSTo1), GST omega 2 (GSTo2), GST pi 1 (GSTp1), GST theta 1 (GSTt1), GST theta 2 (GSTt2), microsomal GST 1 (mGST1) and microsomal GST 2 (mGST2). Large ribosomal protein, P1 (Rplp1) was run as the housekeeping gene along with a reverse transcription control and a positive PCR control. All primer sets were verified by Qiagen for the custom PCR array. PCR was carried out using the Bio-rad iCycler iQ real-time detection system with RT² SYBR Green qPCR mastermix (Qiagen; 330513).

Fluorescence data collection was performed for 40 cycles at 95°C for 15 seconds and 40 cycles at 60°C for 1 minute. The fold change of each target mRNA expression relative to Rplp1 under experimental and control conditions were calculated based on the threshold cycle (C_T) as $r = 2^{-\Delta(\Delta C_T)}$, where $\Delta C_T = C_T(\text{target}) - C_T(\text{Rplp1})$ and $\Delta(\Delta C_T) = \Delta C_T(\text{experimental}) - \Delta C_T(\text{control})$.

GSH Analysis. Total glutathione (GSH) levels were determined using the Cayman Chemical GSH assay kit (Ann Arbor, Michigan). Liver samples (100-200 mg) were homogenized using the Precellys 24 (Bertin Technologies, Rockville, MD) at 5000 rpm, twice for 10 seconds each time and spun at 10,000 x g for 15 minutes at 4 °C. The total protein content of supernatant was measured according to the Bradford method [117] with bovine serum albumin as a protein

standard. Protein levels for all samples were standardized to 10 mg/mL. Samples were deproteinated with metaphosphoric acid followed by the reaction of the sulfhydryl groups of GSH with 5,5'-dithio-*bis*-2-nitrobenzoic acid (DTNB, Ellman's reagent) to produce a yellow colored product, 5-thio-2-nitrobenzoic acid (TNB). The product was measured at 412 nm using the Molecular Devices (Sunnyvale, CA) Spectra Max Plus384, and the absorbance was compared to a standard curve range of 0-8.0 μ M oxidized glutathione (GSSG) using the Softmax Pro (Molecular Devices) data software. All samples were assayed in duplicate, and the results were expressed as nmol GSH/mg protein.

Western Blotting. The same animals from the GST mRNA analysis were used to measure GST protein levels. Protein extracts (75 ng) and low molecular weight standards (Bio-rad, 161-0305) were separated by electrophoresis at 200 V for 50 minutes in a 12% Criterion TGX polyacrylamide gel (Bio-rad; 567-1045). Protein extracts were transferred for 1 hour at 100 V to a nitrocellulose membrane (Bio-rad; 162-0116). Blots were blocked using equal volumes of Li-Cor (Lincoln, NE) Odyssey Blocking Buffer (927-40000) and PBS (.1M; pH 7.2) and placed on a rotator for 1 hour. Blots were incubated overnight at 4°C on a rotator with 12 mL of primary antibody cocktail [Primary antibody cocktails used were as follows: Mouse anti-GST alpha (MyBioSource, San Diego, CA, MBS560696; 1:1000) with Goat anti-GST mu (Abcam, Cambridge, MA, Ab53942; 1:1000) and Rabbit anti-GST omega (Abcam, Ab129106; 1:1000)]. Blots were rinsed and incubated in secondary antibody cocktail [Secondary antibody cocktails used were as follows: Donkey anti-Mouse (Odyssey 680 RD; 926-68072; 1:10,000) with Donkey anti-Goat (Odyssey 800 CW; 926-32214; 1:10,000) and Donkey anti-Rabbit (Odyssey 680 RD; 926-68073; 1:10,000)]. Blots were washed and stored in PBS until imaged. All blots were

imaged using the Li-Cor Odyssey Infrared Imaging System. Blots were analyzed using the Odyssey Software v2.0. Beta-actin (Mouse anti-Actin; Millipore, Billerica, MA, MAB1501; 1:1000) was run as a loading control protein, and protein levels for each GST isoform were standardized to beta-actin levels.

GST Analysis. GST enzymatic activity was determined using the Cayman Chemical GST assay kit. Using 10 mg/mL standardized protein samples, homogenate was diluted to 1 mg/ml in potassium phosphate buffer (100 mM potassium phosphate, 2 mM EDTA, pH 7.0), placed into 3.0 mL sterile ultracentrifuge tubes (Beckman Coulter, 355870), heat sealed and spun in an ultra-speed centrifuge (Beckman L8-70M, Brea, CA) at 100,000 x g for 60 minutes at 4°C. Cytosolic fraction was placed in new sterile tube, and microsomal pellet was resuspended in 500µL of cold homogenization buffer. Protein concentration of both fractions was determined by protein assay (BioRad). GST activity for both fractions were determined spectrophotometrically by measuring the rate of formation of the conjugate of GSH and 1-chloro-2,4-dinitrobenzene (CDNB). The absorbance was read at 340 nm every 60 seconds for 6 minutes using the Molecular Devices Spectra Max Plus384 plate reader. All samples were assayed in duplicate, and enzymatic activity was expressed as nmol/min/mg protein. Data were analyzed using Softmax Pro software.

Real-time PCR Analysis-CYP Enzymes. Real-time PCR analysis was performed using a custom Qiagen RT² Profiler PCR array. Liver samples (4-5) were randomly selected from the 8 liver GST mRNA samples analyzed from the 4-day control and experimental group. mRNA expression levels for 45 isoforms of Cytochrome P450 (CYP) enzymes were analyzed for the 4 day treatment group: CYP11a1, CYP11b1, CYP17a1, CYP19a1, CYP1a1, CYP1a2, CYP1b1,

CYP24a1, CYP26a1, CYP26b1, CYP26c1, CYP27a1, CYP27b1, CYP2a3, CYP2b2, CYP2b3, CYP2c11, CYP2c22, CYP2c23, CYP2c37, CYP2c6, CYP2c7, CYP2c80, CYP2d2, CYP2d4, CYP2e1, CYP2f4, CYP2r1, CYP2s1, CYP2t1, CYP2w1, CYP3a18, CYP3a23/3a1, CYP3a9, CYP4a3, CYP4a8, CYP4b1, CYP4f1, CYP4f18, CYP4f4, CYP4f40, CYP4f6, CYP7a1, CYP7b1 and CYP8b1. Rplp1 was run as the housekeeping gene along with reverse transcription and positive PCR controls. All primer sets were verified by Qiagen for the custom PCR array. After reverse transcription, PCR was carried out using the Bio-rad iCycler iQ real-time detection system with RT² SYBR Green qPCR mastermix (Qiagen; 330513). One cycle was performed at 95°C for 10 minutes to activate the HotStart DNA *Taq* Polymerase. Fluorescence data collection was performed for 40 cycles at 95°C for 15 seconds and 40 cycles at 60°C for 1 minute. The fold change of each target mRNA expression relative to Rplp1 was calculated based on the threshold cycle (C_T) as $r = 2^{-\Delta(\Delta C_T)}$, where $\Delta C_T = C_T(\text{target}) - C_T(\text{Rplp1})$ and $\Delta(\Delta C_T) = \Delta C_T(\text{experimental}) - \Delta C_T(\text{control})$.

Statistical Analysis. GST mRNA expression, GSH, GST protein and GST activity level data were analyzed for all time points using 2-way analysis of variance (ANOVA) for treatment, days of treatment and treatment \times days of treatment interactions with Bonferroni post-hoc tests. Hepatic CYP mRNA expression data were analyzed on day four of ATR treatment and compared to same day control animals using student's t-test. The level of statistical significance was set at $P \leq 0.05$. All values are reported as the mean \pm SEM. Prism 5 for Mac (GraphPad Software, Inc.) was used for all data analysis.

Results

Real-time PCR Analysis-GST. We found a significant interaction for GSTm1 ($F_{3,56}=6.06$; $P<0.05$) as well as GSTm2 ($F_{3,56}=3.80$; $P<0.05$), GSTm3 ($F_{3,56}=3.08$; $P<0.05$), GSTo2 ($F_{3,56}=3.05$; $P<0.05$) and GSTt2 ($F_{3,56}=2.99$; $P<0.05$). However, we found no significant interaction between days of treatment and dosage for GSTa3 ($F_{3,56}=2.26$; $P=0.09$), GSTa4 ($F_{3,56}=0.65$; $P=0.59$), GSTk1 ($F_{3,56}=1.89$; $P=0.14$), GSTo1 ($F_{3,56}=2.55$; $P=0.06$), GSTp1 ($F_{3,56}=1.56$; $P=0.21$), GSTt1 ($F_{3,56}=1.56$; $P=0.21$), mGST1 ($F_{3,56}=2.25$; $P=0.09$) or mGST2 ($F_{3,56}=1.68$; $P=0.18$). The post-hoc *t*-tests showed that atrazine treated animals did not have a significant increase in liver mRNA expression levels after one or two days of exposure for any of the GST enzymes. However, after three days of exposure, ATR-treated animals showed an increase in liver mRNA expression levels compared to their corresponding control group for GSTa3, GSTm1, GSTm3, GSTp1 and mGST2 (**Figure 3; Table 1**). Following four days of atrazine treatment, eleven GST isoforms showed increased mRNA expression levels as compared to control (**Table 1**).

Bioreactive GSH levels. There was a significant interaction for treatment ($F_{1,91}=27.61$; $P<0.05$). ATR-treated animals showed increased liver GSH levels after 3 and 4 days of treatment compared to control (**Figure 4A**). However, there was no significant interaction between days of treatment and dosage ($F_{3,91}=0.48$; $P=0.70$).

GST protein levels. Using western blots, we found no significant difference in protein levels for GST mu (GSTm), GST alpha (GSTa) or GST omega (GSTo) after 1, 2, 3 or 4 days of ATR

treatment (Data not shown). There was no interaction between days of treatment and dosage for GSTm ($F_{3,56}=0.89$; $P=0.45$), GSTa ($F_{3,55}=0.14$; $P=0.93$) or GSTo ($F_{3,56}=0.33$; $P=0.80$).

GST activity. There was an interaction between days of treatment and dosage for cGST activity ($F_{3,83}=3.50$; $P<0.05$), but not mGST activity ($F_{3,56}=0.43$; $P=0.73$). There was no increase in cGST (**Figure 4B**) or mGST (**Figure 4C**) activity after 1 or 2 days of treatment. However, animals treated with ATR showed an increase in cGST activity after 3 and 4 days of treatment.

Real-time PCR Analysis-CYP. ATR-treated animals did show a significant increase in liver mRNA expression for Cyp17a1 ($t=2.63$; $DF=8$; $P<0.05$), Cyp26b1 ($t=3.41$; $DF=8$; $P<0.05$), Cyp27a1 ($t=4.07$; $DF=8$; $P<0.05$), Cyp2b2 ($t=2.96$; $DF=8$; $P<0.05$), Cyp2b3 ($t=4.75$; $DF=8$; $P<0.05$), Cyp2c22 ($t=4.96$; $DF=8$; $P<0.05$), Cyp2c23 ($t=4.07$; $DF=8$; $P<0.05$), Cyp2c7 ($t=4.70$; $DF=8$; $P<0.05$), Cyp2d2 ($t=3.85$; $DF=8$; $P<0.05$), Cyp2e1 ($t=4.20$; $DF=8$; $P<0.05$), Cyp2f4 ($t=4.44$; $DF=8$; $P<0.05$), Cyp2r1 ($t=2.54$; $DF=8$; $P<0.05$), Cyp2t1 ($t=3.14$; $DF=8$; $P<0.05$), Cyp3a18 ($t=3.35$; $DF=8$; $P<0.05$), Cyp3a23/3a1 ($t=3.10$; $DF=8$; $P<0.05$), Cyp3a9 ($t=2.51$; $DF=8$; $P<0.05$), Cyp4a3 ($t=3.05$; $DF=8$; $P<0.05$), Cyp4f1 ($t=6.30$; $DF=8$; $P<0.05$), Cyp4f4 ($t=2.66$; $DF=8$; $P<0.05$) and Cyp4f6 ($t=2.97$; $DF=8$; $P<0.05$) (**Table 2**; **Figure 5**). However, animals treated with atrazine for 4 days did not show a significant increase in liver mRNA expression for CYP1a2 ($t=1.04$; $DF=8$; $P=0.33$), Cyp26a1 ($t=0.18$; $DF=8$; $P=0.86$), Cyp26c1 ($t=0.58$; $DF=8$; $P=0.57$), Cyp2c37 ($t=0.05$; $DF=8$; $P=0.96$), Cyp2c6 ($t=0.72$; $DF=8$; $P=0.49$), Cyp2d4 ($t=1.11$; $DF=8$; $P=0.30$), Cyp4b1 ($t=1.81$; $DF=8$; $P=0.11$), Cyp7a1 ($t=1.29$; $DF=8$; $P=0.23$), Cyp7b1 ($t=1.91$; $DF=8$; $P=0.09$) or Cyp8b1 ($t=0.96$; $DF=8$; $P=0.37$) (**Table 2**). Using PCR analysis,

Cyp11a1, Cyp11b1, Cyp19a1, Cyp1a1, Cyp1b1, Cyp24a1, Cyp27b1, Cyp2a3, Cyp2c11, Cyp2c80, Cyp2s1, Cyp2w1, Cyp4a8, Cyp4f18 and Cyp4f40 were below detection threshold.

Discussion

In this study, we have characterized the changes in expression, protein levels and activity of GST-mediated hepatic phase II xenobiotic metabolism of ATR after 1, 2, 3 and 4 days of ATR treatment, as well as the expression of the hepatic phase I CYP enzymes after four days of ATR exposure. Our results are consistent with previous studies, which show that both hepatic phase I and phase II biotransformation components play a role in the metabolism of ATR, and ATR exposure results in expression changes in hepatic phase I and phase II components. However, our study reveals novel hepatic phase I and phase II xenobiotic metabolism enzymes that might be involved in the metabolism of ATR or its effects on liver function that have not been previously examined.

There was a significant interaction between dosage and days of treatment in the mRNA expression levels for a number of GST isoforms, with significant elevations in mRNA expression levels for five isoforms of GST after three days of ATR treatment, and 11 GST isoforms after four days of treatment when compared to the control group. GSTp1 and GSTm1 showed the largest change in expression with two fold increases in expression. This increase in GSTp1 expression supports previous findings, which demonstrated that GSTp is responsible for the majority of the GSH-dependent biotransformation of ATR in the liver of mice [111, 112]. In contrast, we are the first to identify an increase in hepatic GSTm1 after ATR treatment [115]. The only previous study that measured GSTm1 expression levels after ATR treatment showed no

change. However, in that study, adult male Wistar rats were treated for 14 consecutive days at 400 mg/kg/b.w. Not surprisingly, the researchers report evidence of tissue degeneration and toxicity due to such a high exposure of ATR. The liver necrosis and subsequent inflammation would, most likely, have masked or disrupted the compensatory upregulation of many phase I and phase II enzymes and substrates. Conversely, treatment with lower doses of ATR (10-300 mg/kg of body weight) have been shown to produce no toxic effects in the liver while still activating GST enzymes [102].

There was also a two-fold increase in expression for GSTa3 after four days of ATR treatment, but no significant increase in expression for GSTa4. This suggests that only specific isoforms of GSTa might be affected by ATR treatment. We also found a significant increase in the expression of GSTm2, GSTk1, GSTo1, GSTo2, GSTt1, GSTt2 and two microsomal GST isoforms, mGST1 and mGST2. These enzymes have not been previously examined in ATR-treated animals.

To determine if the mRNA expression changes would result in an increase in GST protein level, we examined the liver protein levels of three GST isoforms, GSTm, GSTo and GSTa. We found no increase in GSTm or GSTo levels, which had not been examined previously. We also found no increase in the level of GSTa, which was consistent with previous findings [102]. These results suggest that ATR might lead to an increase in the mRNA expression levels of specific GST isoforms without altering liver GST protein levels. However, it is also possible that ATR might increase protein levels of specific GST isoforms without altering the level of all detectable GST biotransformation enzymes due to limitations in current antibody specificity.

Considering this limitation in isoform protein quantification, we went on to measure hepatic GST activity and to quantify the GST substrate, GSH. Our study was the first to examine GST activity for both cytosolic and microsomal fractions in correlation with GSH levels following ATR treatment. We found an increase in cGST activity following three and four days of treatment with ATR compared to the control group, which does support previous findings [118]. Hepatic GSH levels were also significantly increased after three and four days in ATR treated animals. This suggests that there is a possible upregulation in the bioavailability of GSH for the GST-mediated phase II biotransformation of ATR. These findings are consistent with previous studies, which have demonstrated that GSH conjugation of ATR in rat and human liver fractions is involved in the phase II xenobiotic metabolism of ATR [108-111]. Although we did not find a significant increase in mGST activity, there was a trend towards increased activity after three and four days of ATR treatment. The increase in cGST activity is consistent with the increase in both GSH and cGST mRNA expression levels. These results indicate that ATR exposure might upregulate mGST and cGST-mediated phase II biotransformation components after a minimum of three days of treatment. Subsequently, the increased availability of GST-mediated phase II biotransformation components might lead to additional GSH conjugation to ATR and its metabolites, and therefore, could potentially increase expulsion rate from the body.

It is known that phase II xenobiotic metabolism typically follows and works synergistically with phase I reactions [70], therefore, we examined the regulation of the hepatic phase I xenobiotic metabolism CYP enzymes. Hepatic mRNA expression levels for 45 CYP enzyme isoforms were examined after four days of treatment with ATR. Animals treated with ATR for four days did not show a significant increase in liver mRNA expression for a number of CYP isoforms. CYP7A1,

CYP7B1 and CYP8B1 are important in the synthesis of the bile acids [60-63], and did not show significant changes in mRNA expression. CYP26A1 and CYP26C1 are all-trans-retinoic acid (atRA) hydrolyses that regulate the cellular concentrations of atRA via oxidative metabolism [59]. CYP26A1 and CYP26C1 also did not show an increase in expression. However, CYP26B1 is also an atRA hydrolyse but did have an almost 3-fold increase in expression. We found an almost 3-fold increase in expression for CYP17A1, an enzyme with 17-alpha-hydroxylase and 17,20-lyase activities that catalyzes the conversion of pregnenolone to dehydroepiandrosterone (DHEA) [58], as well as a two-fold increase in expression of CYP27A1, which is known to perform the 27-hydroxylation of cholesterol. These novel results suggest that ATR might activate specific CYP enzymes that are involved in various biosynthetic pathways, but more research is needed to elucidate the mechanism by which ATR might activate these pathways.

Previous studies have shown that CYP1A1/2, CYP2E1, CYP2B1/2, CYP2C6/11, CYP3A1/2 and CYP4A3 are involved in ATR metabolism or are regulated by ATR treatment. Hanioka et al (1998), using liver microsomes from both male and female SD rats, found that CYP1A2 was not involved in the metabolism of ATR and protein levels were not affected by ATR exposure [100]. However, the same group examined CYP1A2 and its inducibility after ATR treatment using solely male SD rat liver microsomes, and found that CYP1A2 plays a minor role in the *N*-monodealkylation of ATR [99]. Another study using immunoblots in male Fischer rats found that ATR exposure significantly increased CYP1A2 protein levels [102]. Peripubertal male Wistar rats gavaged with 200 mg/kg/b.w. of ATR from postnatal day 23 to day 50 displayed increased CYP1A1/2 activity [103], again suggesting that CYP1A1/2 is involved in the phase I biotransformation of ATR or at the very least is responsive to ATR treatment. Although the

regulation of CYP1A2 is somewhat controversial following ATR exposure, CYP1A2 expression did not increase in the present study. These conflicting results might reveal a sexual dimorphism in the role of CYP1A2 in the metabolism of ATR between male and female rats, particularly since CYP1A2 expression is regulated by sex steroids [119].

CYP2E1 is involved in the biotransformation of ATR in both male and female SD rat liver microsomes [17], but the CYP2E1 protein level and activity remain unaffected due to ATR treatment in male Wistar rat liver microsomes [101]. Our results show an over 3-fold increase in mRNA expression after ATR treatment, indicating ATR treatment leads to an increase in expression of CYP2E1 and regulates CYP2E1 at a transcriptional rather than translational level. CYP2B2 had the largest fold change in expression, with an almost 24-fold increase in expression when compared to control. This is consistent with previous studies which have all shown that CYP2B/1/2 plays a role in the metabolism of ATR [101-103, 120]. CYP2C11/6 has also been shown to be involved in the metabolism of ATR in male rat liver microsomes [100, 101], however, the expression level of CYP2C11 was undetectable using our methods and CYP2C6 expression levels were not significantly different from control after ATR treatment. CYP2C11/6 might play a role in the metabolism of ATR, but the mRNA expression levels were not affected by ATR treatment in the present study. CYP2C6 mRNA expression is increased following estrogen treatment [119], again, suggesting that the current pretreatment with estradiol might have resulted in a ceiling effect of CYP2C6 levels, masking possible ATR effects. Not surprisingly, CYP4A3 showed an almost two-fold increase, and has been shown previously to have a possible role in the metabolism of ATR [120].

CYP2B3, CYP2C22, CYP2C23, CYP2C7, CYP2D2, CYP2F4, CYP2R1, CYP2T1, CYP3A18 and CYP3A9 all showed an increase in expression levels after ATR treatment. CYP1, CYP2 and CYP3 enzyme classes are known to be involved in the majority of drug biotransformations and some steroid metabolism [52], however, these specific CYP enzyme isoforms have not been previously examined after ATR exposure. These results suggest that ATR exposure might induce an upregulation in a number of specific CYP isoforms that could be involved in the phase I biotransformation of ATR but have not yet been previously examined.

ATR treatment also led to an increase in the expression of CYP4F1, CYP4F4 and CYP4F6, which have all been shown to be involved in the omega-hydroxylation of leukotriene B₄, a potent mediator of inflammation. The omega-hydroxylation of leukotriene B₄ helps to reduce the number of inflammatory signals and resolve the inflammation process. Furthermore, mGSTs are usually involved in the biosynthesis of leukotrienes which help to protect against oxidative stress [84]. As previously mentioned, ATR treatment leads to an increase in the mRNA expression levels of both mGST1 and mGST2, and previous research has shown that ATR treatment can lead to oxidative stress in rats if given at high enough doses and duration [121, 122]. This suggests that the potential oxidative stress caused by ATR treatment could lead to an increase in expression of both mGST and CYP4F enzymes.

In conclusion, our research shows that repeated ATR exposure over 4 days upregulates the expression level of hepatic phase I CYP enzymes, as well as the expression level of many GST isoforms, cGST activity and the levels of GSH involved in the metabolism of ATR. We have thoroughly examined the hepatic expression, protein levels and activity levels of the primary

component enzymes and substrates for phase I and phase II biotransformation. We have validated some previous findings but have also identified possible novel players in ATR metabolism and liver adaptation in response to ATR treatment in the rat. Further research is required to elucidate the exact role of many of the isoforms of CYP and GST that have been previously unexamined following ATR exposure. More research is necessary to determine the role of phase I and phase II biotransformation components in the metabolism of ATR after longer ATR treatment.

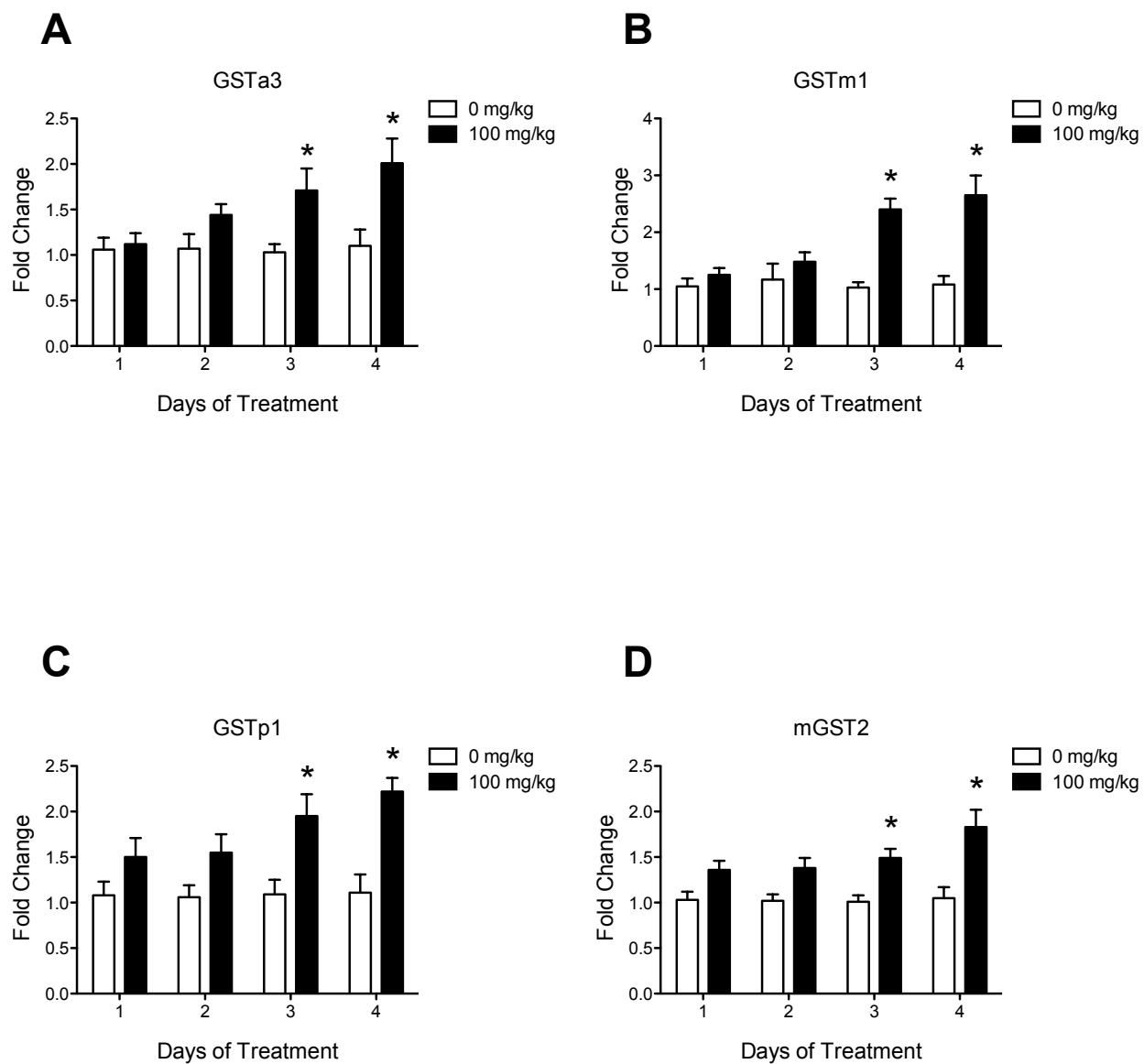


Figure 3: Hepatic mRNA expression levels for GSTa3, GSTm1, GSTp1 and mGST2 following 1, 2, 3 and 4 days of 100 mg/kg of ATR. Histograms depicting fold change in liver mRNA expression for GSTa3 (A), GSTm1 (B), GSTp1 (C) and mGST2 (D) after 1, 2, 3 and 4 days of treatment. Data are presented as mean \pm SEM for 8 randomly selected animals for all groups; *Significant difference ($P < 0.05$) versus corresponding control group.

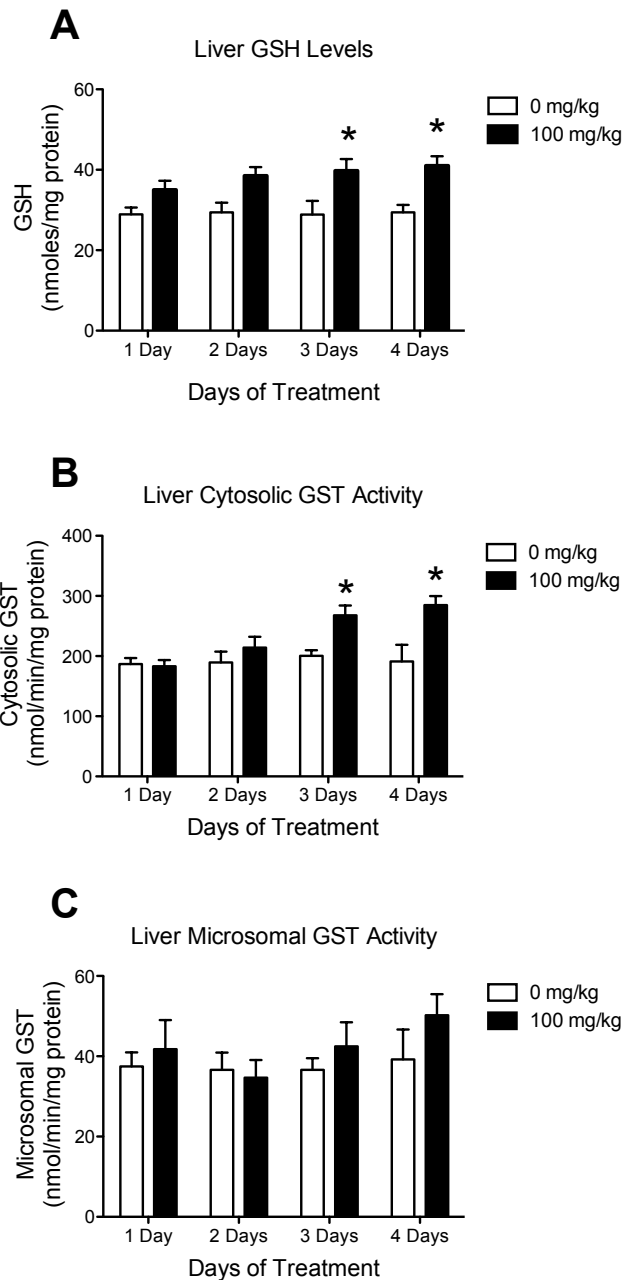


Figure 4: Hepatic GSH levels, cytosolic GST activity and microsomal GST activity following 1, 2, 3 and 4 days of 100 mg/kg of ATR. Histogram depicting liver GSH levels in nmoles/mg protein (A), liver cytosolic GST (cGST) activity in nmol/min/mg protein (B) and liver microsomal GST (mGST) activity in nmol/min/mg protein (C) for all animals after 1, 2, 3 and 4 days of treatment. Data are presented as mean \pm SEM; *Significant difference ($P < 0.05$) versus corresponding control group.

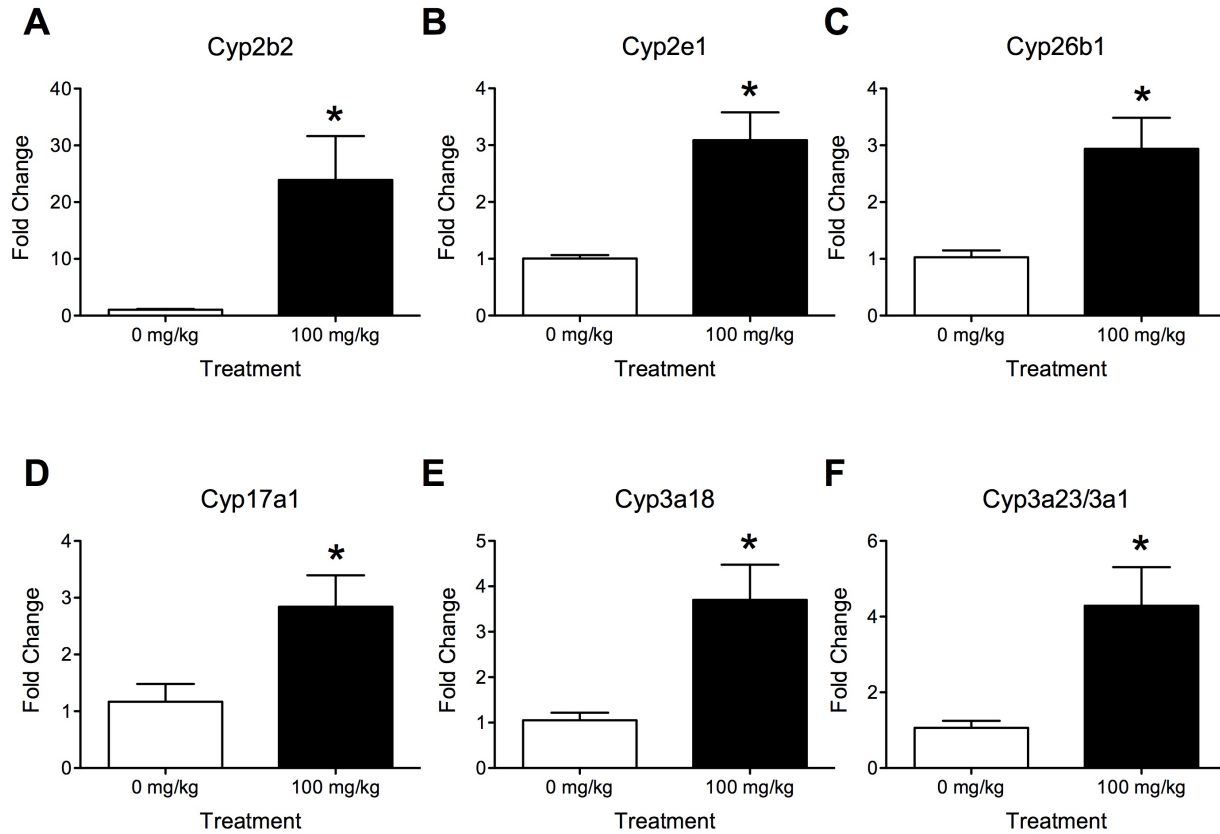


Figure 5: Hepatic mRNA expression for Cyp2b2, Cyp2e1, Cyp26b1, Cyp17a1, Cyp3a18 and Cyp3a23/3a1 following 4 days of 100 mg/kg of ATR. Histograms depicting fold change in liver mRNA expression for Cyp2b2 (A), Cyp2e1 (B), Cyp26b1 (C), Cyp17a1 (D), Cyp3a18 (E) and Cyp3a23/3a1 (F) after 4 days of atrazine treatment. Data are presented as mean \pm SEM for 4-5 animals for all groups; *Significant difference ($P < 0.05$) versus corresponding control group.

LIVER GST mRNA EXPRESSION LEVELS IN OVARIECTOMIZED ESTROGEN-TREATED FEMALES
SUMMARY VALUES FOR GST EXPRESSION IN FOLD CHANGE

GST isoforms	1 Day Treatment		2 Day Treatment		3 Day Treatment		4 Day Treatment	
	Control	Atrazine	Control	Atrazine	Control	Atrazine	Control	Atrazine
GSTa3	1.06 ± .13	1.12 ± .12	1.07 ± .16	1.44 ± .12	1.03 ± .09	1.71 ± .24 *	1.10 ± .18	2.01 ± .27 *
GSTa4	1.03 ± .10	1.21 ± .11	1.06 ± .12	1.17 ± .14	1.04 ± .11	1.33 ± .13	1.11 ± .20	1.60 ± .21
GSTk1	1.03 ± .10	1.14 ± .10	1.05 ± .13	1.08 ± .09	1.04 ± .10	1.41 ± .18	1.06 ± .15	1.63 ± .14 *
GSTm1	1.05 ± .14	1.25 ± .12	1.17 ± .28	1.48 ± .17	1.03 ± .09	2.40 ± .19 *	1.08 ± .15	2.65 ± .35 *
GSTm2	1.03 ± .09	0.92 ± .08	1.08 ± .17	1.16 ± .13	1.12 ± .20	1.80 ± .22	1.12 ± .19	2.15 ± .33 *
GSTm3	1.14 ± .22	0.93 ± .14	1.25 ± .35	1.23 ± .16	1.05 ± .13	2.08 ± .18 *	1.26 ± .34	2.20 ± .39
GSTo1	1.04 ± .10	1.01 ± .07	1.03 ± .10	1.02 ± .06	1.03 ± .08	1.34 ± .15	1.12 ± .24	1.73 ± .17 *
GSTo2	1.03 ± .08	1.00 ± .11	1.02 ± .07	0.89 ± .06	1.03 ± .09	1.20 ± .11	1.03 ± .10	1.39 ± .18 *
GSTp1	1.08 ± .15	1.50 ± .21	1.06 ± .13	1.55 ± .20	1.09 ± .16	1.95 ± .24 *	1.11 ± .20	2.22 ± .19 *
GSTt1	1.02 ± .07	1.35 ± .10	1.07 ± .15	1.34 ± .09	1.04 ± .11	1.34 ± .14	1.10 ± .19	1.88 ± .20 *
GSTt2	1.03 ± .09	1.00 ± .10	1.03 ± .10	0.96 ± .08	1.03 ± .08	1.37 ± .12	1.04 ± .11	1.51 ± .21 *
mGST1	1.01 ± .05	1.08 ± .06	1.03 ± .10	1.09 ± .07	1.02 ± .08	1.26 ± .11	1.03 ± .10	1.48 ± .22 *
mGST2	1.03 ± .09	1.36 ± .10	1.02 ± .07	1.38 ± .11	1.01 ± .07	1.49 ± .10 *	1.05 ± .12	1.83 ± .23 *

Control = 0 mg/kg/day; Atrazine = 100 mg/kg/day

2-way ANOVA with Bonferroni post-hoc (* = p < 0.05)

Table 1: Hepatic GST expression levels following 1, 2, 3 and 4 days of 100 mg/kg of ATR.

LIVER CYTOCHROME P450 ENZYME mRNA EXPRESSION LEVELS IN
OVARECTOMIZED ESTROGEN-TREATED FEMALES
SUMMARY VALUES FOR CYTOCHROME P450 ENZYME EXPRESSION IN
FOLD CHANGE

CYP P450 Enzyme	Treatment		CYP P450 Enzyme	Treatment	
	Control	Atrazine		Control	Atrazine
Cyp17a1	1.17 ± .31	2.84 ± .55 *	Cyp2e1	1.01 ± .06	3.09 ± .49 *
Cyp1a2	1.01 ± .08	0.86 ± .13	Cyp2f4	1.02 ± .10	1.79 ± .14 *
Cyp26a1	1.14 ± .29	1.08 ± .11	Cyp2r1	1.02 ± .10	1.78 ± .28 *
Cyp26b1	1.03 ± .12	2.94 ± .55 *	Cyp2t1	1.03 ± .13	1.82 ± .21 *
Cyp26c1	1.08 ± .23	1.23 ± .10	Cyp3a18	1.06 ± .16	3.70 ± .77 *
Cyp27a1	1.02 ± .11	2.11 ± .24 *	Cyp3a23/3a1	1.06 ± .18	4.29 ± 1.0 *
Cyp2b2	1.04 ± .15	23.92 ± 7.7 *	Cyp3a9	1.02 ± .10	1.64 ± .23 *
Cyp2b3	1.03 ± .12	2.32 ± .24 *	Cyp4a3	1.06 ± .17	1.93 ± .23 *
Cyp2c22	1.04 ± .16	2.59 ± .27 *	Cyp4b1	1.02 ± .11	1.57 ± .28
Cyp2c23	1.02 ± .11	2.12 ± .25 *	Cyp4f1	1.02 ± .09	1.93 ± .11 *
Cyp2c37	1.04 ± .14	1.06 ± .21	Cyp4f4	1.06 ± .18	2.04 ± .32 *
Cyp2c6	1.05 ± .17	1.27 ± .25	Cyp4f6	1.10 ± .24	2.08 ± .22 *
Cyp2c7	1.00 ± .05	1.74 ± .15 *	Cyp7a1	1.34 ± .53	0.62 ± .15
Cyp2d2	1.04 ± .15	2.02 ± .21 *	Cyp7b1	1.01 ± .08	0.77 ± .10
Cyp2d4	1.38 ± .53	2.70 ± 1.1	Cyp8b1	1.02 ± .10	0.84 ± .16

Control = 0 mg/kg/day; Atrazine = 100 mg/kg/day

T-test (* = p < 0.05)

Table 2: Hepatic CYP expression levels following 1, 2, 3 and 4 days of 100 mg/kg of ATR.

Chapter III

Changes in Hepatic Phase I and Phase II Biotransformation Enzyme Expression and Substrate Availability Following Long-term Atrazine Exposure

Abstract

Atrazine (2-chloro-4-ethylamino-6-isopropylamino-s-triazine; ATR) is one of the most commonly used herbicides worldwide, and is known to affect the expression of both hepatic phase I and phase II metabolism components. However, much of the previous work has been limited in scope when considering ATR doses/duration used and the hepatic components examined. In the present study, adult ovariectomized Sprague-Dawley (SD) rats were gavaged daily with 1% methylcellulose vehicle or 6.5, 50 or 100 mg/kg/b.w. of ATR for 4, 8 or 14 consecutive days. On the afternoon of the final treatment day, livers were removed and stored at -70°C until assaying for CYP and GST mRNA expression levels, total GSH, GST protein levels and GST (cytosolic and microsomal) activity. Cytosolic GST (cGST) activity and GSH levels were increased after 14 days of ATR treatment but only in animals treated with 100 mg/kg. Hepatic CYP2B2 showed a dose-dependent increase in mRNA expression, with an almost 21-fold increase in expression after 14 days of 100 mg/kg ATR treatment. We also found an increase in expression for CYP2E1 and CYP3A23/3A1 as previously reported. However, the expression of multiple CYP enzymes was upregulated following 4 and 8 days of ATR treatment but not after 14 days of treatment. We also found an increase in expression levels for multiple GST isoforms following 4 and 8 days of treatment, but by 14 days of treatment, only mGST2

showed an increase in expression. These novel findings indicate that there may be a habituation or adaptation of liver metabolism components following long-term ATR treatment, which might indicate the role both phase I and phase II hepatic biotransformation components play in ATR metabolism.

Introduction

Atrazine (2-chloro-4-ethylamino-6-isopropylamino-s-triazine; ATR) belongs to the chloro-s-triazine family of herbicides, and is used to stop both pre- and post-emergence broadleaf and grassy weeds in a number of different crops including corn, sorghum and sugarcane [1]. ATR prevents the electron transfer at the reducing site of photosystem complex II in chloroplasts by binding to the plastoquinone-binding protein [2, 4]. This results in the breakdown of the electron transport process which leads to plant death due to starvation and oxidative damage.

Both hepatic phase I and phase II biotransformation components have been examined following ATR exposure. Previously, we examined the short-term effects of high-dose ATR exposure on the regulation and expression of both hepatic phase I and phase II xenobiotic metabolism components. We found that multiple days of ATR exposure leads to an increase in the expression of numerous glutathione-s-transferase (GST) and cytochrome P450 (CYP) isoforms, glutathione (GSH) levels and GST activity. We discovered a number of novel GST and CYP enzymes that are regulated by ATR exposure and could potentially be involved in the metabolism of ATR. We also verified previous findings that reported CYP2B1/2 [99-101], CYP2E1 [17] and CYP4A3 [120] are likely involved in ATR metabolism.

In the present study, we examined the effects of ATR exposure on the expression levels of hepatic GST and CYP enzymes, GST protein and activity levels and GSH levels after a range of ATR exposure both dosage (0, 6.5, 50 or 100 mg/kg/b.w.) and duration (daily for 4, 8 or 14 days). In doing so, we are able to better understand the changes in hepatic phase I and phase II metabolism over longer term ATR exposure. By using lower doses of ATR, we will also be able to better characterize the physiological effects ATR has on liver biotransformation components that could possibly be involved in ATR metabolism.

Materials and Methods

Animals. All animal surgical procedures and experimental protocols were approved by the WIL Research Institutional Animal Care and Use Committee. All animal procedures were performed by WIL Research Laboratories. Adult female Sprague-Dawley (SD) rats (minimum of 12 weeks old) were individually housed in suspended wire cages on a 14h schedule (lights on 0500) with *ad libitum* access to food and water. All animals were ovariectomized and implanted with a 12-14 mm long estradiol (4 mg/mL in sesame oil) silastic capsule before additional procedures were performed. All animals received a single daily dose of vehicle (1% carboxymethylcellulose sodium salt (CBC)) in deionized water (5 mL/kg) 7 days prior to the first day of treatment. Animals were administered ATR or vehicle by gavage once daily (6.5, 50 or 100 mg/kg of body weight) for 4, 8 or 14 consecutive days (24-25 animals per group). Following completion of the last treatment, animals were euthanized by carbon dioxide inhalation and the right lobe of the liver was collected and weighed. Tissue was flash frozen in liquid nitrogen and stored at -70°C until analyzed.

RNA Extraction. RNA extraction was performed using the Qiagen® (Valencia, CA) RNeasy® Microarray Tissue kit (73304). Tissue (40-60 mg) from the right lobe of the liver was weighed and placed in 1 mL of QIAzol® lysis reagent in a DNase/Rnase free 1.7 mL microcentrifuge tube. Tissue was homogenized for 30-40 seconds using the pellet mixer (VWR, Radnor, PA; 47747-370). Following homogenization, the homogenate was placed on the bench top at room temperature for 5 minutes to promote dissociation of the nucleoprotein complexes. Chloroform (200 µL) was added, mixed and allowed to sit at room temperature for 3 minutes. Homogenates were then centrifuged at 12,000 x g for 15 minutes at 4°C. The upper aqueous layer was transferred to a new microcentrifuge tube and mixed with 600 µL of 70% ethanol. The mixture was transferred to an Rneasy Mini spin column in a 2 mL collection tube and centrifuged at 8,000 x g for 15 seconds at room temperature. On-column Dnase Digestion was performed using the Rnase-free Dnase set (Qiagen; 79254). RNA was eluted off the spin column and collected in a 1.5 mL collection tube. Sample concentration (ng/µL) and purity (260/280 ratio) were determined using the Thermo Scientific (Pittsburgh, PA) NanoDrop ND-1000 Spectrophotometer. cDNA synthesis was performed using the Qiagen RT² First Strand Kit (330401).

Real-time PCR Analysis-GST. Real-time PCR analysis was performed using a custom Qiagen RT² Profiler PCR array. Eight liver samples were selected at random from each control and experimental group, and mRNA expression levels for 13 isoforms of GST were analyzed: GST alpha 3 (GSTa3), GST alpha 4 (GSTa4), GST kappa 1 (GSTk1), GST mu 1 (GSTm1), GST mu 2 (GSTm2), GST mu 3 (GSTm3), GST omega 1 (GSTo1), GST omega 2 (GSTo2), GST pi 1 (GSTp1), GST theta 1 (GSTt1), GST theta 2 (GSTt2), microsomal GST 1 (mGST1) and

microsomal GST 2 (mGST2). Large ribosomal protein, P1 (Rplp1) was run as the housekeeping gene along with a reverse transcription control and a positive PCR control. All primer sets were verified by Qiagen for the custom PCR array. PCR was carried out using the Bio-rad iCycler iQ real-time detection system with RT² SYBR Green qPCR mastermix (Qiagen; 330513).

Fluorescence data collection was performed for 40 cycles at 95°C for 15 seconds and 40 cycles at 60°C for 1 minute. The fold change of each target mRNA expression relative to Rplp1 under experimental and control conditions were calculated based on the threshold cycle (C_T) as $r = 2^{-\Delta(\Delta C_T)}$, where $\Delta C_T = C_T(\text{target}) - C_T(\text{Rplp1})$ and $\Delta(\Delta C_T) = \Delta C_T(\text{experimental}) - \Delta C_T(\text{control})$.

GSH Analysis. Total glutathione (GSH) levels were determined using the Cayman Chemical GSH assay kit (Ann Arbor, Michigan). Liver samples (100-200 mg) were homogenized using the Precellys 24 (Bertin Technologies, Rockville, MD) at 5000 rpm, twice for 10 seconds each time and spun at 10,000 x g for 15 minutes at 4 °C. The total protein content of supernatant was measured according to the Bradford method [117] with bovine serum albumin as a protein standard. Protein levels for all samples were standardized to 10 mg/mL. Samples were deproteinated with metaphosphoric acid followed by the reaction of the sulfhydryl groups of GSH with 5,5'-dithio-*bis*-2-nitrobenzoic acid (DTNB, Ellman's reagent) to produce a yellow colored product, 5-thio-2-nitrobenzoic acid (TNB). The product was measured at 412 nm using the Molecular Devices (Sunnyvale, CA) Spectra Max Plus384, and the absorbance was compared to a standard curve range of 0-8.0 μM oxidized glutathione (GSSG) using the Softmax Pro (Molecular Devices) data software. All samples were assayed in duplicate, and the results were expressed as nmol GSH/mg protein.

Western Blotting. The same animals from the GST mRNA analysis were used to measure GST protein levels. Protein extracts (75 ng) and low molecular weight standards (Bio-rad, 161-0305) were separated by electrophoresis at 200 V for 50 minutes in a 12% Criterion TGX polyacrylamide gel (Bio-rad; 567-1045). Protein extracts were transferred for 1 hour at 100 V to a nitrocellulose membrane (Bio-rad; 162-0116). Blots were blocked using equal volumes of Li-Cor (Lincoln, NE) Odyssey Blocking Buffer (927-40000) and PBS (.1M; pH 7.2) and placed on a rotator for 1 hour. Blots were incubated overnight at 4°C on a rotator with 12 mL of primary antibody cocktail [Primary antibody cocktails used were as follows: Mouse anti-GST alpha (MyBioSource, San Diego, CA, MBS560696; 1:1000) with Goat anti-GST mu (Abcam, Cambridge, MA, Ab53942; 1:1000) and Rabbit anti-GST omega (Abcam, Ab129106; 1:1000)]. Blots were rinsed and incubated in secondary antibody cocktail [Secondary antibody cocktails used were as follows: Donkey anti-Mouse (Odyssey 680 RD; 926-68072; 1:10,000) with Donkey anti-Goat (Odyssey 800 CW; 926-32214; 1:10,000) and Donkey anti-Rabbit (Odyssey 680 RD; 926-68073; 1:10,000)]. Blots were washed and stored in PBS until imaged. All blots were imaged using the Li-Cor Odyssey Infrared Imaging System. Blots were analyzed using the Odyssey Software v2.0. Beta-actin (Mouse anti-Actin; Millipore, Billerica, MA, MAB1501; 1:1000) was run as a loading control protein, and protein levels for each GST isoform were standardized to beta-actin levels.

GST Analysis. GST enzymatic activity was determined using the Cayman Chemical GST assay kit. Using 10 mg/mL standardized protein samples, homogenate was diluted to 1 mg/ml in potassium phosphate buffer (100 mM potassium phosphate, 2 mM EDTA, pH 7.0), placed into 3.0 mL sterile ultracentrifuge tubes (Beckman Coulter, 355870), heat sealed and spun in an ultra-

speed centrifuge (Beckman L8-70M, Brea, CA) at 100,000 x g for 60 minutes at 4°C. Cytosolic fraction was placed in new sterile tube, and microsomal pellet was resuspended in 500µL of cold homogenization buffer. Protein concentration of both fractions was determined by protein assay (BioRad). GST activity for both fractions were determined spectrophotometrically by measuring the rate of formation of the conjugate of GSH and 1-chloro-2,4-dinitrobenzene (CDNB). The absorbance was read at 340 nm every 60 seconds for 6 minutes using the Molecular Devices Spectra Max Plus384 plate reader. All samples were assayed in duplicate, and enzymatic activity was expressed as nmol/min/mg protein. Data were analyzed using Softmax Pro software.

Real-time PCR Analysis-CYP Enzymes. Real-time PCR analysis was performed using a custom Qiagen RT² Profiler PCR array. Liver samples (4-5) were randomly selected from the 8 liver GST mRNA samples analyzed from the four day control and experimental group. mRNA expression levels for 45 isoforms of Cytochrome P450 (CYP) enzymes were analyzed for the 4 day treatment group: CYP11a1, CYP11b1, CYP17a1, CYP19a1, CYP1a1, CYP1a2, CYP1b1, CYP24a1, CYP26a1, CYP26b1, CYP26c1, CYP27a1, CYP27b1, CYP2a3, CYP2b2, CYP2b3, CYP2c11, CYP2c22, CYP2c23, CYP2c37, CYP2c6, CYP2c7, CYP2c80, CYP2d2, CYP2d4, CYP2e1, CYP2f4, CYP2r1, CYP2s1, CYP2t1, CYP2w1, CYP3a18, CYP3a23/3a1, CYP3a9, CYP4a3, CYP4a8, CYP4b1, CYP4f1, CYP4f18, CYP4f4, CYP4f40, CYP4f6, CYP7a1, CYP7b1 and CYP8b1. Rplp1 was run as the housekeeping gene along with reverse transcription and positive PCR controls. All primer sets were verified by Qiagen for the custom PCR array. After reverse transcription, PCR was carried out using the Bio-rad iCycler iQ real-time detection system with RT² SYBR Green qPCR mastermix (Qiagen; 330513). One cycle was performed at 95°C for 10 minutes to activate the HotStart DNA *Taq* Polymerase. Fluorescence data collection

was performed for 40 cycles at 95°C for 15 seconds and 40 cycles at 60°C for 1 minute. The fold change of each target mRNA expression relative to Rplp1 was calculated based on the threshold cycle (C_T) as $r = 2^{-\Delta(\Delta C_T)}$, where $\Delta C_T = C_T(\text{target}) - C_T(\text{Rplp1})$ and $\Delta(\Delta C_T) = \Delta C_T(\text{experimental}) - \Delta C_T(\text{control})$.

Statistical Analysis. All data were analyzed for all time points using 2-way analysis of variance (ANOVA) for treatment, days of treatment and treatment \times days of treatment interactions with Bonferroni post-hoc tests. The level of statistical significance was set at $P \leq 0.05$. All values are reported as the mean \pm SEM. Prism 5 for Mac (GraphPad Software, Inc.) was used for all data analysis.

Results

Real-time PCR Analysis-GST. We found a significant interaction for all GST enzymes examined: GSTa3 ($F_{6,84}=32.60$; $P<0.05$) as well as GSTa4 ($F_{6,83}=14.19$; $P<0.05$), GSTk1 ($F_{6,84}=24.20$; $P<0.05$), GSTm1 ($F_{6,84}=9.07$; $P<0.05$), GSTm2 ($F_{6,84}=13.58$; $P<0.05$), GSTm3 ($F_{6,84}=6.72$; $P<0.05$), GSTo1 ($F_{6,84}=9.67$; $P<0.05$), GSTo2 ($F_{6,84}=3.72$; $P<0.05$), GSTp1 ($F_{6,84}=6.84$; $P<0.05$), GSTt1 ($F_{6,84}=22.06$; $P<0.05$), GSTt2 ($F_{6,84}=7.37$; $P<0.05$), mGST1 ($F_{6,83}=10.36$; $P<0.05$) and mGST2 ($F_{6,84}=2.45$; $P<0.05$). All data are presented in **Table 3** with a select few depicted in **Figure 6**. The Bonferroni post-hoc *t*-tests revealed that ATR treatment led to a dose-dependent increase in GST enzyme mRNA expression levels. Animals treated with ATR for four days with 50 and 100 mg/kg/b.w. showed a significant increase in expression levels for GSTa3 and mGST2 compared to control and 6.5 mg/kg/b.w. (**Figure 6**). After 4 days of treatment, ATR-treated animals also showed an increase in GSTa4 and GSTo1 at 100 mg/kg/b.w. compared to all other

experimental groups. In the case of GSTo1, 50 mg/kg/b.w. treated animals were also elevated compared to vehicle treated animals (**Figure 6; Table 3**). After 8 days of treatment, all but GSTo2, mGST1 and mGST2 showed an increase in expression at 100 mg/kg/b.w. compared to control and 6.5 mg/kg/b.w. (**Table 3**). Furthermore, animals treated for 8 days with ATR also showed an increase in expression for GSTt1 at 6.5 mg/kg/b.w. compared to control, and GSTp1 and mGST1 at 50 mg/kg/b.w. compared to control (**Figure 6; Table 3**). GSTa3, GSTa4, GSTk1, GSTm2, GSTm3, GSTo1 and GSTt1 showed an increase in expression after 8 days at 50 mg/kg/b.w. compared to control and 6.5 mg/kg/b.w. GSTm1, GSTm2 and GSTp1 showed an increase in expression at 100 mg/kg/b.w. compared to all other treatment groups (**Figure 1; Table 3**). Conversely, after 14 days of treatment, only mGST2 at 100 mg/kg/b.w. was significantly elevated above control (**Figure 6; Table 3**). All other GST expression levels after 14 days of treatment were at or below control levels, with 50 mg/kg/b.w. ATR-treated animals expressing GSTa4 below control and 6.5 mg/kg/b.w. treated animals, and 100 mg/kg/b.w. animals possessing GSTa4 levels below those at 6.5 mg/kg.b.w. of ATR treatment. Similarly, hepatic mGST1 levels of 50 mg/kg/b.w. treated animals was below all other treatment groups (**Figure 6; Table 3**).

Bioreactive GSH levels. ATR-treated animals showed increased liver GSH levels at 6.5, 50 and 100 mg/kg/b.w. after 4 days of treatment compared to control (**Figure 7A**) and at 100 mg/kg/b.w. after 14 days of treatment. There was a significant interaction for treatment ($F_{3,251}=20.18$; $P<0.05$), but there was not a significant interaction between days of treatment and dosage ($F_{6,251}=1.59$; $P=0.15$). ATR treatment did not have a significant effect on liver GSH levels after 8 days of treatment at any dose.

GST protein levels. Using western blots, we did find a significant increase in protein level for GST omega (GSTo) after 4 days of treatment for 100 mg/kg atrazine treated animals versus control ($P < 0.05$) (**Figure 8**). There was a significant interaction between days of treatment and dosage for GSTo ($F_{6,84} = 2.76$; $P < 0.05$). We did not find a significant difference for GST alpha (GSTa) or GST mu (GSTm) after atrazine treatment (data not shown). There was no interaction between days of treatment and dosage for GSTm ($F_{6,82} = 1.09$; $P = 0.37$) or GSTa ($F_{6,80} = 0.68$; $P = 0.67$).

GST activity. We then wanted to determine if overall GST activity was increased for both cytosolic and microsomal fractions due to ATR exposure. There was a significant treatment ($F_{3,234} = 3.75$; $P < 0.05$) and days of treatment ($F_{2,234} = 4.06$; $P < 0.05$) effect for cytosolic GST (cGST) activity, but there was not a significant interaction between days of treatment and dosage for cGST activity ($F_{6,234} = 0.89$; $P = 0.50$). For microsomal GST (mGST) activity, there was no significant treatment ($F_{3,249} = 0.52$; $P = 0.67$), days of treatment ($F_{2,249} = 1.74$; $P = 0.18$) or interaction ($F_{6,249} = 1.03$; $P = 0.40$). There was no increase in cGST or mGST activity after 4 or 8 days of treatment (**Figure 8B-C**), but ATR treated animals showed an increase in cGST activity after 14 days of treatment in the 100 mg/kg/b.w. group compared to control (**Figure 8**).

Real-time PCR Analysis-CYP. We found a significant interaction between days of treatment and dosage for Cyp1a2 ($F_{6,42} = 8.81$; $P < 0.05$), as well as Cyp2b3 ($F_{6,42} = 2.76$; $P < 0.05$), Cyp2c7 ($F_{6,42} = 4.44$; $P < 0.05$), Cyp2d2 ($F_{6,42} = 5.94$; $P < 0.05$), Cyp2f4 ($F_{6,42} = 5.04$; $P < 0.05$), Cyp2r1 ($F_{6,42} = 2.89$; $P < 0.05$), Cyp3a9 ($F_{6,42} = 4.77$; $P < 0.05$), Cyp4a3 ($F_{6,42} = 4.81$; $P < 0.05$), Cyp4b1

($F_{6,42}=3.12$; $P<0.05$), Cyp4f1 ($F_{6,42}=4.40$; $P<0.05$), Cyp4f4 ($F_{6,42}=2.33$; $P<0.05$), Cyp4f6 ($F_{6,42}=2.43$; $P<0.05$), Cyp7a1 ($F_{6,42}=3.09$; $P<0.05$) and Cyp7b1 ($F_{6,42}=4.03$; $P<0.05$). However, we found no interaction in the expression levels of Cyp17a1 ($F_{6,42}=0.07$; $P=0.99$), Cyp26a1 ($F_{6,42}=1.68$; $P=0.15$), Cyp26c1 ($F_{6,42}=1.68$; $P=0.15$), Cyp27a1 ($F_{6,42}=1.32$; $P=0.27$), Cyp2b2 ($F_{6,42}=0.98$; $P=0.45$), Cyp2c22 ($F_{6,42}=1.13$; $P=0.36$), Cyp2c23 ($F_{6,42}=1.44$; $P=0.22$), Cyp2c37 ($F_{6,42}=1.45$; $P=0.22$), Cyp2c6 ($F_{6,42}=1.22$; $P=0.31$), Cyp2d4 ($F_{6,42}=0.70$; $P=0.65$), Cyp2e1 ($F_{6,42}=1.84$; $P=0.12$), Cyp2t1 ($F_{6,42}=1.01$; $P=0.43$), Cyp 3a18 ($F_{6,42}=1.47$; $P=0.21$), Cyp3a23/3a1 ($F_{6,42}=1.71$; $P=0.14$) or Cyp8b1 ($F_{6,42}=1.90$; $P=0.10$). ATR-treated animals showed a dose-dependent increase in liver mRNA expression for a number of CYP enzymes, including Cyp2b2, Cyp2e1 and Cyp4f6 (**Table 4; Figure 9**). Using PCR analysis, Cyp11a1, Cyp11b1, Cyp19a1, Cyp1a1, Cyp1b1, Cyp24a1, Cyp26b1, Cyp27b1, Cyp2a3, Cyp2c11, Cyp2c80, Cyp2s1, Cyp2w1, Cyp4a8, Cyp4f18 and Cyp4f40 were below detection threshold.

Discussion

In the present study, we have characterized the changes in hepatic GST and CYP enzyme expression, GST protein levels, GSH levels and GST activity after 4, 8 and 14 days of ATR treatment at 6.5, 50 and 100 mg/kg/b.w. of ATR. The current study helps to elucidate the regulation and expression of hepatic GST-mediated phase I metabolism components and phase II CYP enzymes that are altered following both short- and long-term exposure to ATR.

We found a significant interaction between dosage and days of treatment in the mRNA expression levels of GSTa3, GSTa4, GSTk1, GSTo1, mGST1 and mGST2 at 100 mg/kg/b.w. of ATR after 4 days of treatment compared to control. GSTo1 was also increased above control at

50 mg/kg/b.w. after 4 days of treatment. After 8 days of 100 mg/kg/b.w. of ATR treatment, the expression level of all GST isoforms with the exception of GSTo2, mGST1 and mGST2 were elevated above control. Animals treated for 8 days with 50 mg/kg/b.w. of ATR also showed significant increases compared to control in the expression of the majority of GST isoforms examined. The expression level of GSTt1 after only 6.5 mg/kg/b.w. of ATR increased compared to control as well, which is the lowest dose of ATR that has been shown to alter the expression level of any GST isoform. Islam et al (2002) reported an increase in GSTp following treatment with 10 mg/kg/b.w. of ATR [102], suggesting that the regulation of phase II metabolism components are responsive to relatively lower doses of ATR.

The most striking finding was that after 14 days of ATR treatment, only mGST2 showed a significant increase in expression compared to control. Considering the reduction in expression of multiple GST isoforms of the liver of after 14 consecutive days with high doses of ATR, the possibility of liver necrosis was considered. Indeed, Campos-Pereira et al (2012) treated animals for 14 consecutive days with 400 mg/kg/b.w. of ATR [115], and reported evidence of liver degeneration and toxicity due to long-term and/or high-dose exposure of ATR. However, lower doses of ATR (10-200 mg/kg/b.w.) for similar durations fails to produce toxic effects in the liver [102], therefore, it is unlikely that using much lower doses of ATR would have led to liver toxicity or degeneration in the present study. The normalized expression of hepatic GST enzymes after 14 days of ATR exposure could be due to a regulatory mechanism in the liver, and might give insight into the long-term regulation and role of the hepatic GST enzymes following long-term exposure to ATR.

We also examined protein levels for three GST isoforms after 14 days of ATR treatment, and found no difference between ATR-treated animals at any dose compared to control. Campos-Pereira (2012) also found no significant difference in the protein levels of GST1 following 14 consecutive days ATR treatment [115]. The ATR-induced increase in GST isoform mRNA expression levels without a corresponding rise in protein levels in the same liver samples suggests that repeated ATR treatment upregulates transcription of GST isoforms without driving translation and protein production. The more likely rationale is that ATR might increase protein levels of specific GST isoforms without altering the level of all detectable GST biotransformation enzymes. Increased protein levels and/or activity in a specific isoforms will be difficult to discern due to limitations in current antibody and assay specificity.

In the current study, we found an increase in liver GSH levels after 4 days of ATR treatment at all doses examined when compared to control levels. There was also an increase in GSH levels after 14 days of ATR treatment. At the intervening time point of 8 days, liver GSH levels were the same as those found in control animals. The 8-day time point is also the duration when the majority of GST isoforms were at their highest expression levels, suggesting that the increased GST levels led to increased utilization of GSH. However, overall GST activity does not support this supposition. Overall, these results indicate that ATR might induce changes in hepatic GSH levels and phase II metabolism at much lower doses than previously reported [103]. However, control GSH levels for the 4 day treatment group were lower than the control levels compared to the 8 and 14 day control groups ($F_{2,72}=28.58$; $P<0.05$), which might have skewed our results. Regardless, other studies have demonstrated that GSH conjugation of ATR by rat liver fractions

is involved in the phase II xenobiotic metabolism of ATR [107], and our results support this finding.

In the current study, we found there was a significant interaction between days of treatment and dosage for cGST activity. Surprisingly, although the expression levels of almost all GST isoforms and GST protein levels were not significantly different from control after 14 days of ATR treatment, we did find an increase in cGST activity in the 100 mg/kg/b.w. ATR-treated group. These results are somewhat consistent with previous findings which have shown that GST enzyme activity in the liver is higher in animals treated with 50 and 200 mg/kg/b.w. of ATR, treated from postnatal day 23 to 50 [103]. The present report of a lack of effect of 50 mg/kg/b.w. could be explained by the inconsistencies in duration or that the previous study was performed in male Wistar rats compared to the current female SD. Regardless, the rise in GST activity at the later time point suggests that although the expression and protein levels of GST are not significantly elevated after long-term ATR treatment, hepatic GST enzymes might still play an active role in the long-term metabolism of ATR.

In the current study, we wanted to characterize the changes in CYP expression levels after longer term ATR treatment and over multiple doses. We found an almost 2-fold increase in expression compared to control for CYP17A1, an enzyme that catalyzes the conversion of pregnenolone to dehydroepiandrosterone (DHEA) [58], after 14 days of ATR treatment at 50 and 100 mg/kg/b.w. as well as a significant increase in expression for CYP27A1, which performs the 27-hydroxylation of cholesterol, in the 50 and 100 mg/kg/b.w. ATR-treated groups after 8 and 14 days of treatment compared to control. These novel results suggest that ATR upregulates these

CYP enzymes following both short- and long-term exposure, but more research is needed to elucidate the mechanism by which ATR might activate these pathways and any changes in liver function that might occur due to changes in the expression of these CYP enzymes.

Previous studies have shown that CYP1A1/2 is involved in ATR metabolism or is regulated by ATR treatment [99, 102, 103]. In the current study, CYP1A2 was significantly elevated after 4 days of ATR treatment compared to all other treatment groups, but only in the 50 mg/kg/b.w. group. There were numerous CYP enzymes that showed similar regulation patterns to CYP1A2. CYP2C37 showed an almost 2-fold increase after 4 days of ATR treatment in the 50 mg/kg/b.w. group and no increase in the 100 mg/kg/b.w. group compared to control. After 8 days of treatment, there was a three-fold increase in the 50 mg/kg/b.w. group compared to only a 2-fold change in the 100 mg/kg/b.w. group, and an over 2-fold change after 14 days in the 50 mg/kg/b.w. group compared to only a 1.5-fold change in the 100 mg/kg/b.w. group. CYP26A1, CYP26C1, CYP2T1 and CYP7A1 also showed a significant increase in expression at 50 mg/kg/b.w. of ATR compared to control at 8 days but not at 100 mg/kg/b.w. Furthermore, CYP2C6, which has been shown previously to be involved in the metabolism of ATR in male rat liver microsomes [100, 101], did not show an increase in expression compared to control until after 8 days of ATR treatment and remained elevated after 14 days of treatment. It appears that varying doses and durations of ATR exposure leads to differential regulation of several CYP enzymes. These findings might reveal novel changes in CYP-mediated liver metabolism or the regulation of ATR or other xenobiotic compounds after prolonged exposures.

In this study, CYP4F1, CYP4F4 and CYP4F6 isoforms showed no increase after 4 days of ATR treatment. However, expression levels were increased compared to control after 8 days of treatment. Surprisingly, the expression levels of all 3 isoforms were not increased above control after 14 days of ATR treatment. Furthermore, the expression of only mGST2 and not mGST1 was increased above control after 14 days of treatment. CYP4F1, CYP4F4 and CYP4F6 are all involved in the omega-hydroxylation of leukotriene B₄, a potent mediator of inflammation, and mGSTs are usually involved in the biosynthesis of leukotrienes. Both of these processes help to protect against oxidative stress [84]. Previous research has shown that ATR treatment can lead to oxidative stress in rats [121, 122], but these results suggest again that there could be an adaptation or habituation to ATR exposure after long-term ATR treatment.

Similarly, CYP2D2, CYP2C7, CYP2R1, CYP3A18 and CYP3A23/3A1 showed an increase in expression after 4 and 8 days of ATR treatment compared to control, but by 14 days of ATR treatment, expression levels were back to control levels. These CYP isoforms are regulated following short-term ATR exposure and might be involved in the initial metabolism of or response to ATR, but it is possible there is an adaptation or habituation in the liver following long-term exposure that no longer leads to an upregulation in the expression of these CYP isoforms or requires them for ATR metabolism. Perhaps alternate compensatory enzymes are upregulated making the early responding enzymes unnecessary. For instance, many CYP isoforms including CYP2B2, CYP2B3, CYP2C22, CYP2C23 and CYP2E1 showed increased expression levels in a dose-dependent manner following 4, 8 and 14 days of exposure. Hepatic CYP2B2 showed the largest increase in expression compared to control, supporting previous evidence that CYP2B2 plays a major role in the metabolism of ATR [101-103, 120]. These

findings could reveal novel roles of CYP2B2, CYP2B3, CYP2C22, CYP2C23 and CYP2E1 in the long-term metabolism of ATR.

In the current study, we thoroughly examined the hepatic expression, protein levels and activity levels of the primary component enzymes and substrates for GST-mediated phase II biotransformation as well as the expression of 45 CYP isoforms involved in phase I xenobiotic metabolism. Our research reports novel findings that long-term ATR exposure differentially regulates the expression of a number of CYP and GST isoforms as well as GST-mediated metabolism components. ATR treatment leads to variations in the expression of hepatic phase I CYP and phase II GST enzymes compared to shorter-term ATR treatment, which could be due to possible liver habituation or adaptation. We have validated some previous findings, but have also identified novel players in the initial as well as long-term hepatic effects of high dose ATR treatment. Further research is required to elucidate the exact role of these CYP and GST isoforms following ATR exposure. More research is also needed to elucidate the potential adaptation or habituation in the liver following ATR exposure.

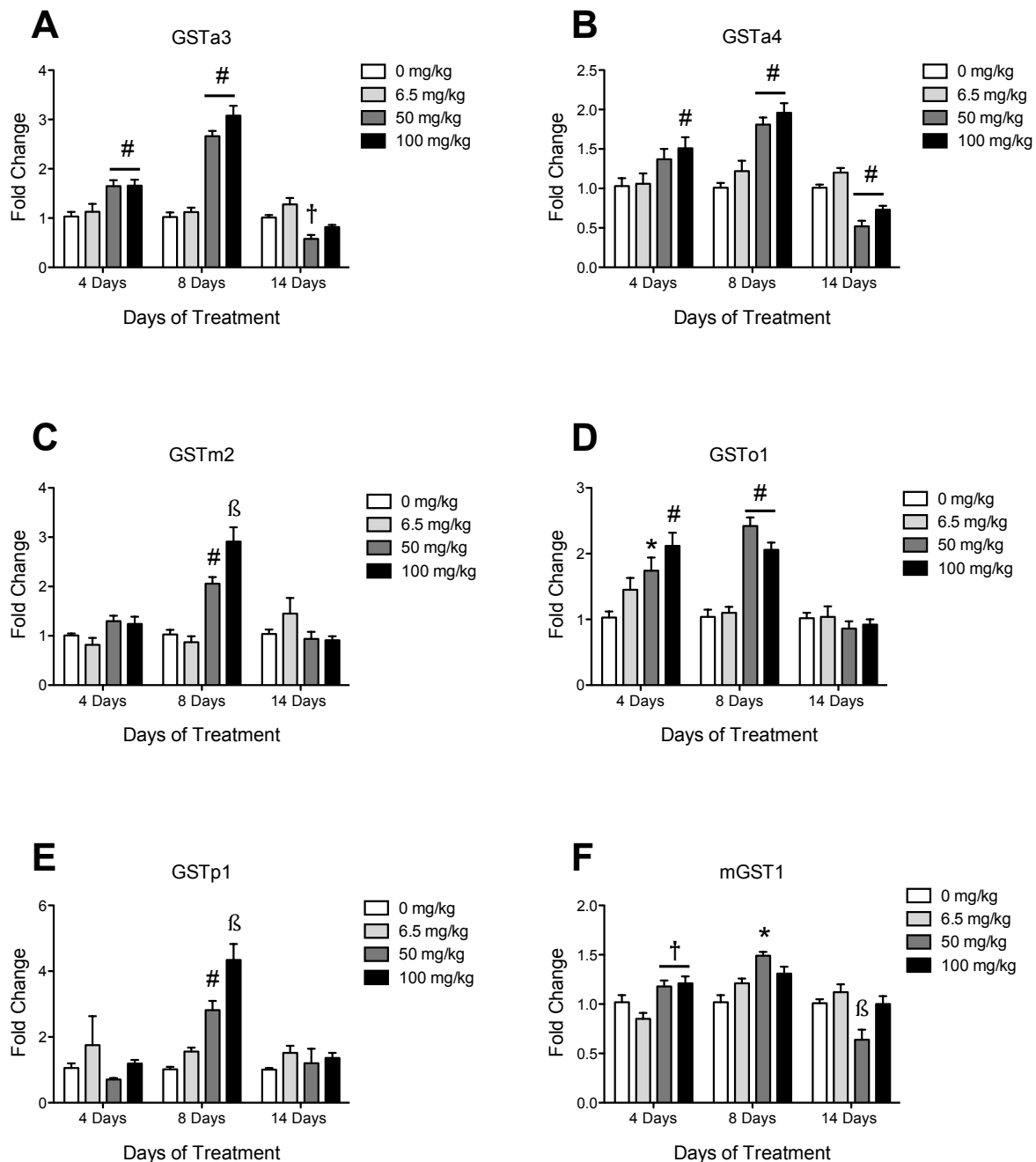


Figure 6: Hepatic mRNA expression levels for GSTa3, GSTa4, GSTm2, GSTo1, GSTp1 and mGST1 following 4, 8 and 14 days of 6.5, 50 or 100 mg/kg of ATR. Histograms depicting fold change in liver mRNA expression for GSTa3 (A), GSTa4 (B), GSTm2 (C), GSTo1 (D), GSTp1 (E) and mGST1 (F) after 4, 8 and 14 days of treatment. Data are presented as mean \pm SEM for 7-8 randomly selected animals for all groups; Significant difference ($P < 0.05$; * = compared to 0 mg/kg; # = compared to 0 mg/kg and 6.5 mg/kg; † = compared to 6.5 mg/kg; β = compared to all other groups).

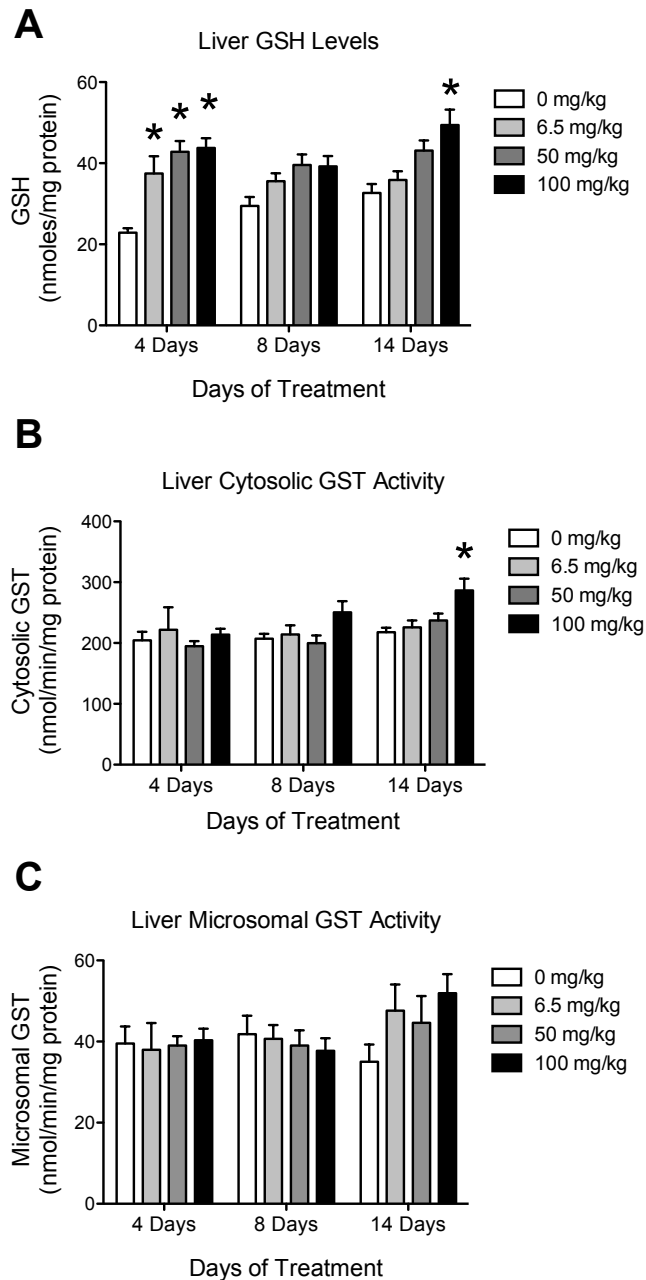


Figure 7: Hepatic GSH levels, cytosolic GST activity and microsomal GST activity following 4, 8 and 14 days of 6.5, 50 or 100 mg/kg of ATR. Histogram depicting liver GSH levels in nmoles/mg protein (A), liver cytosolic GST (cGST) activity in nmol/min/mg protein (B) and liver microsomal GST (mGST) activity in nmol/min/mg protein (C) for all animals after 4, 8 and 14 days of treatment. Data are presented as mean \pm SEM; *Significant difference ($P < 0.05$) versus control.

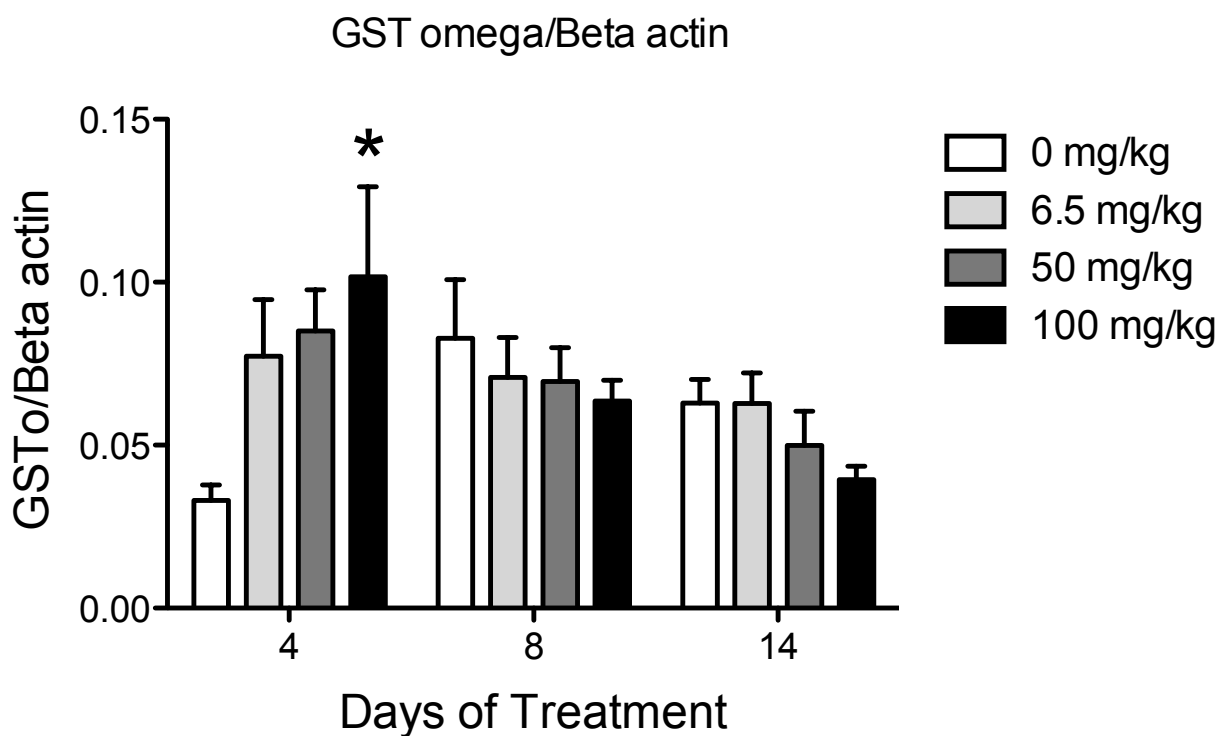


Figure 8: Hepatic GST omega protein levels following 4, 8 and 14 days of 6.5, 50 or 100 mg/kg of ATR. Histogram depicting GST omega protein levels after 4, 8 and 14 days of 6.5, 50 or 100 mg/kg/b.w. ATR treatment or control (0 mg/kg/b.w.). Protein levels are presented as GST omega levels/Beta actin levels. Data are presented as mean \pm SEM; *Significant difference ($P < 0.05$) versus corresponding control.

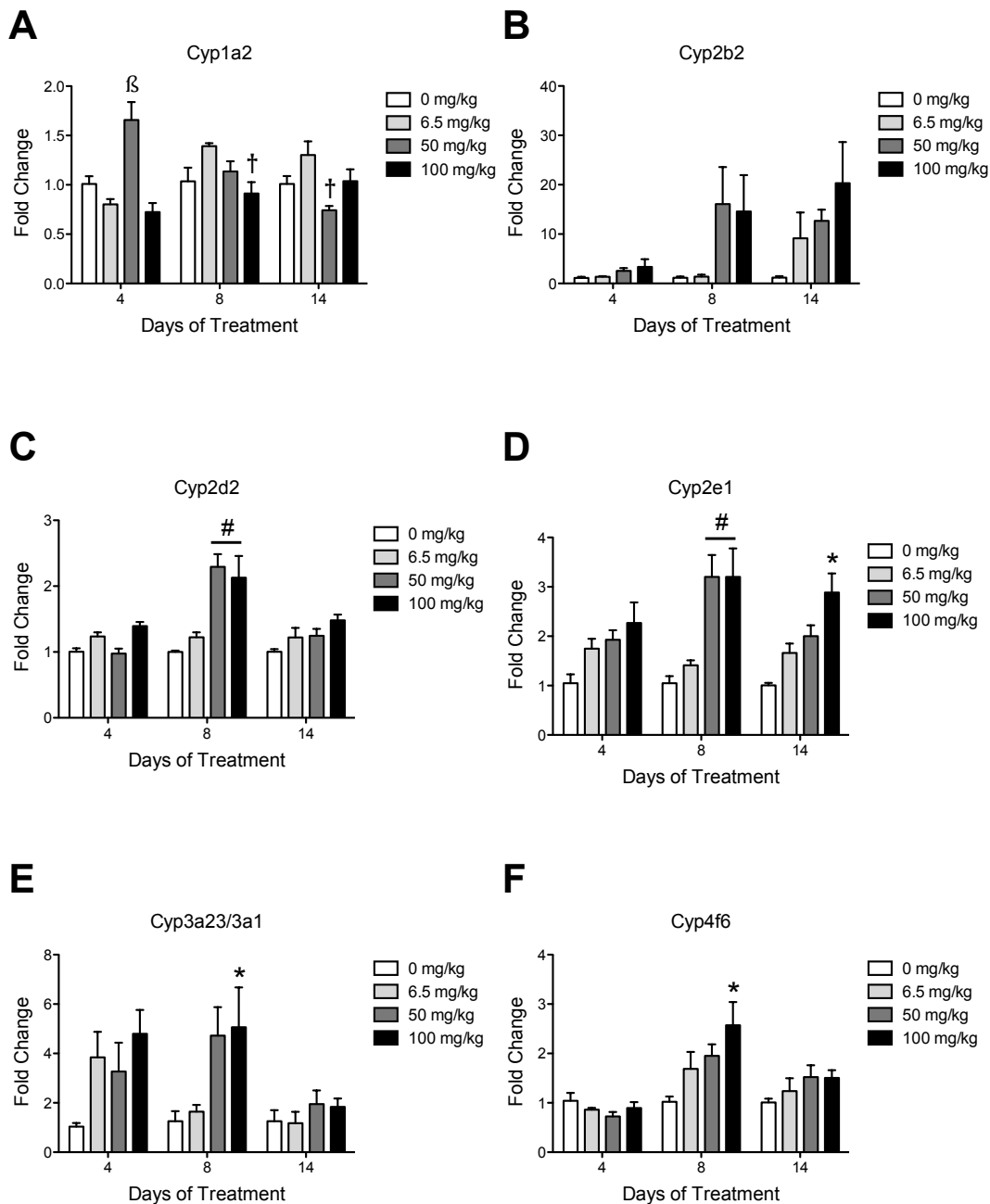


Figure 9: Hepatic mRNA expression levels for Cyp1a2, Cyp2b2, Cyp2d2, Cyp2e1, Cyp4f6 and Cyp3a23/3a1 following 4, 8 and 14 days of 6.5, 50 or 100 mg/kg of ATR. Histograms depicting fold change in liver mRNA expression for Cyp1a2 (A), Cyp2b2 (B), Cyp2d2 (C), Cyp2e1 (D), Cyp3a23/3a1 (E) and Cyp4f6 (F) after 4, 8 and 14 days of atrazine treatment. Data are presented as mean \pm SEM for 4-5 animals for all groups. Significant difference ($P < 0.05$; * = compared to 0 mg/kg; # = compared to 0 mg/kg and 6.5 mg/kg; † = compared to 6.5 mg/kg; β = compared to all other groups; ω = compared to 0 mg/kg and 100 mg/kg).

LIVER GST mRNA EXPRESSION LEVELS IN OVARIECTOMIZED ESTROGEN-TREATED
FEMALES DUE TO LONG-TERM ATRAZINE TREATMENT
SUMMARY VALUES FOR GST EXPRESSION IN FOLD CHANGE

GST isoforms	4 Day Treatment (mg/kg)				8 Day Treatment (mg/kg)				14 Day Treatment (mg/kg)			
	0	6.5	50	100	0	6.5	50	100	0	6.5	50	100
GSTa3	1.03	1.13	1.65 #	1.66 #	1.02	1.12	2.66 #	3.08 #	1.01	1.28	0.58 †	0.82
GSTa4	1.03	1.06	1.37	1.51 #	1.01	1.22	1.81 #	1.96 #	1.01	1.20	0.52 #	0.73 †
GSTk1	1.01	1.19	1.39	1.51 *	1.01	1.12	2.32 #	2.50 #	1.01	1.17	0.57 †	0.84
GSTm1	1.05	0.90	1.44	1.55	1.05	1.10	1.89	3.56 β	1.05	1.33	1.06	1.15
GSTm2	1.01	0.82	1.30	1.24	1.03	0.87	2.06 #	2.91 β	1.04	1.45	0.94	0.91
GSTm3	1.06	0.45	1.24	0.86	1.08	1.29	3.17 #	3.93 #	1.15	1.13	0.70	0.62
GSTo1	1.03	1.45	1.74 *	2.12 #	1.04	1.10	2.42 #	2.06 #	1.02	1.04	0.86	0.92
GSTo2	1.05	0.73	0.80	0.82	1.03	0.93	1.35	1.27	1.03	1.20	0.88	1.14
GSTp1	1.06	1.75	0.71	1.19	1.02	1.56	2.82 *	4.34 β	1.01	1.52	1.20	1.36
GSTt1	1.02	0.66	0.77	0.81	1.78	2.64 *	4.52 #	3.96 #	1.02	1.29	0.69	1.03
GSTt2	1.05	0.75	0.89	1.05	1.03	1.07	1.51	1.68 #	1.10	1.57	0.95 †	0.81 †
mGST1	1.02	0.75	1.18 †	1.21 †	1.02	1.21	1.49 *	1.31	1.01	1.12	0.64 β	1.00
mGST2	1.08	1.24	2.07 #	2.24 #	1.05	0.93	1.34	1.40	1.03	1.03	1.24	1.69 #

2-way ANOVA; significance $p < 0.05$ (* = compared to 0 mg/kg; # = compared to 0 mg/kg and 6.5 mg/kg; † = compared to 6.5 mg/kg; β = compared to all other groups)

Table 3: Hepatic GST expression levels following 4, 8 and 14 days of 6.5, 50 or 100 mg/kg of ATR.

LIVER CYTOCHROME P450 ENZYME mRNA EXPRESSION LEVELS IN OVARECTOMIZED ESTROGEN-TREATED FEMALES
SUMMARY VALUES FOR CYTOCHROME P450 ENZYME EXPRESSION IN FOLD CHANGE

CYP P450 Enzyme	4 Day Treatment (mg/kg)				CYP P450 Enzyme	8 Day Treatment (mg/kg)				CYP P450 Enzyme	14 Day Treatment (mg/kg)			
	0	6.5	50	100		0	6.5	50	100		0	6.5	50	100
Cyp17a1	1.04	0.84	0.89	1.20	Cyp17a1	1.06	0.89	1.39	1.56	Cyp17a1	1.68	1.47	1.75	1.99
Cyp1a2	1.01	0.80	1.65	β 0.73	Cyp1a2	1.04	1.40	1.14	0.91 †	Cyp1a2	1.01	1.30	0.74 †	1.04
Cyp26a1	1.05	1.44	1.52	1.20	Cyp26a1	1.02	1.77	2.72 *	1.81	Cyp26a1	1.16	1.39	1.59	2.07
Cyp26c1	1.02	0.76	0.68	0.55	Cyp26c1	1.01	1.53	1.92	1.55	Cyp26c1	1.13	1.54	1.73	1.55
Cyp27a1	1.03	1.46	1.59	1.83	Cyp27a1	1.01	1.48	2.40 #	1.99	Cyp27a1	1.06	1.53	1.64 *	2.18 *
Cyp2b2	1.10	1.34	2.56	3.36	Cyp2b2	1.14	1.39	16.08	14.59	Cyp2b2	1.20	9.14	12.67	20.32
Cyp2b3	1.02	1.94	1.44	2.63 ω	Cyp2b3	1.01	1.21	2.59 #	2.98 #	Cyp2b3	1.01	1.03	2.04	2.75 #
Cyp2c22	1.02	1.30	1.46	2.38	Cyp2c22	1.05	1.57	2.45 *	2.04	Cyp2c22	1.07	1.42	1.41	2.16
Cyp2c23	1.07	1.71	1.72	2.39 *	Cyp2c23	1.06	1.26	2.13 #	2.26 #	Cyp2c23	1.03	1.06	1.47	1.88 #
Cyp2c37	1.17	1.20	1.93	1.01	Cyp2c37	1.12	1.00	3.02	2.01	Cyp2c37	1.14	2.57	2.12	1.54
Cyp2c6	1.20	0.37	0.77	0.26	Cyp2c6	1.58	0.91	3.32	1.64	Cyp2c6	1.07	2.53	2.43	2.82
Cyp2c7	1.00	1.05	0.85	0.90	Cyp2c7	1.01	1.37	2.10 #	1.84 *	Cyp2c7	1.02	1.40	1.49	1.57
Cyp2d2	1.00	1.24	0.98	1.39	Cyp2d2	1.00	1.22	2.29 #	2.13 #	Cyp2d2	1.00	1.22	1.25	1.48
Cyp2d4	1.02	6.00	3.20	5.95	Cyp2d4	1.55	4.11	2.95	2.62	Cyp2d4	2.05	1.56	1.58	3.84
Cyp2e1	1.05	1.75	1.93	2.27	Cyp2e1	1.05	1.41	3.20 #	3.20 #	Cyp2e1	1.00	1.66	2.01	2.88 *
Cyp2f4	1.01	1.12	1.09	1.14	Cyp2f4	1.03	1.22	2.14 #	2.25 #	Cyp2f4	1.01	1.28	1.41	1.30
Cyp2r1	1.02	1.78	1.66	2.23 *	Cyp2r1	1.04	1.67	2.10 *	1.46	Cyp2r1	1.01	1.03	0.99	1.10
Cyp2t1	1.01	1.28	1.32	1.44	Cyp2t1	1.01	1.33	1.89 *	1.33	Cyp2t1	1.04	0.99	1.47	1.45
Cyp3a18	1.02	2.65	2.82	2.81	Cyp3a18	1.24	1.71	4.27	4.93 #	Cyp3a18	1.26	1.38	2.00	1.78
Cyp3a23/3a1	1.04	3.84	3.27	4.79	Cyp3a23/3a1	1.26	1.64	4.73	5.06 *	Cyp3a23/3a1	1.26	1.18	1.95	1.84
Cyp3a9	1.05	2.59	1.80	3.31 *	Cyp3a9	1.04	1.53	2.93 *	1.51	Cyp3a9	1.06	1.00	1.62	2.71 #
Cyp4a3	1.01	0.92	0.53	0.75	Cyp4a3	1.12	1.33	2.59 #	2.38 #	Cyp4a3	1.08	1.35	2.56 #	1.67
Cyp4b1	1.08	0.72	0.75	0.48	Cyp4b1	1.09	1.13	1.54	1.22	Cyp4b1	1.01	1.61	1.35	1.62
Cyp4f1	1.00	1.13	0.86	1.05	Cyp4f1	1.01	1.29	1.89 #	1.66 *	Cyp4f1	1.01	1.22	1.39	1.41
Cyp4f4	1.07	0.71	0.91	0.77	Cyp4f4	1.05	1.29	1.78	1.52	Cyp4f4	1.02	1.61	1.15	1.60
Cyp4f6	1.04	0.86	0.73	0.89	Cyp4f6	1.02	1.69	1.95	2.57 *	Cyp4f6	1.01	1.24	1.52	1.51
Cyp7a1	1.03	1.12	1.04	0.77	Cyp7a1	1.02	1.92	3.54 ω	1.56	Cyp7a1	1.42	1.50	0.58	1.67
Cyp7b1	1.01	0.47 *	0.63	0.33 *	Cyp7b1	1.01	1.24	0.96	1.01	Cyp7b1	1.04	1.04	0.78	0.85
Cyp8b1	1.02	0.62	0.84	0.39	Cyp8b1	1.04	1.43	0.82	0.97	Cyp8b1	1.03	1.30	0.63	0.87

2-way ANOVA; significance $p < 0.05$ (* = compared to 0 mg/kg; # = compared to 0 mg/kg and 6.5 mg/kg; † = compared to 6.5 mg/kg; β = compared to all other groups; ω = compared to 0 mg/kg and 100 mg/kg)

Table 4: Hepatic CYP expression levels following 4, 8 and 14 days of 6.5, 50 or 100 mg/kg of ATR.

Chapter IV

Review of Literature (Part 2)

Hypothalamic-Pituitary-Adrenal (HPA) Axis

Adrenal Gland Structure and Function

The adrenal gland is comprised of two embryologically distinct tissues, the adrenal medulla and the adrenal cortex. The medullary cells, or chromaffin cells, are of neurodermal origin, while the cortical cells are of mesodermal origin [123]. The adrenal cortex is subdivided into three cortical layers: the outermost layer is the zona glomerulosa (zG), the middle layer is the zona fasciculata (zF) and the innermost layer is the zona reticularis (zR). In rats, the zG is responsible for the production of the mineralocorticoids, such as aldosterone (ALDO), while both the zF and zR produce the glucocorticoids, such as corticosterone (CORT). In humans and some other species but not the rat, the zR has the capability to produce adrenal androgens [123].

The localized production of the mineralocorticoids and glucocorticoids can be attributed to the differential expression of two distinct genes, CYP11B1 and CYP11B2 [124, 125]. The CYP11B1 gene codes for the 11 β -hydroxylase enzyme and is found in the zF and zR. This enzyme is responsible for the synthesis of CORT, and does not have the ability to synthesize ALDO because it does not possess 18-oxidase activity. CYP11B2 is found only in the zG and codes for the enzyme ALDO synthase, which, as its name implies, is responsible for the production of ALDO [126].

Hypothalamic-Pituitary-Adrenal (HPA) Axis

Corticotropin-releasing hormone (CRH) is synthesized in neurons of the paraventricular nucleus (PVN) of the hypothalamus and secreted from neurosecretory nerve terminals of CRH neurons at the median eminence. CRH enters the hypophyseal portal system and is carried to the anterior pituitary by the hypophyseal portal blood. CRH binds to corticotrophs and activates an internal cascade that results in the synthesis and secretion of the adrenocorticotrophic hormone (ACTH). ACTH is released into general circulation, and is carried to the adrenal cortex where it stimulates the biosynthesis and secretion of CORT. In a negative feedback manner, CORT is transported through general circulation to the hypothalamus or anterior pituitary where it reduces the secretion of CRH or ACTH respectively.

Regulation of Aldosterone Secretion and Synthesis

The primary physiological stimulus for the synthesis and secretion of ALDO from the zG is angiotensin II (Ang II) [127]. Ang II is the effector of the renin-angiotensin system (RAS). Ang II is an octapeptide and is produced when angiotensin I (Ang I) is cleaved by angiotensin I-converting enzyme (ACE), which is secreted by pulmonary and renal endothelial cells and is expressed mainly in lungs [127]. Ang I is converted from angiotensinogen by the enzyme renin [128], which is secreted by cells of the juxtaglomerular afferent arterioles in the kidney [129].

Cells in the zG respond to Ang II stimulation via G-protein coupled Ang II receptors. There are two types of Ang II receptors in the zG, but ALDO secretion is stimulated by the binding of Ang II to Ang II type 1 receptors (AT₁R) [130]. AT₁R are located in both the zG and zF/zR [131], and binding of Ang II to AT₁R has been shown to increase inositol phosphate levels [132]. However,

due to the lack of inositol phosphate receptors in the zF/zR [133], production of CORT is not activated by the binding of Ang II. Elevated extracellular potassium levels can also stimulate the production and secretion of ALDO. Ang II and potassium work via calcium secondary messenger systems to stimulate ALDO synthesis and secretion. Atrial natriuretic peptide (ANP), which is secreted by heart muscle cells to control water, sodium and potassium levels, is also a known inhibitor of ALDO secretion [130].

ACTH can also stimulate ALDO production; however, these effects are not sustained [134]. Following long-term stimulation of high levels of ACTH, most zG cells containing ALDO synthase expression atrophy [135], which could indicate not only a reduced cell function but also an overall decrease in zG thickness and cell number. Engeland et al. (1999) reported that during adrenal regeneration following a unilateral adrenal enucleation, or removal of all parts of the adrenal except the zG, with contralateral adrenalectomy treatment, ACTH treatment was shown to suppress the regeneration of the zG cell phenotype and restore the zF cell phenotype compared to regenerating adrenals without ACTH stimulation [136]. Furthermore, restoration of the zF preceded the reestablishment of the zG, and full recovery of ALDO synthase expression did not occur after 30 days of regeneration, whereas 11 β -hydroxylase expression was restored by 20 days. In addition, when ALDO synthase expression was increased in enucleated adrenals by the presence of an intact adrenal, recovery of 11 β -hydroxylase expression was suppressed. The suppression was partially reversed by ACTH treatment, suggesting that elevated plasma ACTH resulting from the loss of steroid negative feedback contributes to the suppression of the zG cell phenotype and the restoration of the zF cell phenotype. To date, the physiologic relevance of ACTH in ALDO production and CYP11B2 transcription is unclear.

Chronic ACTH treatment affects the expression of steroid hydroxylases primarily via increases in intracellular cyclic adenosine monophosphate (cAMP) and activation of protein kinase A, but the mechanism through which ACTH inhibits the expression of CYP11B2 is still unclear [137]. Studies have shown that treatment with cAMP analogues preferentially increase CYP11B1 mRNA expression over CYP11B2 [138, 139], and cAMP signaling has been shown to have a negative effect on the expression of Ang II receptors in adrenocortical cells [140, 141], desensitizing adrenal cells to Ang II. Furthermore, the induction of CYP11B1 for production of CORT by ACTH could also decrease ALDO synthase expression by removing precursors from the pathway leading to ALDO production [137]. However, in the presence of normal ACTH stimulation, the zG is able to maintain CYP11B2 expression by controlling intracellular levels of cAMP. In isolated zG cells, but not zF cells, Ang II will inhibit ACTH-stimulated cAMP production [142, 143], and secondly, the zG, but not zF, expresses adenylyl cyclases types 5 and 6, which are both inhibited by intracellular calcium, the second messenger involved in signaling from Ang II and potassium [144].

Aldosterone is synthesized from cholesterol via a CYP-mediated biosynthesis pathway. In rats, cholesterol is synthesized either de novo in cortical cells from acetate or is absorbed as high-density lipoproteins. Shuttling of steroid hormone precursors is vital during multiple steps of ALDO synthesis, which begins in the mitochondria, continues in the endoplasmic reticulum and is completed in the mitochondria. The rate-limiting step in the production of ALDO is mediated by steroidogenic acute regulatory (StAR) protein, which transports cholesterol from the outer to the inner mitochondrial membrane [127]. The next step in the pathway in the synthesis of ALDO is the conversion of cholesterol to pregnenolone, which is mediated by the side-chain cleaving

enzyme (P450_{scc}; CYP11A1). In the final step of the pathway, ALDO is produced from CORT by ALDO synthase (CYP11B2), which has 11 β -hydroxylation, 18-hydroxylation and 18-oxidation activities. The full biosynthesis pathway can be found in **Figure 10**.

Secretion of ALDO and other steroid hormones is immediate due to their lipid solubility [145]. Blood concentrations of steroid hormones reflect rates of synthesis due to a lack of storage of preformed hormone in adrenal cortical cells. For nocturnal animals such as rats, secretion is greatest in the early evening.

Effects of ATR Exposure on the HPA Axis

ATR has been shown to not only disrupt the HPG axis, but studies have also revealed that ATR exposure affects the hypothalamic-pituitary-adrenal (HPA) axis. ATR treatment increases serum concentrations of CORT in female rats and mice [146, 147] as well as castrated male rats [148]. These effects have been shown to persist for up to 21 days of dosing in rats [148] and 28 days in mice [146].

In order to elucidate the mechanism by which ATR exposure leads to an increase in CORT concentrations, Laws et al. (2009) examined the effects of ATR and its metabolites on pituitary and adrenal hormone secretion in male Wistar rats (50-60 days old) [96]. Animals were gavaged with ATR (5, 50, 100 or 200 mg/kg/b.w.), DEA (173.4 mg/kg/b.w.), DIA (4, 10, 40, 80 or 160 mg/kg/b.w.) or DACT (3.4, 33.7, 67.5 or 135 mg/kg/b.w.). CORT, P and ACTH levels were measured 5, 15, 30, 60 or 180 minutes after dosing.

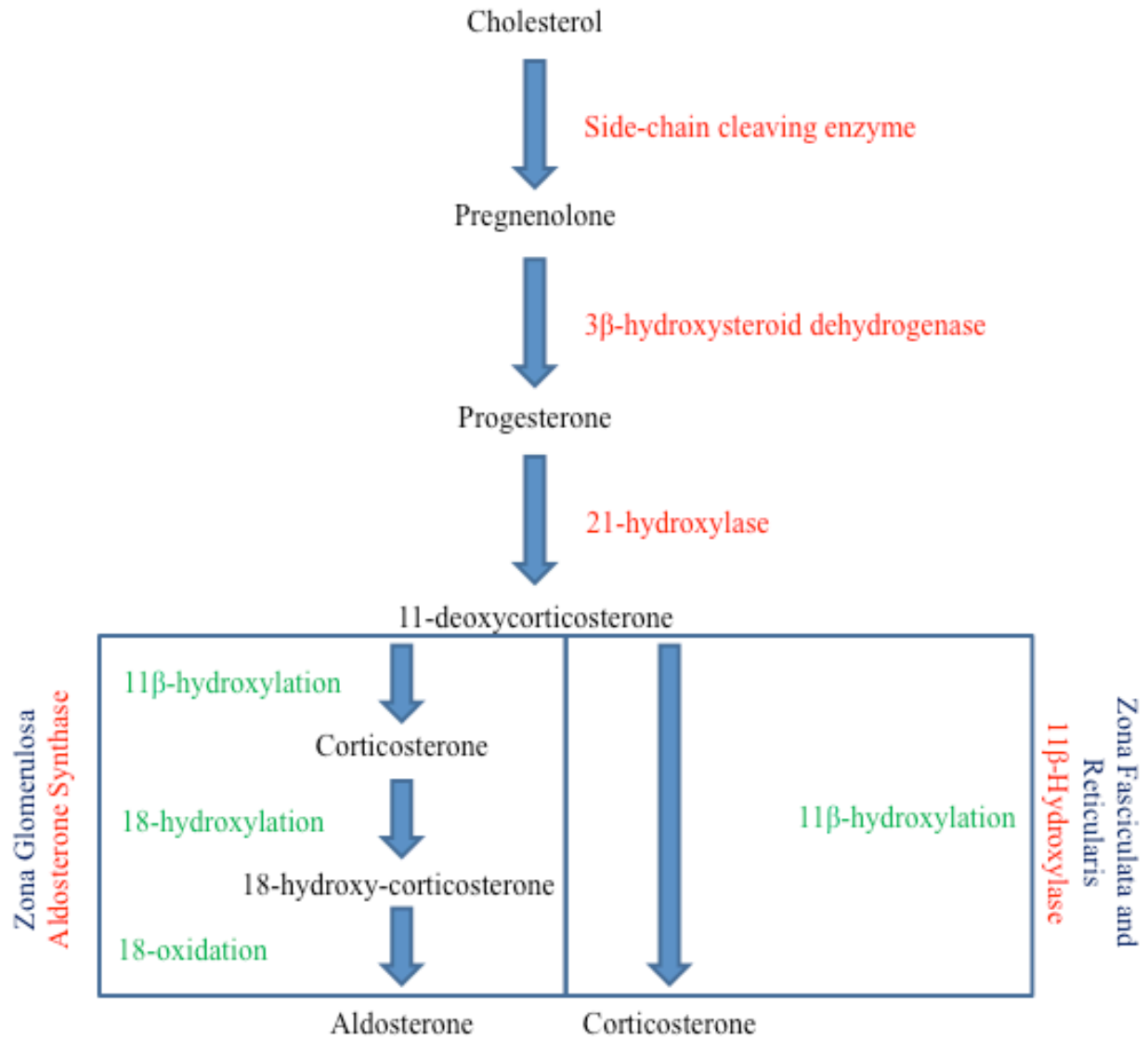


Figure 10: Steroidogenesis in rat adrenal cortex.

Treatment with ATR led to a dose-dependent increase in the plasma levels of ACTH, CORT and P. ACTH levels were significantly elevated above control 5 minutes after dosing, and peak ACTH levels were measured after 15 minutes of dosing. CORT and P levels were significantly elevated after 15 minutes of dosing and remained high after 180 minutes in the 50, 100 and 200 mg/kg/b.w. of ATR-treated groups. Peak levels of CORT and P were reached within 30 minutes after dosing. Treatment with DACT also leads to significant increases in ACTH, CORT and P levels; however, these levels were substantially less than the levels observed after treatment with ATR, which suggests that DACT is a less potent activator of the HPA axis. Furthermore, equimolar concentrations of DIA led to dose-dependent increases in ACTH, CORT and P levels, while treatment with DEA also resulted in significant increases in these hormone levels.

Another group of animals were subject to restraint stress for 15 minutes in order to elicit an acute stress response. Previous studies have shown that an acute stress-mediated response causes elevated ACTH, CORT and prolactin levels. In this study, restraint stressed animals did show elevated ACTH, CORT and prolactin levels, however, ATR-treated animals only showed an increase in ACTH and CORT levels without an elevation in the level of prolactin.

These results suggest that animals treated with ATR have elevated adrenal hormone levels as a result of increased ACTH secretion from the pituitary, which is not a direct result of an acute stress-mediated response. However, the mode by which ATR activates this ACTH-mediated response is unclear. Furthermore, P is a precursor in the synthesis of CORT, and the rapid increase in P levels suggest that P secretion is from the adrenal gland as a direct result of ACTH stimulation or direct stimulation of ATR on the adrenal [149]. Tinfo et al. (2011) found

consistent results and determined that HPA axis activation after a single gavage of ATR is unlikely due to gastrointestinal distress [150]. Again, this indicates that the increase in CORT and P secretion might be an ACTH-mediated response or a direct effect of ATR on adrenal gland steroidogenesis.

In another study, female Long-Evans Hooded rats were gavaged with control, ATR (75 mg/kg/b.w.) or the equimolar equivalent dose of DIA or DACT either on the day of proestrus or for 4 consecutive days beginning 4 days before proestrus [147]. Another group was restraint stressed for 5 minutes either on the day of proestrus or for 4 consecutive days beginning 4 days before proestrus. As shown previously, treatment with ATR or DIA for both groups significantly increased the levels of ACTH, CORT and P, while treatment with DACT had no significant effect. This study also found a significant attenuation effect of ACTH secretion following multiple doses of ATR or DIA. However, the CORT response remained similar between the two treatment groups. Restraint stress-treated animals for both groups also had increased levels of ACTH, CORT and P as compared to the control group with no attenuation of ACTH levels due to multiple restraint stress treatments. Due to the attenuation of ACTH after multiple exposures to ATR, it is possible ATR acts directly at the adrenal to increase adrenal hormone secretion.

Effects of Activation of the HPA Axis on the HPG Axis

Previous studies have shown that activation of the HPA axis can lead to direct or indirect effects on the function of the HPG axis at all levels of the axis in many different species [151-155]. The inhibition of reproduction due to stimuli that activate the HPA axis has been studied in humans [156] and many other species; however, the mechanism by which the HPA axis might alter the

HPG axis is still unclear. There is evidence that an interaction exists between CRH and GnRH [157], which could lead to alterations in HPG function. In addition, secretion of corticosteroids and P from the adrenal gland has been shown to alter the secretion of GnRH and LH [158, 159], as well as pituitary responsiveness to GnRH secretion [152, 155, 160]. The effects of corticosteroids and P on the pituitary are secondary but result in the observed decrease of circulating LH levels [161]. Furthermore, specific corticosteroids known as the glucocorticoids, also exert their effects at the cellular level through binding to the glucocorticoid receptor (GR), which are localized to specific cell types within both the testis and ovary which suggests a possible direct influence on reproductive function at the level of the gonads [162, 163].

Effects of ATR Exposure on HPG Axis in Adrenalectomized (ADX) Rats

Using an adrenalectomized (ADX) rat model, Foradori et al. (2011) examined the effects of the adrenal gland on the hormone-induced LH surge and LH pulsatility following ATR treatment [164]. Young female ovariectomized Wistar rats (60-90 days old) received either a sham operation or a bilateral ADX. Animals were then treated daily for 4 days with vehicle or 200 mg/kg of ATR. A hormone-induced surge was measured on the evening on the final day of treatment. Similarly treated animals not given hormone replacement were used to measure pulsatile LH release, following a sham operation or a bilateral ADX.

Both sham and ADX animals showed an inhibition of the hormone-induced LH surge following ATR treatment in both AUC and peak LH levels. However, in the final experiment, LH pulsatility was only affected in the sham surgery group reporting a reduced pulse frequency and

increased pulse amplitude. In contrast, LH pulsatility in ADX animals was not affected after ATR treatment.

These results show that ATR has different modes of action on the two types of GnRH/LH secretion. In the absence of the adrenal glands, ATR treatment still led to an inhibition of the hormone-induced LH surge, suggesting that ATR might act via the central nervous system. Conversely, the adrenal gland is critical for the ATR-induced inhibition of LH pulsatility, which suggests that CORT and/or P are involved in this inhibition. It has been postulated that CORT and P might be intermediaries in ATR's ability to inhibit GnRH/LH pulsatility because GnRH neurons do not express type II GR or progesterone receptors (PR) [165, 166]. These two hormones might act via a common inhibitory interneuronal system(s), and the interneuronal system(s) involved in the regulation of GnRH secretion might include endogenous opioids [167, 168]. As shown with ATR treatment, administration of opioid peptides inhibits LH pulse frequency [169, 170]. Specifically, dynorphin and β -endorphin neurons located in the arcuate nucleus contain GR and PR receptors. Increases in P have been shown to increase the number of GR-immunoreactive cells in the arcuate nucleus [166, 171-173], and furthermore, neurons expressing endogenous opioid peptides are activated during stress or increases in glucocorticoids, which could lead to inhibition of LH release [174-176]. It is possible that high doses of ATR might lead to an increase in CORT and/or P levels, which would lead to the activation of endogenous opioid neurons in the arcuate nucleus, and subsequently, the inhibition of GnRH pulsatility.

Conclusions and Objectives

Disruption of adrenal gland hormone secretions is known to affect the function of the HPG axis. An ATR treatment leads to altered adrenal gland steroidogenesis, and has been shown to disrupt the two types of GnRH/LH secretion via different modes of action. The adrenal gland is required for disruption of GnRH/LH pulsatility, while ATR is still able to disrupt the hormone-induced surge in the absence of the adrenals. In order to better understand ATR's effect on GnRH/LH pulsatility, we examined the effects of ATR treatment on adrenal gland morphology, enzymatic immunoreactivity and enzyme mRNA expression levels. Specifically, we wanted to fully characterize ATR's effects on the expression of ALDO synthase and 11 β -hydroxylase after ATR treatment.

Chapter V

Changes in Adrenal Gland Morphology and Enzymatic Expression in the Rodent

Following Atrazine Exposure or Restraint Stress

Abstract

Atrazine (ATR) is one of the most commonly used herbicides worldwide, and is used to stop a variety of pre- and post-emergence broadleaf and grassy weeds. ATR's effects on the hypothalamic-pituitary-gonadal (HPG) axis have been widely studied including the inhibition of pulsatile luteinizing hormone (LH) release. Recent evidence suggests that these effects are mediated by ATR's effects on the hypothalamic-pituitary-adrenal (HPA) axis. ATR treatment leads to an increase in adrenocorticotrophic hormone (ACTH) and corticosterone (CORT), which is a known inhibitor of the HPG axis. In addition, adrenalectomy will abolish ATR's inhibition of LH pulsatile release. To determine the effects of repeated ATR exposure on the adrenal gland, adult ovariectomized (OVX) Sprague Dawley rats were gavaged daily with vehicle or 100 mg/kg/b.w. of ATR for 1, 2, 3 or 4 consecutive days, or 6.5, 50 or 100 mg/kg/b.w. of ATR for 4, 8 or 14 consecutive days in a subsequent study. On the final day of treatment adrenals were taken for histological and gene expression. ATR-treatment resulted a reduction in zona glomerulosa (zG) thickness, as well as a decrease in aldosterone (ALDO) synthase expression in a dose and time dependent manner. In a subsequent study, rats were treated for 4 or 14 days with vehicle or 100 mg/kg/b.w. of ATR or restraint stressed for 30 min in order to compare the effects of ATR treatment with a known stressor. One hour after the final treatment, trunk blood was taken along

with adrenal glands. ATR treatment mimicked those of restraint stress with a reduction in zG thickness and a decrease in ALDO synthase immunoreactivity with no change to zona fasciculata (zF) or 11β -hydroxylase. In conclusion, ATR's effects on circulating adrenal hormone levels and adrenal morphology mimic those of repeated restraint stress, suggesting ACTH mediated effects.

Introduction

Atrazine (2-chloro-4-ethylamino-6-isopropylamino-s-triazine; ATR) is one of the most commonly used herbicides, with approximately 80 million pounds applied each year in the U.S. alone [1]. It belongs to the triazine family of herbicides, and is used to stop both pre- and post-emergence broadleaf and grassy weeds. In rats, the effects of ATR exposure on the hypothalamic-pituitary-gonadal (HPG) axis have been well documented (see Cooper et al 2007 [26] for review). In particular, we have shown that high doses of ATR will inhibit pulsatile release of gonadotropin releasing hormone (GnRH) and the subsequent release of luteinizing hormone (LH) from the pituitary [32, 44].

More recently, ATR has been shown to affect the hypothalamic-pituitary-adrenal (HPA) axis as well. ATR treatment results in increased serum adrenocorticotropic hormone (ACTH) in rats, and subsequently, increased corticosterone (CORT) levels and adrenal-derived progesterone (P) [96, 147, 148, 150]. Considering the known inhibitory actions of HPA activation has on reproductive output, we postulated a role of adrenal stimulation in ATR's inhibition of LH release [151-155, 158, 159]. Indeed, ATR-induced inhibition of pulsatile LH is abolished in adrenalectomized rats. Evidence to date suggests ATR stimulates the adrenal gland, most likely, via ACTH release from the pituitary, and the subsequent release of adrenal hormones (CORT, P,

etc.) is necessary for ATR to inhibit pulsatile release. In addition, we investigated the effects of ATR treatment may have adrenal exposure on the synthesis and release of mineralocorticoid, aldosterone (ALDO). Synthesized and released from the zona glomerulosa (zG) from the adrenal cortex, ALDO secretion is thought to be primarily controlled by the renin-angiotensin system and secondarily by ACTH, suggesting it, along with the previous mentioned adrenal steroids, will be upregulated after repeated ATR treatment.

In the current study, we examined the effects of ATR treatment on adrenal gland morphology, enzymatic immunoreactivity, enzyme mRNA expression levels and circulating levels of CORT and ALDO after multiple doses and treatment durations. We also went on to compare the effects of restraint stress and ATR treatment on the same adrenal measures.

Materials and Methods

Animals: Experiments 1 and 2. Animal surgical procedures and experimental protocols were carried out and approved by the WIL Research Institutional Animal Care and Use Committee. Adult female Sprague-Dawley (SD) rats (60-90 days olds) were individually housed on a 14h schedule (lights on 0500) with ad libitum access to food and water. All animals were ovariectomized and implanted with a 12-14 mm long estradiol (4 mg/mL in sesame oil) silastic capsule before additional procedures were performed. All animals received a single daily dose of vehicle (1% carboxymethylcellulose sodium salt (CBC)) in deionized water (5 mL/kg) at least 4 days prior to the first day of treatment to habituate animals to gavage.

Animals: Experiment 3. Animal surgical procedures and experimental protocols were carried out and approved by the Auburn University Institutional Animal Care and Use Committee. Adult female Sprague-Dawley (SD) rats (60-90 days olds) were used, and animals were housed 2-3 per cage on a 14h schedule (lights on 0500) with ad libitum access to food and water. All animals were ovariectomized and allowed one week to recuperate. Animals received a single daily dose of vehicle (CBC) in deionized water (5 mL/kg) at least 4 days prior to the first day of treatment to habituate animals to gavage.

Experiment 1: Effects of Short-term Atrazine Exposure on Adrenal Gland Morphology and Steroidogenic Enzymes. Animals were administered ATR in CBC by gavage once daily (100 mg/kg/b.w.) for 1, 2, 3 or 4 consecutive days (10 animals per group). Control animals received CBC only (15 animals per group). Following completion of the last treatment, animals were euthanized by carbon dioxide inhalation and left and right adrenal tissue samples were collected and weighed separately. The right adrenal gland was placed in 10% neutral-buffered formalin for immunohistochemical examination. The left adrenal gland and pituitary were flash frozen in liquid nitrogen and stored at -70°C until RNA extraction.

Experiment 2: Effects of Long-term Atrazine Exposure and Atrazine Dosage on Adrenal Gland Morphology and Steroidogenic Enzymes. Animals were administered ATR in CBC by gavage once daily (6.5 mg/kg, 50 mg/kg or 100 mg/kg/b.w) for 4, 8 or 14 consecutive days (24-25 animals per group). Control animals received CBC only (24-25 animals per group). Following completion of the last treatment, animals were euthanized by carbon dioxide inhalation and left and right adrenal tissue samples were collected and weighed separately. The right adrenal gland

was placed in 10% neutral-buffered formalin for immunohistochemical examination. The left adrenal gland was flash frozen in liquid nitrogen and stored at -70°C until RNA extraction.

Experiment 3: Effects of Atrazine and Stress on Adrenal Gland Morphology and Steroidogenic Enzymes. ATR-treated animals were administered ATR in CBC by gavage once daily (100 mg/kg/b.w.) for 4 or 14 consecutive days (5 animals per group). Control animals received CBC only (5 animals per group). Stress animals were restraint stressed daily for 30 minutes in Plas-Labs Scientific restraint stress (Lansing, MI; 553-BSRR) for 4 or 14 consecutive days (4-5 animals per group). Following 1 hour after final treatment, animals were decapitated. Trunk blood was collected along with left and right adrenal tissue samples. The right adrenal gland was placed in 10% neutral-buffered formalin for immunohistochemical examination. The left adrenal gland was flash frozen in methyl-butane and stored at -70°C until RNA extraction.

Immunohistochemistry. Right adrenal glands were paraffin-embedded and 6µm sections were placed on HistoBond slides. Before beginning immunohistochemical analysis, slides were warmed at 55°C for 45 minutes. Slides were then deparaffinized and rehydrated through xylene and graded ethanol. Sections were then antigen-unmasked by boiling in TRIS buffer (10mM Tris; 1mM EDTA) at pH 9.0 for 15 minutes. Slides were washed in phosphate buffer saline (PBS; pH 7.2) and then placed in blocking solution (1% bovine serum albumin (BSA) in PBS) for 20 minutes. Slides were incubated in hybridization chambers overnight in a primary antibody cocktail in blocking solution [1:50 rabbit anti-Ki67 (abcam, Cambridge, MA; ab16667); 1:100 mouse anti-cytochrome P450 aldosterone synthase (CYP11B2; Millipore, Billerica, MA; MAB6021); 1:500 goat anti-11β-hydroxylase (CYP11B1; Santa Cruz Biotechnology, Dallas,

TX; sc-47652)]. After incubation in primary antibody, slides were washed three times in PBS and then incubated in a fluorescent secondary antibody cocktail for one hour [1:250 Alexa Fluor 488 donkey-anti mouse (Invitrogen, Carlsbad, CA; A21202); 1:250 Alexa Fluor 546 donkey-anti rabbit (A10040); 1:250 Alexa Fluor 594 donkey-anti goat (A11058)]. After incubation in secondary, slides were rinsed in phosphate buffer (PB; pH 7.2) and then coverslipped with hardset mounting media with DAPI counterstain (Vector Laboratories, Inc., Burlingame, CA; H-1500). Slides were then imaged at 20X magnification using a Perkin Elmer Cri-Nuance fluorescent multispectral imaging camera (Model FX; Waltham, MA) in conjunction with the Zeiss Axioskop microscope (Carl Zeiss Microscopy, LLC, Thornwood, NY). The nuance camera enables imaging of multiple molecular markers in tissue sections for fluorescence microscopy, and can help eliminate problems with autofluorescence. Using tunable filters matched to the bandwidths of common molecular markers, the camera can acquire spectral information from a sample resulting in component images. The various signals from multiple labels in the resulting image are “unmixed” by the software and a composite image is produced, allowing for spectral characterization and quantitation for each of the multi-labeled components in an image.

Adrenal Gland Analysis. Slides were analyzed using the ImageJ Software to measure the thickness of each adrenal cortical layer. Layers were measured in μm using the immunofluorescence and DAPI counterstain to distinguish the morphological differences in each layer (zona glomerulosa (zG), zona fasciculata (zF) and zona reticularis(zR)). Aldosterone (ALDO) synthase immunoreactivity was measured using NIH image software. Images were uploaded into NIH image, and a constant threshold was set. Immunoreactivity was measured as total pixel density in a 50 x 200 μm region of interest (ROI). Ki67 positive cells were counted to

examine cell proliferation in a 50 x 200 μm ROI in each cortical layer. Total cell number/ROI was counted in three separate ROI to get an average cell count for each layer.

RNA Extraction. RNA extraction was performed using the Qiagen (Valencia, CA) RNeasy Microarray Tissue kit (73304). Each whole, left adrenal was weighed (40-60 mg) and placed in 1 mL of QIAzol lysis reagent. Tissue was homogenized for 30-40 seconds. Following homogenization, the homogenate was placed on the bench top at room temperature for 5 minutes to promote dissociation of the nucleoprotein complexes. Chloroform (200 μL) was added, mixed and allowed to sit at room temperature for 3 minutes. Homogenates were then centrifuged at 12,000 x g for 15 minutes at 4°C. The upper aqueous layer was removed and mixed with 600 μL of 70% ethanol. An RNeasy Mini spin column used along with DNase digestion set (Qiagen; 79254) were used for purification. Concentration (ng/ μL) and purity (260/280 ratio) were determined using the Thermo Scientific (Pittsburgh, PA) NanoDrop ND-1000 Spectrophotometer. cDNA synthesis was performed using the Bio-Rad iScript cDNA synthesis kit (Hercules, CA; 170-88912).

Real-time PCR Analysis. PCR analysis was performed for angiotensin II type 1 receptor (AT₁R) [177] (Forward primer: GCTAAGCAGCTCACTCACTAC; Reverse primer: AACTCTTGACCTCCCATCTC), 11 β -hydroxylase (Forward primer: TTACCCAAGAGCTTGACTCGTTGGAC; Reverse primer: ACCATCTCGGATATGACACTCCAG) and ALDO synthase (Forward primer: ACGAGGTAGCAAGGGACTTCTTGGA; Reverse primer: GCATGGATGAACTTCAGGCTACCA), and glyceraldehyde 3-phosphate dehydrogenase

(GAPDH; Forward primer: GGTGATGCTGGTGCTGAGTA; Reverse primer: GGATGCAGGGATGATGTTCT) was used as the housekeeping gene. PCR was carried out using the Bio-rad iCycler iQ real-time detection system with Bio-Rad iQ SYBR Green Supermix. One cycle was performed at 95°C for 10 minutes to activate polymerase and denature the DNA. Fluorescence data collection was performed for 40 cycles at 95°C for 15 seconds and 40 cycles at 58°C for 1 minute. The fold change of each target mRNA expression relative to GAPDH under experimental and control conditions were calculated based on the threshold cycle (C_T) as $r = 2^{-\Delta(\Delta C_T)}$, where $\Delta C_T = C_T(\text{target}) - C_T(\text{GAPDH})$ and $\Delta(\Delta C_T) = \Delta C_T(\text{experimental}) - \Delta C_T(\text{control})$. The amplicons for 11 β -hydroxylase and ALDO synthase were sequenced and validated.

Corticosterone (CORT) Analysis. CORT was measured using an EIA kit (ENZO® Life Sciences, Farmingdale, NY; ADI-900-097). CORT samples were prepared by diluting the sample 1:50 in assay buffer. CORT binding globulin (CBG) was inactivated by incubating the diluted sample at 75°C for one hour. The optical density of each sample was read at 405 nm using the Molecular Devices Spectra Max Plus384 (Sunnyvale, CA). The concentration of CORT (ng/mL) was determined using the Softmax Pro microplate data software.

Aldosterone (ALDO) Analysis. ALDO was measured using an EIA kit (ENZO® Life Sciences; ADI-900-173). The optical density of each sample was read at 405 nm using the Molecular Devices Spectra Max Plus384. The concentration of aldosterone (pg/mL) was determined using the Softmax Pro microplate data software.

Statistical Analysis. Adrenal layer measurements, ALDO synthase immunoreactivity (Experiment 1), Ki67, ALDO level and CORT level data were analyzed for all time points using 2-way analysis of variance (ANOVA) for treatment, days of treatment and treatment \times days of treatment interactions with Bonferroni post-hoc tests. Data for ALDO synthase immunoreactivity for experiment 2 were analyzed for all ATR doses on each day using one-way ANOVA with Bonferroni post-hoc tests. Adrenal mRNA expression data were analyzed on day 4 of ATR treatment and compared to same day control animals using student's t-test. The level of statistical significance was set at $P \leq 0.05$. All values are reported as the mean \pm SEM. Prism 5 for Mac (GraphPad Software, Inc.) was used for all data analysis.

Results

Experiment 1. There was a significant treatment ($F_{3,91}=10.87$; $P<0.05$) effect on zG thickness, with ATR-treated animals having a significantly reduced layer compared to same day controls after 4 days but no other duration of treatment (**Figure 11A**). There was no significant treatment effect on zF thickness ($F_{1,91}=1.54$; $P=0.22$; **Figure 11B**), zR thickness ($F_{1,91}=0.85$; $P=0.36$; **Figure 11C**) or overall adrenal cortex thickness ($F_{1,91}=0.57$; $P=0.45$; **Figure 11D**). To control for adrenal size, we also examined the thickness of the zG relative to the total adrenal cortex thickness, and again saw a decrease in zG thickness following 4 days of treatment with 100 mg/kg/b.w. of ATR ($F_{1,91}=11.11$; $P<0.05$; **Figure 12A**). Aldosterone synthase immunoreactivity was significantly decreased following 2, 3 and 4 days of ATR treatment compared to control ($F_{1,55}=33.25$; $P<0.05$; **Figure 13**). There was no significant change in the average total number of cells in the zG ($F_{6,200}=2.01$; $P=0.07$; **Table 5**) or zF ($F_{1,91}=7.66$; $P<0.05$; **Table 5**) per ROI following ATR treatment, but there was a significant treatment effect on the total number of cells

in the zR ($F_{1,91}=10.21$; $P<0.05$; **Table 5**), with a decrease in the total number of cells after 4 days of treatment with 100 mg/kg/b.w. of ATR compared to control. There was a significant treatment effect ($F_{1,91}=6.24$; $P<0.05$), on relative right adrenal weight (**Figure 14A**), but not relative pituitary weight ($F_{3,91}=0.12$; $P=0.95$; **Figure 15A**). Adrenal weights were significantly increased above control following 2 days of treatment with 100 mg/kg/b.w. of ATR.

When examining adrenal steroidogenic enzyme expression, we also found a significant decrease in ALDO synthase expression after 4 days of ATR treatment ($t=7.43$; $DF=6$; $P<0.05$; **Figure 16A**), but there was no effect of ATR treatment on adrenal AT_1R expression ($t=2.10$; $DF=6$; $P=0.08$; **Figure 16B**) or 11β -hydroxylase ($t=1.21$; $DF=10$; $P=0.25$; **Figure 16C**) after 4 days of treatment.

Experiment 2. There was a significant reduction in zG thickness after 4 and 8 days of ATR treatment ($F_{3,268}=9.97$; $P<0.05$; **Figure 17A**). In animals treated for 4 days of ATR, both the 50 and 100 mg/kg/b.w. treated animals had reduced zG thickness when compared to controls. After 8 days of treatment, only the 100 mg/kg/b.w. ATR-treated animals displayed reduced zG thickness with no significant reduction in zG thickness after 14 days of treatment in any ATR treated groups. There was no significant effect of ATR on zF thickness ($F_{3,267}=1.06$; $P=0.37$; **Figure 17B**), zR thickness ($F_{3,267}=1.24$; $P=0.29$; **Figure 17C**) or overall adrenal cortex thickness ($F_{3,267}=0.94$; $P=0.42$; **Figure 17D**). After controlling for overall adrenal cortical thickness, we found a significant treatment effect on zG ($F_{3,266}=4.38$; $P<0.05$; **Figure 18A**) and zR ($F_{3,267}=3.43$; $P<0.05$; **Figure 18B**) thickness but no change in zF thickness. Aldosterone synthase immunoreactivity was reduced after 4 ($F_{3,27}=5.56$; $P<0.05$; **Figure 19**) and 8 ($F_{3,24}=5.19$; $P<0.05$;

Figure 19) days of 50 and 100 mg/kg/b.w. of ATR, and 14 days of 100 mg/kg/b.w. ($F_{3,27}=4.12$; $P<0.05$; **Figure 19**) of ATR compared to control. There was no significant change in the total number of cells in the zG ($F_{3,91}=0.20$; $P=0.89$; **Table 6**) or zF ($F_{3,91}=0.82$; $P=0.56$; **Table 6**), but similar to experiment 1, there was a significant treatment effect in the zR ($F_{3,200}=4.61$; $P<0.05$; **Table 6**). Also similar to experiment 1, there was a significant treatment ($F_{3,276}=6.89$; $P<0.05$) effect on relative adrenal weight (**Figure 14B**). There was a significant increase in adrenal weight following 4 and 8 days of 100 mg/kg/b.w. of ATR treatment. However, there was no significant change in relative pituitary weight ($F_{6,276}=1.87$; $P=0.09$; **Figure 15B**).

Experiment 3. There was a significant treatment of effect of ATR on zG thickness ($F_{2,16}=7.76$; $P<0.05$; **Figure 20A**). Zona glomerulosa thickness was reduced in the 100 mg/kg/b.w. ATR and restraint stress treated group compared to control group after 14 but not 4 days of treatment. There was no significant difference in adrenal cortical layer thickness for the zF ($F_{2,14}=0.19$; $P=0.83$; **Figure 20B**), zR ($F_{2,14}=2.85$; $P=0.09$; **Figure 20C**) or overall adrenal cortex ($F_{2,14}=0.62$; $P=0.55$; **Figure 20D**) thickness. After controlling for total adrenal cortex thickness, we still found a significant decrease in zG thickness ($F_{2,16}=7.81$; $P<0.05$; **Figure 21A**). However, neither zF or zR displayed any significant change in layer thickness. There was a significant decrease in aldosterone synthase immunoreactivity following 4 days of ATR treatment and restraint stress compared to control ($F_{2,10}=13.40$; $P<0.05$; **Figure 22**). There was no significant change in the number of Ki67 positive cells following ATR treatment or restraint stress compared to control in the zG ($F_{2,16}=0.37$; $P=0.7$; **Table 7**), outer zF ($F_{2,16}=1.48$; $P=.26$; **Table 7**), inner zF ($F_{2,14}=0.22$; $P=0.81$; **Table 7**) or zR ($F_{2,14}=0.78$; $P=0.48$; **Table 7**).

There was a significant treatment effect of ATR and restraint stress on CORT levels ($F_{2,24}=29.35$; $P<0.05$; **Figure 23A**). CORT levels for several control animals were below the detection threshold for our assay, therefore, CORT levels for these animals were set at assay detection. CORT levels in ATR were significantly elevated above control and restraint stress following 4 and 14 days of treatment with 100 mg/kg/b.w. of ATR. There was also a significant treatment ($F_{2,23}=14.84$; $P<0.05$; **Figure 23B**) effect of ATR and restraint stress on plasma ALDO levels. Furthermore, plasma ALDO levels were significantly higher in the 4 day ATR treatment group compared to the 14 day ATR treatment group ($t=3.966$; $DF=9$; $P<0.05$).

Discussion

In the current study, we have examined the effects of multiple doses and durations of ATR treatment as well as repeated restraint stress on adrenal gland morphology, enzymatic expression and immunoreactivity and circulating CORT and ALDO levels. ATR treatment led to changes in zG thickness, ALDO synthase expression immunoreactivity and adrenal hormone secretions, results which mimic the effects of repeated restraint stress. Our study reveals novel changes in adrenal gland morphology and enzymatic expression following ATR exposure as well as a potential ACTH-mediated mode of action by which ATR affects adrenal gland secretions and morphology.

ATR treatment led to a significant reduction in zG thickness following 4 and 8 days of 100 mg/kg/b.w. of ATR compared to control, with a continuing trend in reduction after 14 days of treatment. Furthermore, 50 mg/kg/b.w. also led to a significant reduction in zG thickness after 4 days of ATR treatment. Similarly, repeated restraint stress led to a reduction in zG thickness

following 14 days of treatment compared to control. Previous work has shown that chronic stress decreases the size of the zG and its cells [135, 178, 179], suggesting that ATR might lead to a reduction in zG thickness via a similar ACTH-mediated pathway as restraint stress.

Exogenous ACTH treatment has been shown to induce adrenal hypertrophy leading to an increase in adrenal weight [135]. Moreover, prolonged treatment with ACTH leads to an increase in adrenal weight, RNA and protein that is followed by an increase in DNA [180-183]. In the current study, we found an increase in adrenal weight following 2 days of treatment with 100 mg/kg of ATR, and a sustained increase in adrenal weight after 4 and 8 days of ATR treatment with adrenal weights returning closer to controls after 14 days. While we did not find an increase in the overall thickness of the adrenal cortex after ATR treatment, we did find a reduced number of total cells in the zR, suggesting possible hypertrophy at a cellular level. We also found a trend toward increased zR thickness, both overall thickness and the ratio of zR over total cortical thickness similar to that of restraint stressed animals compared to controls, which could be due to a zone-specific increase in cholesterol uptake. Ulrich-Lai et al. (2006) reported hypertrophy specific to the inner zones of the adrenal cortex following chronic stress [135], consistent with our findings. Furthermore, treatment with ACTH [184, 185] has been shown to increase cholesterol accumulation in adrenocortical mitochondria, which could be one reason for the observed increases in adrenal weight without an increase in overall cortical thickness following treatment with ATR. We measured adrenal medulla thickness and found no change following treatment with ATR in experiment 1 ($F_{1,91}=0.57$; $P=0.45$) or experiment 2 ($F_{3,267}=0.94$; $P=0.42$), which shows an increase in medullary thickness does not contribute to the observed increase in adrenal weight. Ulrich-Lai et al. (2006) also reports increased cell proliferation or hyperplasia,

marked by an increase in Ki67 positive cells, in the outer zones of the cortex. While we did not find a significant increase in the number of Ki67 positive cells following ATR treatment or restraint stress, we did find the majority of Ki67 positive cells in the outer zF and zG, indicating that any possible cell hyperplasia following ATR treatment could be due to an increase in ACTH stimulation. Additionally, the same study also reports reduced cell size in the zG after chronic stress. It is plausible this reduced cell size could lead to the overall reduction in zG thickness following ATR treatment or restraint stress.

Treatment with ATR and some of its metabolites has been shown to an increase ACTH, CORT and progesterone levels, and in the same studies, restraint stress also led to an similar increase in ACTH and CORT [96, 147]. The effects of restraint stress on the adrenal gland has been shown to mimic increased ACTH stimulation [186], suggesting that the ATR-induced increase in ACTH release could lead to the change in adrenal morphology present here. ACTH has been shown to inhibit ALDO synthase expression and inhibit zG regeneration in favor of zF cell proliferation and may cause zG cells to morph into a zF-like phenotype possessing 11 β -hydroxylase expression [136]. Immunohistochemical staining and cell number per ROI from the current study supports the hypothesis that increased ACTH levels following treatment with ATR or restraint stress is suppressing ALDO synthase and might cause a dedifferentiation of the zG cell phenotype into the zF cell phenotype, leading to an overall reduction in zG thickness with no change to overall cortical thickness.

As previously mentioned, ATR treatment has been shown to cause an increase in CORT secretion from the adrenal gland [96, 147]. In the current study, we show an increase in

circulating CORT levels following both 4 and 14 days of ATR treatment compared to control. Furthermore, ATR treatment also led to an increase in circulating ALDO levels after 4 and 14 days of treatment compared to control, with lower circulating ALDO levels after 14 days of ATR treatment compared to 4 days of ATR treatment. ACTH has been shown to stimulate ALDO production [187-190], but overtime, these effects are not sustained [134], suggesting that there might be a partial adaptation at the level of the adrenal gland following prolonged, elevated exposure to ATR and subsequently, ACTH. As mentioned earlier, we observed alterations in zG thickness and adrenal weight up to 8 days following ATR treatment with zG thickness and adrenal weight returning closer to control levels after 14 days of treatment, further suggesting a likely adaptation at the level of the adrenal gland due to increased ACTH stimulation following ATR treatment.

In the current study, we found that circulating CORT levels were not significantly different following 4 days of ATR treatment compared to 14 days of treatment, and circulating CORT levels were significantly higher in ATR-treated animals compared to restraint stress after both 4 and 14 days of treatment. Laws et al. (2009) showed that there is a significant attenuation of ACTH secretion following multiple doses of ATR while the CORT response remains unaffected after repeated exposure [147]. It is plausible that ATR treatment could lead to alterations in adrenal gland hormone secretions solely via an ACTH-mediated pathway, which is a likely cause of the attenuated response in ALDO secretion following prolonged exposure. However, the possibility does exist that ATR, in conjunction with the ATR-induced ACTH-mediated effects, could be mediating the lack of CORT habituation effects via a subsequent pathway either indirectly or directly at the level of the adrenal gland.

ATR treatment both in vivo and in vitro has been shown to induce cyclic adenosine monophosphate (cAMP) levels through inhibition of phosphodiesterase activity [105, 191, 192]. ATR or its metabolites might have the ability to potentiate ACTH stimulation through a pathway involving cAMP downstream of the ACTH receptor [193], leading to an increase in CORT and ALDO significantly higher compared to restraint stress animals and resulting in the lack of CORT attenuation over time when ACTH levels are shown to drop in the same animals [147]. Studies have shown that treatment with cAMP analogues preferentially increase 11 β -hydroxylase mRNA expression over ALDO synthase expression [138, 139], which could explain why CORT secretion remained high following 14 days of ATR treatment. ATR might be inducing increased cAMP levels through inhibition of phosphodiesterase activity, resulting in increased CORT levels following both short- and long-term ATR exposure. This, along with the atrophy of the zG due to increased ACTH release, could also explain why ALDO levels are elevated following short- but not long-term ATR exposure. Atrophy of the zG due to elevated ACTH precedes the drop in ALDO secretion following long-term ATR treatment, but the increased cAMP stimulation might still be potentiating the ACTH-induced ALDO secretion at levels significantly higher than those observed after restraint-stress. It is difficult to discern the exact reason for the hormonal response difference between two vastly different experimental treatments as ATR and restraint stress, however, if ATR treatment results in increased cAMP due to phosphodiesterase inhibition then the same ACTH treatment would be potentiated in ATR-treated animals over levels seen in restraint stress treated animals. This theory needs to be investigated further.

In the rat, the localized production of CORT and ALDO can be attributed to the differential expression of two distinct genes, CYP11B1 and CYP11B2 [124, 125]. The CYP11B1 gene codes for the 11 β -hydroxylase enzyme and is found in the zF and zR. This enzyme is the primary enzyme involved in the production of CORT in both the zF and zR in the rat. ACTH treatment has been shown to differentially regulate the expression of 11 β -hydroxylase and ALDO synthase, therefore, we wanted to examine the effects of ATR exposure on the expression of ALDO synthase and 11 β -hydroxylase. Four days of ATR (100 mg/kg) treatment led to a decrease in expression of ALDO synthase compared to control, indicating the changes in ALDO synthase immunoreactivity could in part be due to a decrease in ALDO synthase mRNA levels. Again, similar findings have been reported in animals following long-term stimulation of high levels of ACTH [134]. Furthermore, restraint stress has also been shown to alter the expression of ALDO synthase [194], indicating that increased ACTH might be the mediator by which ATR leads to a reduction in ALDO synthase expression and immunoreactivity. The possibility also exists that the induction of 11 β -hydroxylase for production of CORT by ACTH following ATR treatment could also decrease ALDO synthase expression by removing precursors from the pathway leading to ALDO production [137].

We found no change in expression of 11 β -hydroxylase following 4 days of ATR treatment, but this was not surprising due to the number of conflicting studies addressing this topic. There is evidence that ACTH stimulation increases the expression of 11 β -hydroxylase after repeated exposure [195], but other studies have shown that repeated ACTH treatment does not alter 11 β -hydroxylase expression or activity [196]. Aguilera et al. (1996) showed that chronic stress and ACTH administration alter the levels of CORT without a change in 11 β -hydroxylase levels

[186], suggesting ATR and restraint stress might also mediate an increase in CORT levels independent of a change in 11 β -hydroxylase expression regulation.

We also examined the expression of AT₁R, the primary angiotensin II (Ang II) receptor found in the zG, and the key receptor involved in the binding of Ang II and stimulation of ALDO secretion [130]. Although we found no change in the expression of AT₁R, previous studies have also shown that treatment with ACTH does not alter total AT₁R mRNA [197]. Furthermore, restraint stress differentially regulates the two AT₁R subtypes, AT₁R_A and AT₁R_B [198], with an increase in AT₁R_A expression and a decrease in AT₁R_B expression following restraint stress. Primers used in the current study would have picked up both AT₁R_A and AT₁R_B, which suggests the differential regulation of the AT₁R subtypes could explain why, although we found a reduction in the thickness of the zG, we did not see a change in AT₁R expression. Additionally, although AT₁R have their highest expression the zG they are located in the zF/zR [131], and due to the fact we found no change in overall cortical thickness following ATR treatment, we might not have been able to detect a change in expression. However, this does not rule out the possibility that ATR treatment might differentially regulate AT₁R expression in a region-specific manner, and future studies could examine this possibility by separating the zG and zF/zR specific mRNA pools.

The mechanism through which ACTH inhibits the expression of ALDO synthase is still unclear [137]. In the presence of normal ACTH stimulation, the zG is able to maintain normal ALDO synthase expression by controlling intracellular levels of cAMP. In isolated zG cells, Ang II will inhibit ACTH-stimulated cAMP production [142, 143], and secondly, the zG, but not zF,

expresses adenylyl cyclases types 5 and 6, which are both inhibited by intracellular calcium, the second messenger involved in signaling from Ang II and potassium [144]. In the case of increased ACTH due to ATR treatment, ACTH might be causing an increase in intracellular cAMP alongside an ATR-induced increase in cAMP independent of ACTH stimulation, which might drive down the expression of ALDO synthase and cause hypotrophy of zG at the same time it is setting up the layers to respond more robust following the ACTH spike after ATR treatment. Furthermore, this decrease in ALDO synthase expression and immunoreactivity is a probable indication of decreased Ang II stimulation as well. Indeed, Aguilera et al. (1995) has shown that in isolated zG cells from chronically stressed rats, maximum ALDO responses to Ang II was significantly reduced, potentially due to a decreased binding of Ang II [194]. Moreover, the possible decrease in Ang II stimulation following ATR treatment might amplify the ATR-induced ACTH-mediated effects observed at the level of the adrenal. Further studies are needed to examine the possible physiological effects of ATR exposure on Ang II binding and the responsiveness of zG cells to Ang II stimulation following ATR treatment. Considering ATR exposure has been shown to significantly increase the elimination of sodium and chloride in rats [199] as well as correlate with increased urinary sodium in people with occupational exposure to ATR [200], it was prudent to investigate whether the changes described here result in physiological changes.

Further work is needed to determine the exact mechanism by which ATR, and therefore ACTH, leads to morphological changes in the adrenal gland. More importantly, more work is needed to determine if the pronounced changes in zG thickness and ALDO synthase expression/protein levels will result in physiological changes *in vivo*. Animals could be treated with vehicle or ATR

via gavage for the 4 days, as we have established, that is required for zG morphological and enzymatic changes, then treated with dexamethasone to block endogenous ACTH. The animals could then be challenged with a high-dose of Ang II to stimulate maximal ALDO steroidogenesis and secretion. We predict that ATR-treated animals will have lower ALDO levels than controls due to reduced ALDO synthase availability and zG size.

An alternate, but no less pertinent study would be to test the before mentioned theory that ATR treatment results in an inhibition of phosphodiesterase activity in the adrenal gland. Therefore, we predict that animals treated with a single dose of ATR will respond more robustly when stimulated by exogenous Ang II or ACTH than vehicle treated animals. If our theory is correct, ATR treatment would result in reduced phosphodiesterase activity, and therefore, when stimulated, adrenal cells would respond to a greater extent because cAMP levels would rise higher and longer unchecked by phosphodiesterase. Phosphodiesterase activity and cAMP levels would need to be measured in adrenal tissue to corroborate this theory.

In the present study, we have characterized changes in adrenal gland morphology, steroidogenesis and enzymatic expression following treatment with multiple doses (6.5, 50 and 100 mg/kg/b.w.) and durations (1, 2, 3, 4, 8 and 14 days) of ATR treatment. In all measures examined following 4 and 14 days of restraint stress, the effects of ATR treatment mimicked those of restraint stress when compared to control. It appears that an increase in ACTH secretion from the pituitary following ATR treatment might, at least partially, lead to the effects seen at the level of the adrenal gland. However, more research is needed to elucidate the mechanism by which ATR causes an increase in ACTH secretion, and whether ATR acts solely via an ACTH-

mediated response or multiple pathways either indirectly or directly at the level of the adrenal gland. It will also important to determine if the changes seen at the level of the adrenal gland affect overall functionality following ATR treatment.

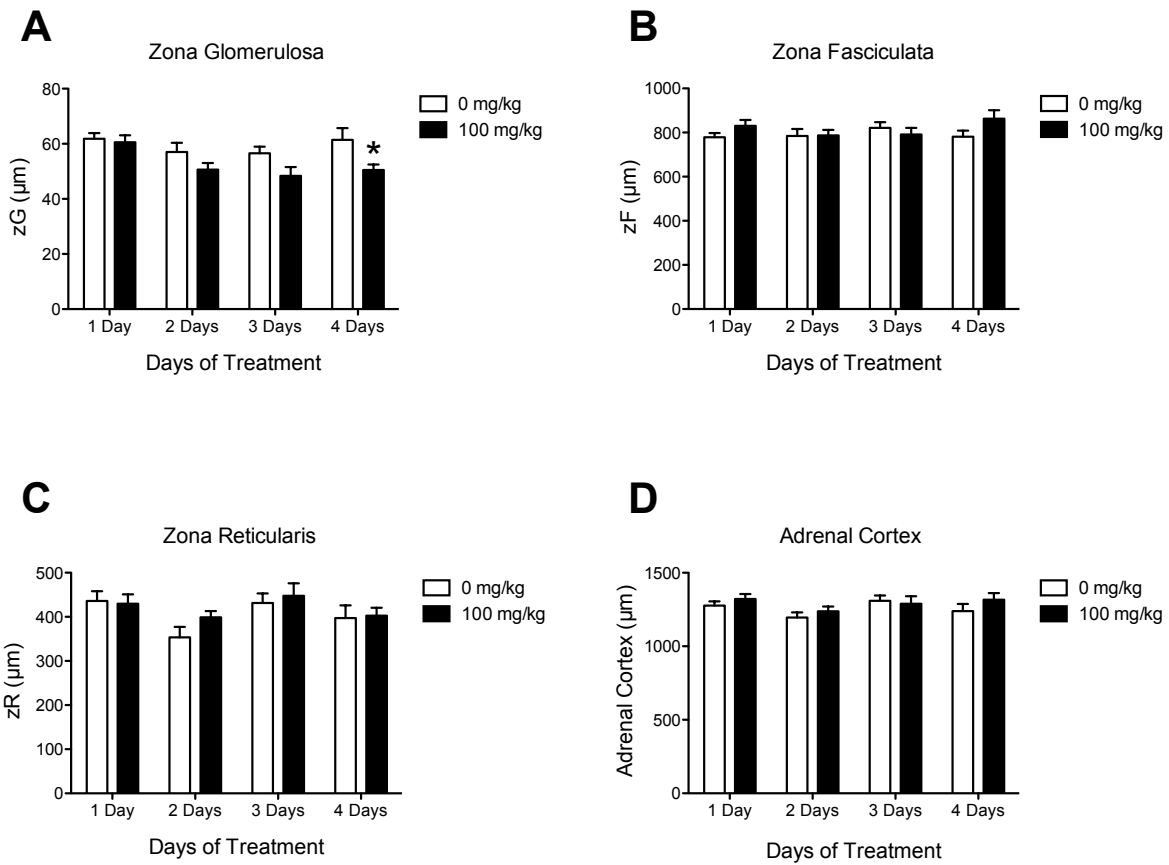


Figure 11: Individual adrenal cortical layer and overall cortical thickness following 1, 2, 3 and 4 days of 100 mg/kg of ATR. Histograms depicting zona glomerulosa (A), zona fasciculata (B), zona reticularis (C) and overall adrenal cortical thickness (D) in µm following 1, 2, 3 and 4 days of ATR treatment (100 mg/kg/b.w.) or control (0 mg/kg). Data are presented as mean ± SEM for all animals for all groups; Significant difference ($P < 0.05$; * = compared to control (0 mg/kg/b.w.)).

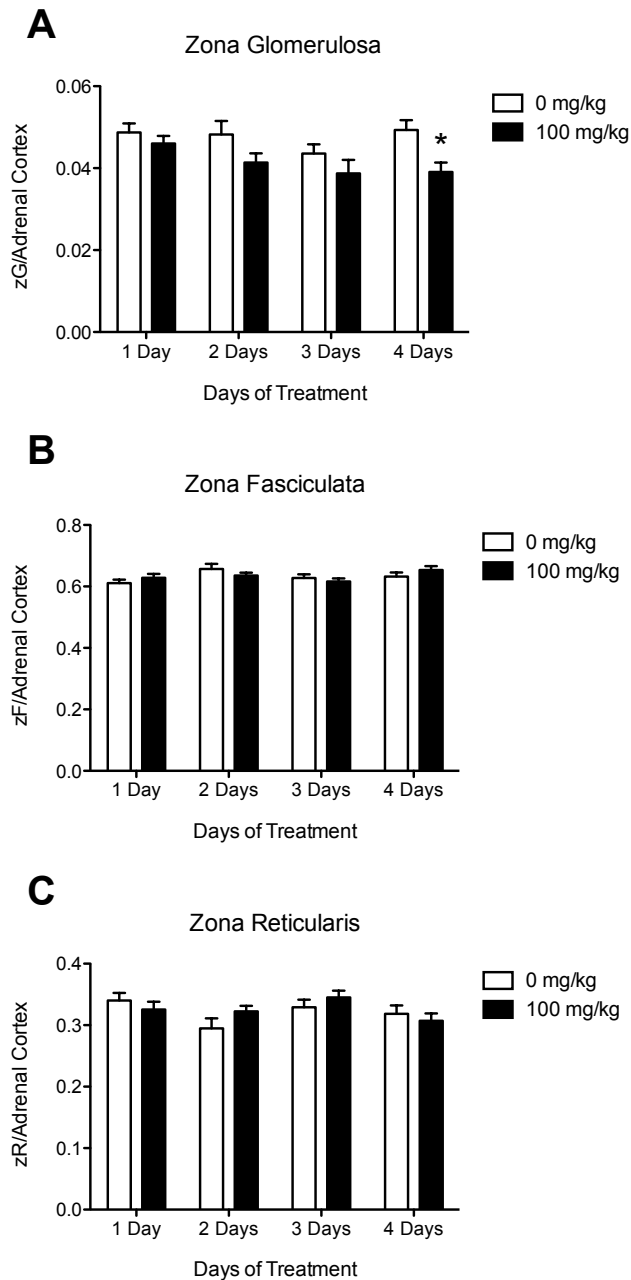


Figure 12: Individual adrenal cortical layer thickness relative to body weight following 1, 2, 3 and 4 days of 100 mg/kg of ATR. Histograms depicting zona glomerulosa (A), zona fasciculata (B) and zona reticularis (C) thickness relative to total adrenal cortex thickness following 1, 2, 3 and 4 days of ATR treatment (100 mg/kg/b.w.) or control (0 mg/kg). Data are presented as mean \pm SEM for all animals for all groups; Significant difference ($P < 0.05$; * = compared to control (0 mg/kg/b.w.)).

Aldosterone Synthase Immunoreactivity

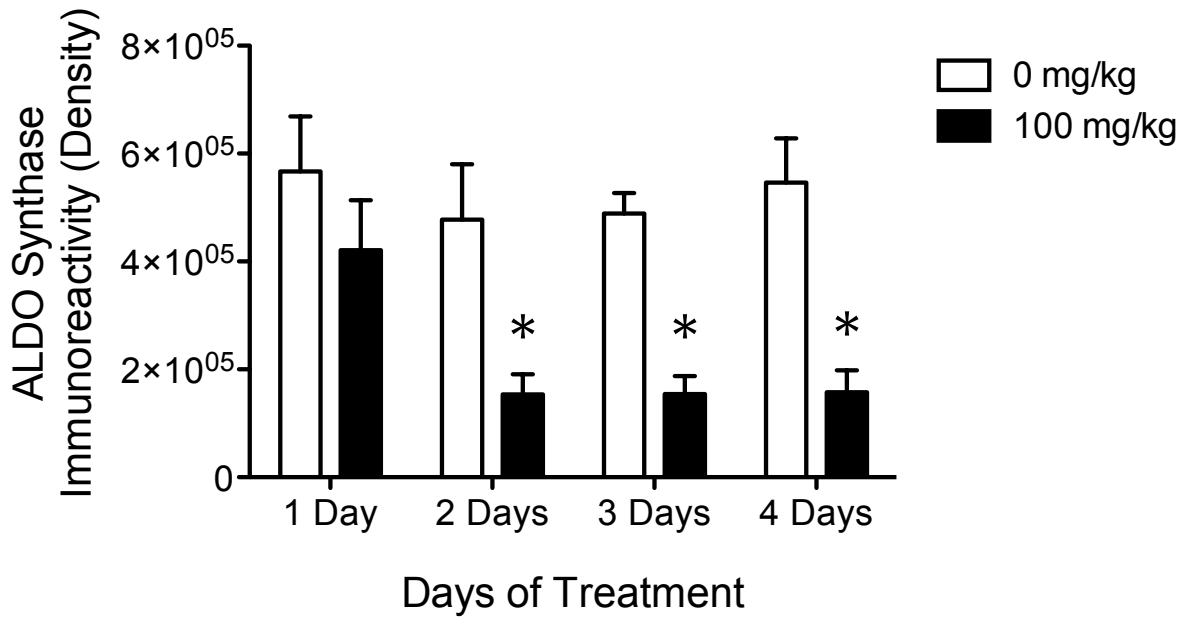


Figure 13: Aldosterone synthase immunoreactivity following 1, 2, 3 and 4 days of 100 mg/kg of ATR. Histograms depicting aldosterone synthase immunoreactivity as total pixel density per ROI following 1, 2, 3 and 4 days of ATR treatment (100 mg/kg/b.w.) or control (0 mg/kg). Data are presented as mean \pm SEM for all animals for all groups; Significant difference ($P < 0.05$; * = compared to control (0 mg/kg/b.w.)).

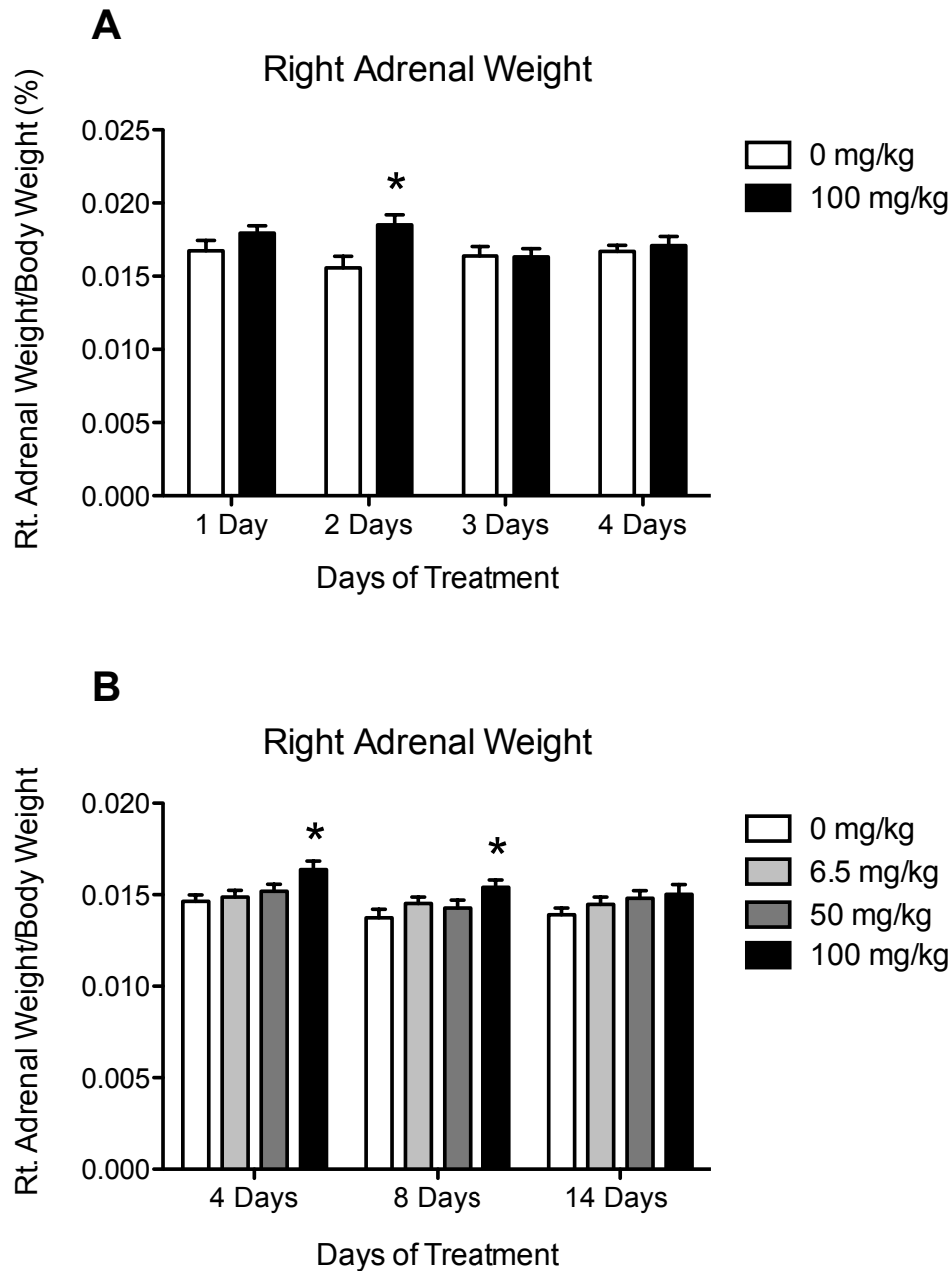


Figure 14: Percent right adrenal weight relative to total body weight following 1, 2, 3 and 4 days of 100 mg/kg of ATR or 4, 8 and 14 days of 6.5, 50 or 100 mg/kg of ATR. Histogram depicting right adrenal weight presented as percent right adrenal weight relative to total body weight following 1, 2, 3 and 4 days of ATR treatment (100 mg/kg/b.w.) or control (0 mg/kg) (A) or 4, 8 and 14 days of ATR treatment (6.5, 50 or 100 mg/kg/b.w.) or control (0 mg/kg) (B). Data are presented as mean \pm SEM; ($P < 0.05$; * = compared to control (0mg/kg/b.w.)).

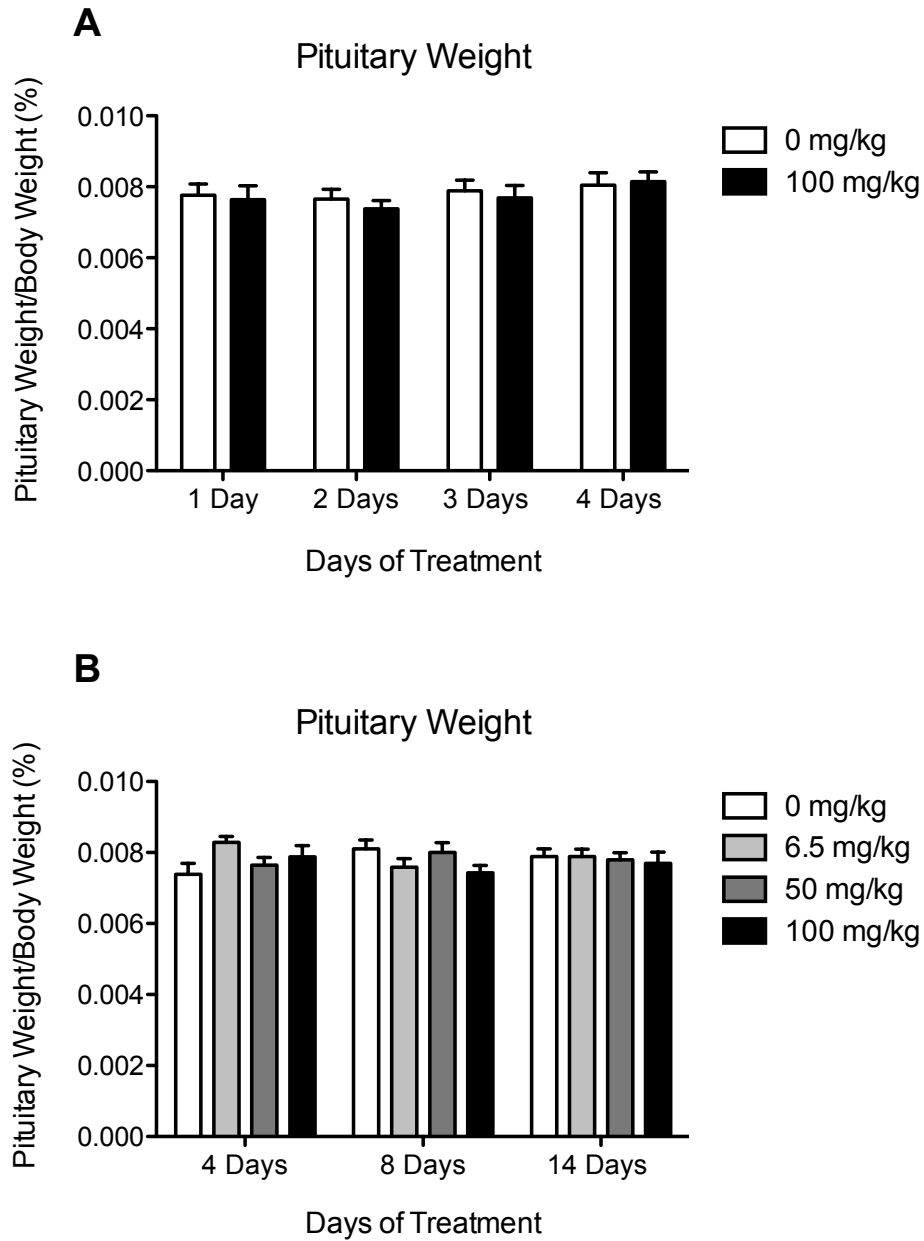


Figure 15: Percent pituitary weight relative to total body weight following 1, 2, 3 and 4 days of 100 mg/kg of ATR or 4, 8 and 14 days of 6.5, 50 or 100 mg/kg of ATR. Histogram depicting pituitary weight presented as percent pituitary weight relative to total body weight following 1, 2, 3 and 4 days of ATR treatment (100 mg/kg/b.w.) or control (0 mg/kg) (A) or 4, 8 and 14 days of ATR treatment (6.5, 50 or 100 mg/kg/b.w.) or control (0 mg/kg) (B). Data are presented as mean \pm SEM; ($P < 0.05$; * = compared to control (0mg/kg/b.w.)).

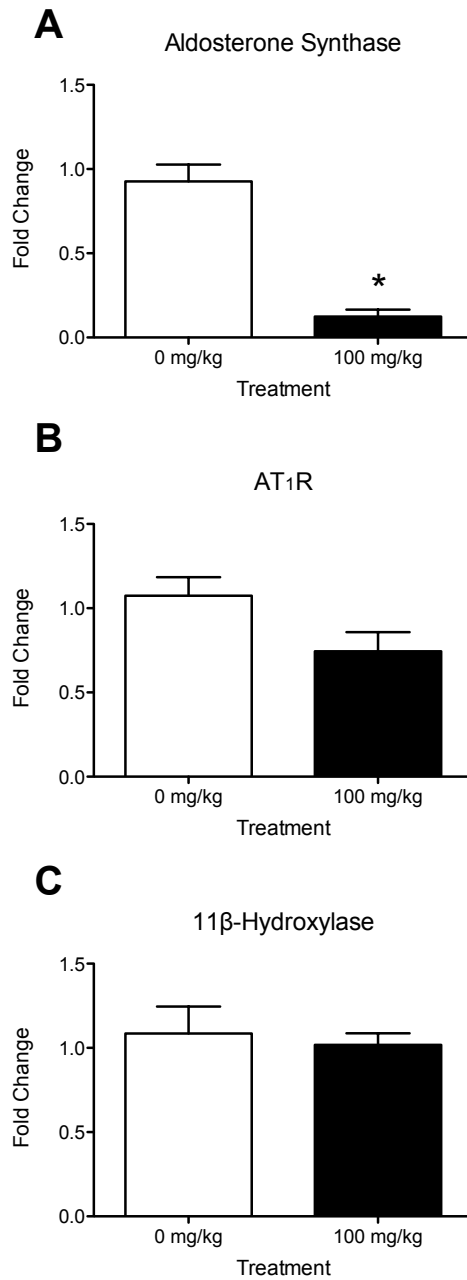


Figure 16: Adrenal mRNA expression levels for aldosterone synthase, 11 β -hydroxylase and AT₁R following 4 days of 100 mg/kg of ATR. Histograms depicting fold change in mRNA expression for aldosterone synthase following 4 days of 100 mg/kg/b.w. ATR treatment (**A**), AT₁R following 4 days of 100 mg/kg/b.w. ATR treatment (**B**) and 11 β -hydroxylase following 4 days of 100 mg/kg/b.w. ATR treatment (**C**) for 4-6 animals per group. Data are presented as mean \pm SEM; Significant difference ($P < 0.05$; * = compared to control (0 mg/kg/b.w.)).

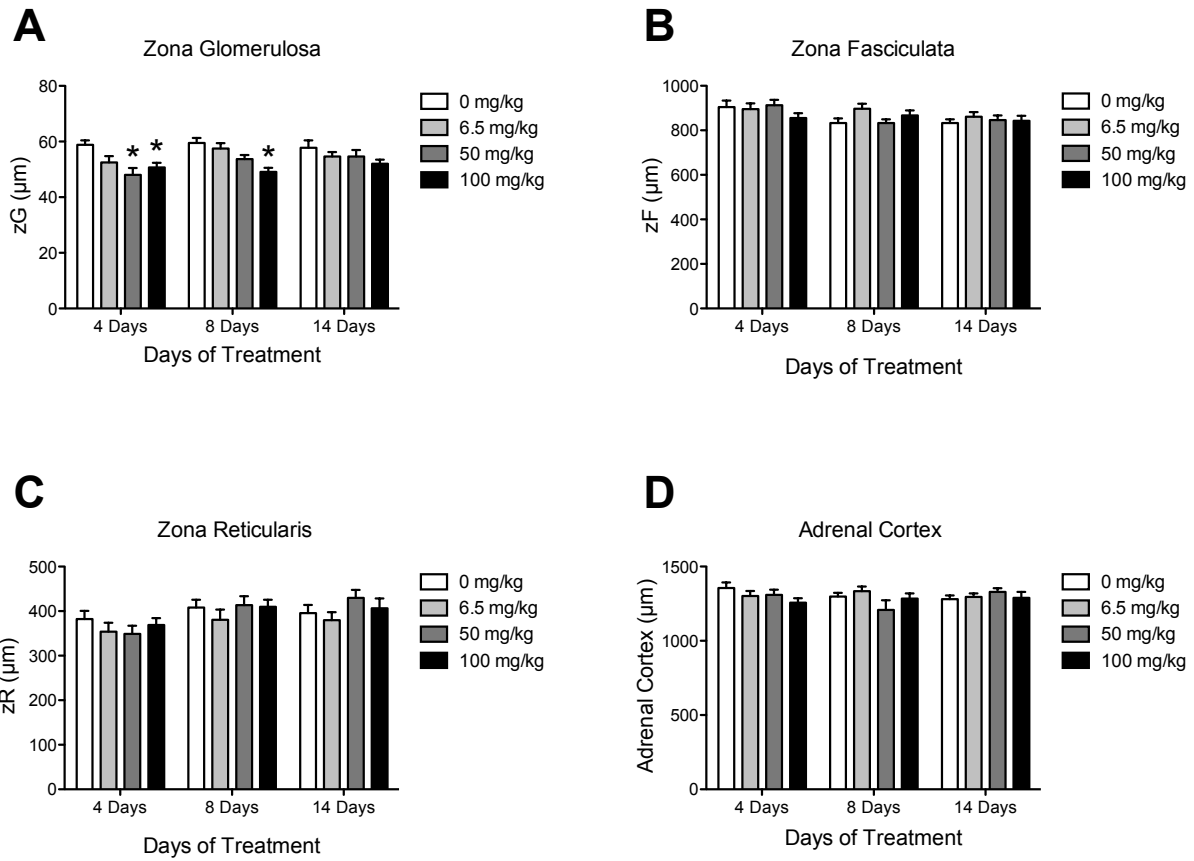


Figure 17: Individual adrenal cortical layer and overall cortical thickness following 4, 8 and 14 days of 6.5, 50 or 100 mg/kg of ATR. Histograms depicting zona glomerulosa (A), zona fasciculata (B), zona reticularis (C) and overall adrenal cortical thickness (D) in μm following 4, 8 and 14 days of ATR treatment (6.5, 50 or 100 mg/kg/b.w.) or control (0 mg/kg). Data are presented as mean \pm SEM for all animals for all groups; Significant difference ($P < 0.05$; * = compared to control (0 mg/kg/b.w.)).

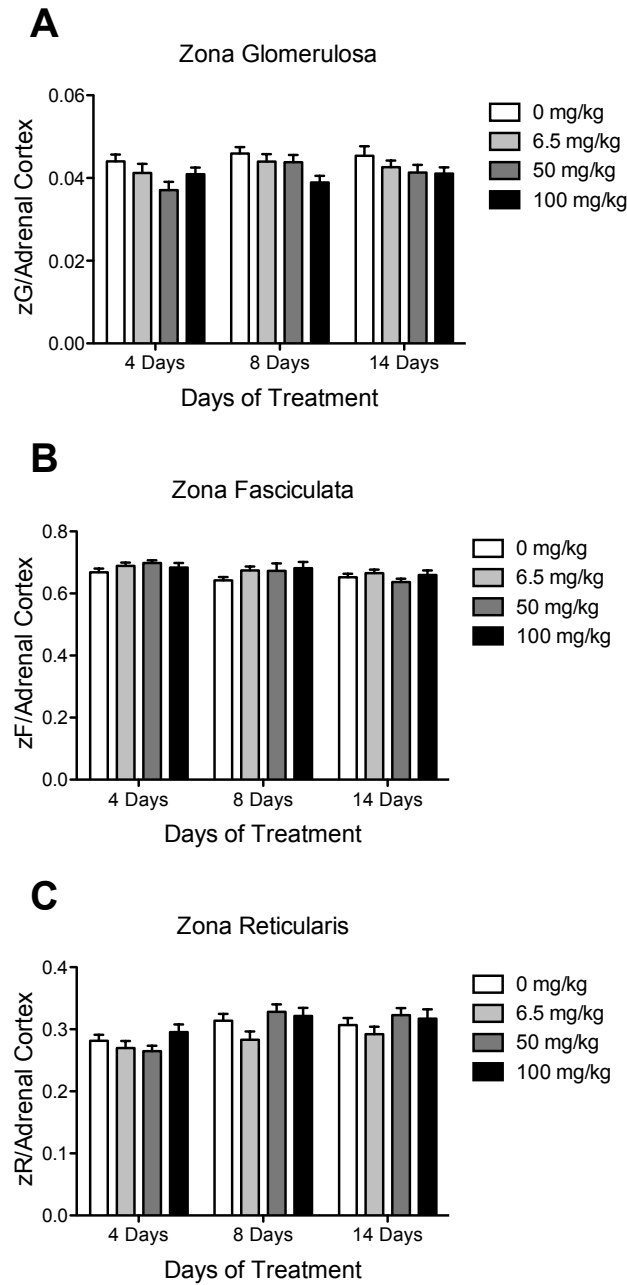


Figure 18: Individual adrenal cortical layer thickness relative to body weight following 4, 8 and 14 days of 6.5, 50 or 100 mg/kg of ATR. Histograms depicting zona glomerulosa (A), zona fasciculata (B) and zona reticularis (C) thickness relative to total adrenal cortex thickness following 4, 8 and 14 days of ATR treatment (6.5, 50 or 100 mg/kg/b.w.) or control (0 mg/kg). Data are presented as mean \pm SEM for all animals for all groups; Significant difference ($P < 0.05$; * = compared to control (0 mg/kg/b.w.)).

Aldosterone Synthase Immunoreactivity

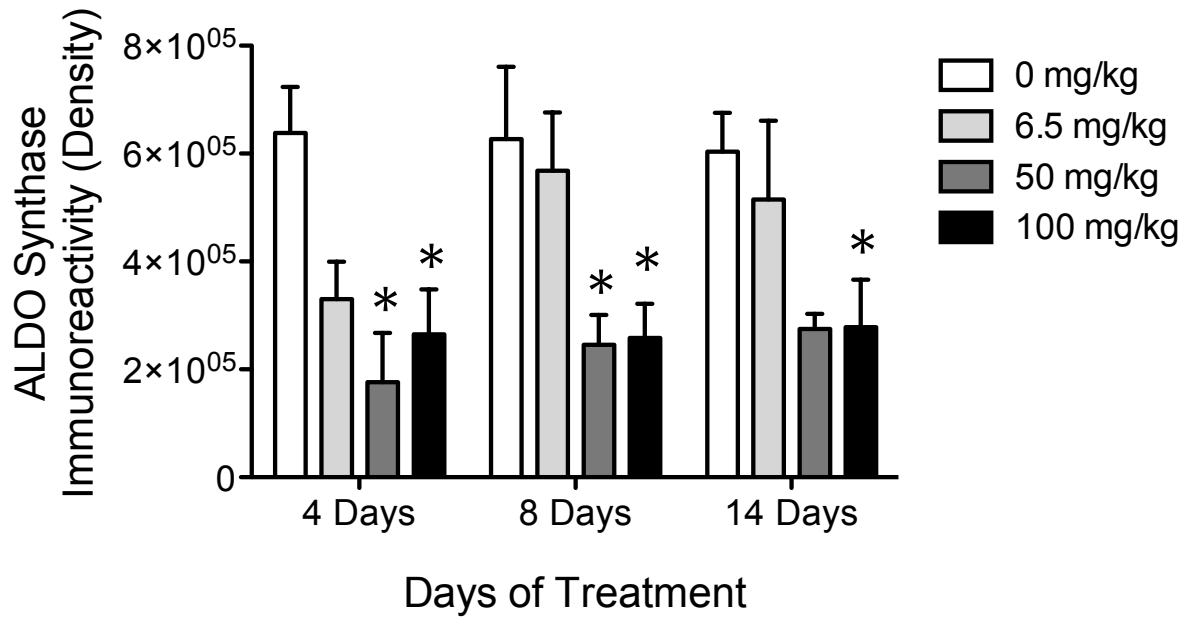


Figure 19: Aldosterone synthase immunoreactivity following 4, 8 and 14 days of 6.5, 50 or 100 mg/kg of ATR. Histograms depicting aldosterone synthase immunoreactivity as total pixel density per ROI following 4, 8 and 14 days of ATR treatment (6.5, 50 or 100 mg/kg/b.w.) or control (0 mg/kg). Data are presented as mean \pm SEM for all animals for all groups; Significant difference ($P < 0.05$; * = compared to control (0 mg/kg/b.w.)).

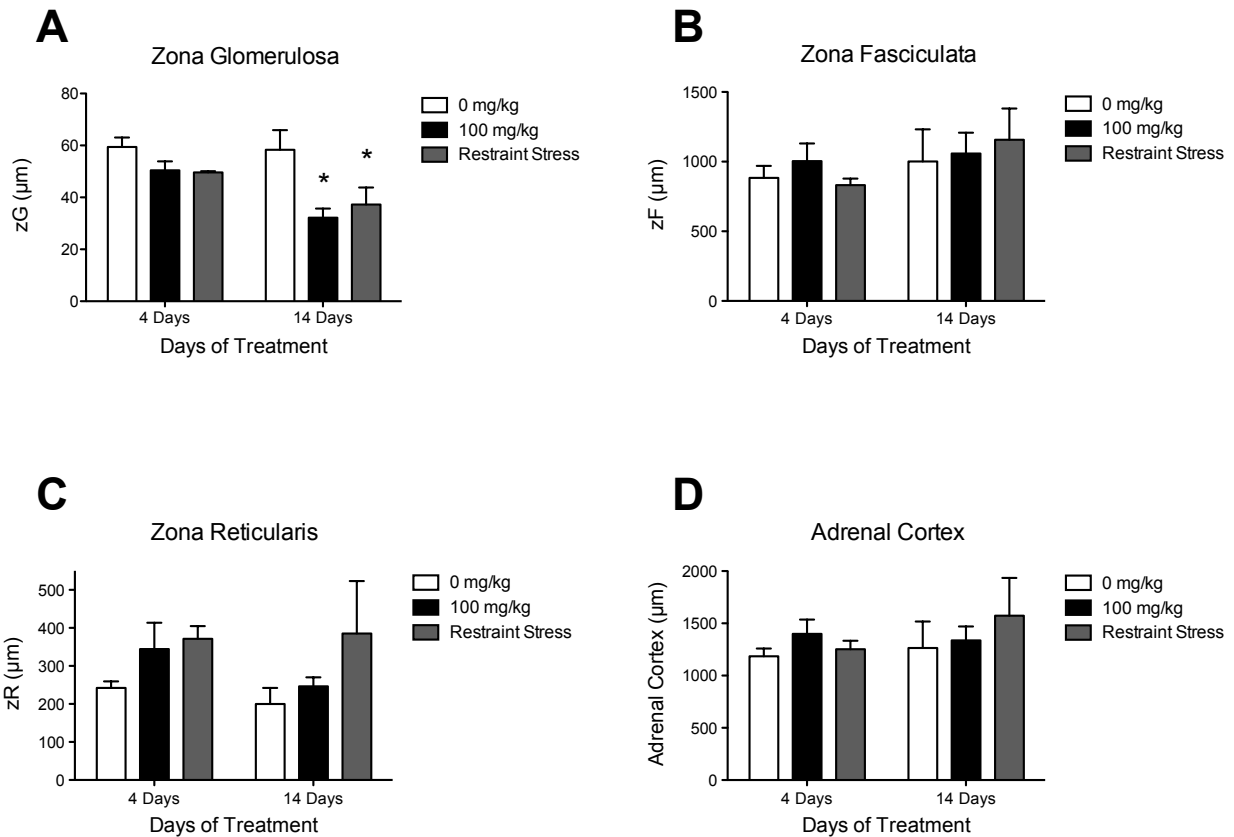


Figure 20: Individual adrenal cortical layer and overall cortical thickness following 4 and 14 days of 100 mg/kg of ATR or restraint stress. Histograms depicting zona glomerulosa (A), zona fasciculata (B), zona reticularis (C) and overall adrenal cortical thickness (D) in μm following 4 and 14 days of ATR treatment (100 mg/kg/b.w.), restraint stress or control (0 mg/kg). Data are presented as mean \pm SEM for all animals for all groups; Significant difference ($P < 0.05$; * = compared to control (0 mg/kg/b.w.)).

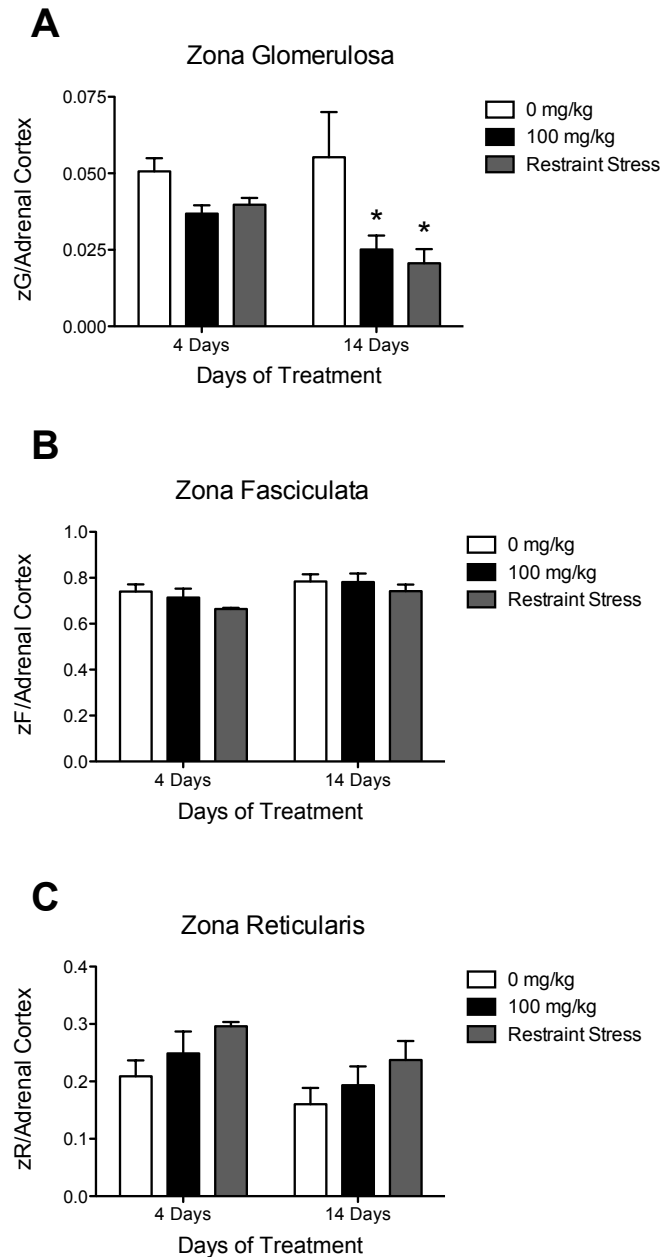


Figure 21: Individual adrenal cortical layer thickness relative to body weight following 4 and 14 days of 100 mg/kg of ATR or restraint stress. Histograms depicting zona glomerulosa (A), zona fasciculata (B) and zona reticularis (C) thickness relative to total adrenal cortex thickness following 4 and 14 days of ATR treatment (100 mg/kg/b.w.), restraint stress or control (0 mg/kg). Data are presented as mean \pm SEM for all animals for all groups; Significant difference ($P < 0.05$; * = compared to control (0 mg/kg/b.w.)).

Aldosterone Synthase Immunoreactivity

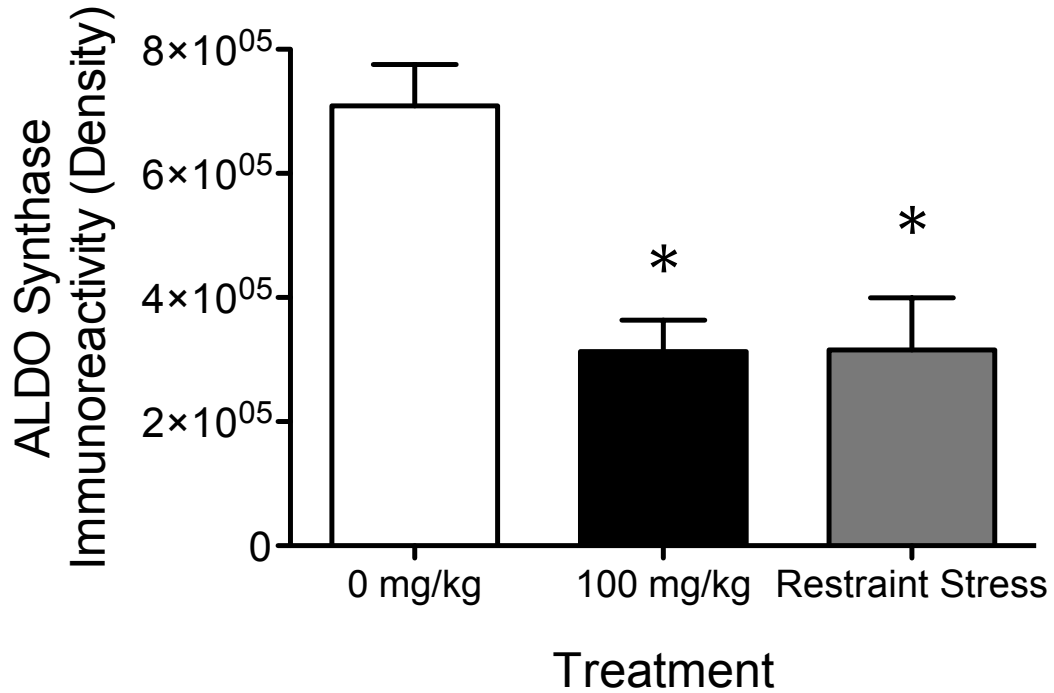


Figure 22: Aldosterone synthase immunoreactivity following 4 days of 100 mg/kg of ATR or restraint stress. Histograms depicting aldosterone synthase immunoreactivity as total pixel density per ROI following 4 days of ATR treatment (100 mg/kg/b.w.), restraint stress or control (0 mg/kg). Data are presented as mean \pm SEM for all animals for all groups; Significant difference ($P < 0.05$; * = compared to control (0 mg/kg/b.w.)).

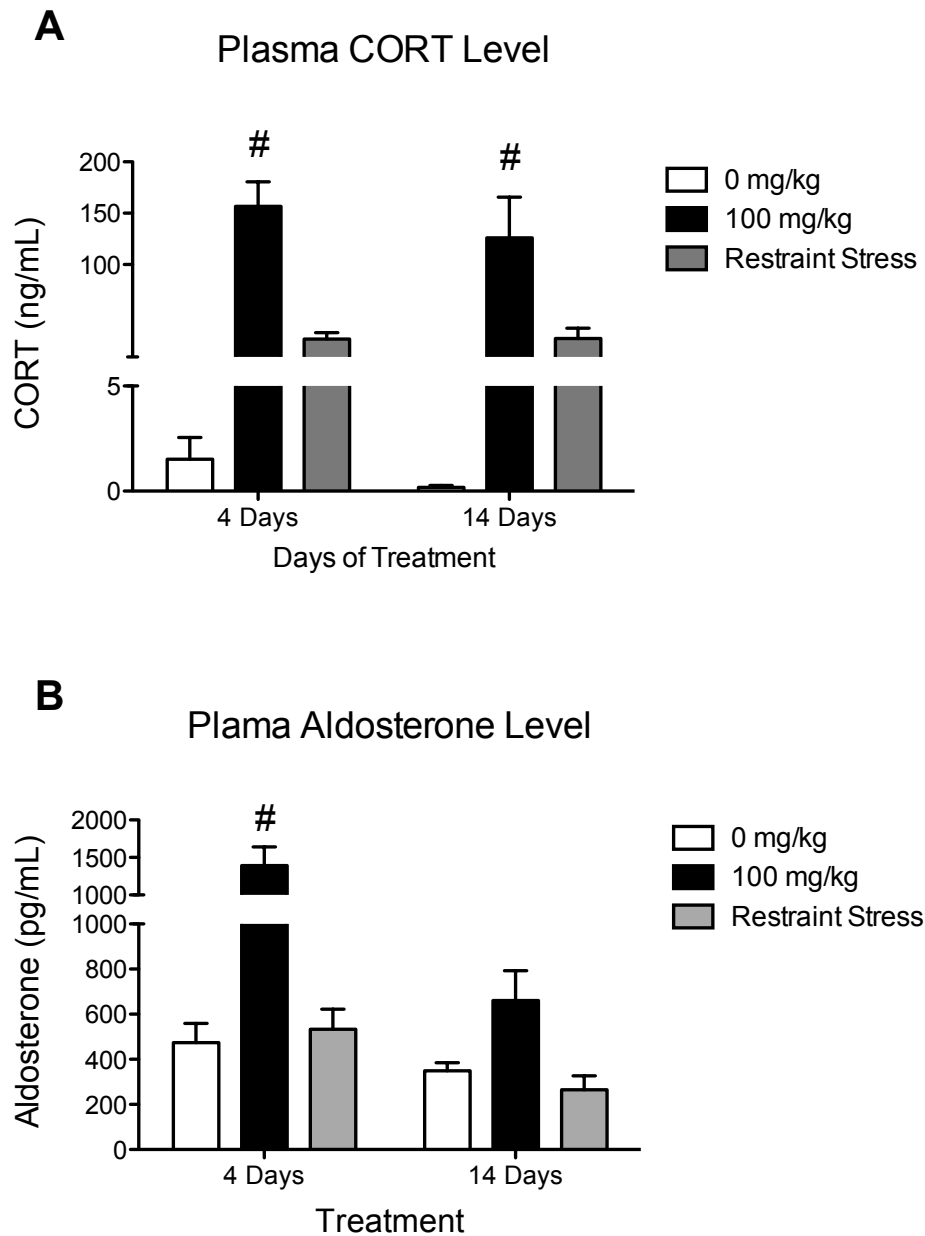


Figure 23: Plasma CORT and aldosterone levels following 4 and 14 days of 100 mg/kg of ATR or restraint stress. Histogram depicting plasma CORT (**A**) and aldosterone (**B**) levels following 4 and 14 days of ATR treatment (100 mg/kg/b.w.), restraint stress or control (0 mg/kg). Data are presented as mean \pm SEM; ($P < 0.05$; * = compared to control (0mg/kg/b.w.); # = compared to control (0 mg/kg/b.w.) and restraint stress).

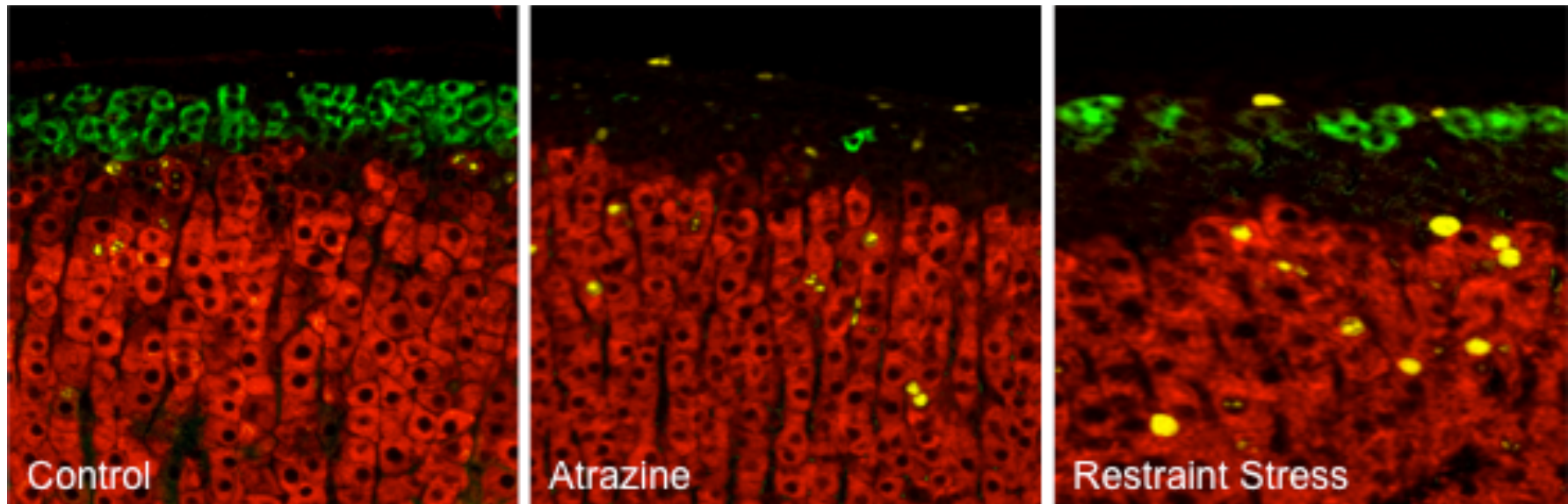


Figure 24: Fluorescent immunohistochemical staining following 4 days of 100 mg/kg or ATR or restraint stress. Fluorescent immunohistochemical staining following 4 days treatment for control (A), 100 mg/kg/b.w. ATR-treated (B) and restraint stress (C) animals. Aldosterone synthase (CYP11B2) is the marker for the zona glomerulosa and is stained green. 11 β -hydroxylase (CYP11B1) is the marker for the zona fasciculata and is stained red. Ki67 positive cells are stained yellow and are proliferating cells.

Average Total Number of Cells per ROI

Adrenal Layer	1 Day Treatment		2 Day Treatment		3 Day Treatment		4 Day Treatment	
	Control	Atrazine	Control	Atrazine	Control	Atrazine	Control	Atrazine
zG	42.13	41.24	41.77	41.02	42.77	43.16	43.73	42.67
zF	11.87	10.82	11.63	10.78	12.93	11.62	12.43	11.86
zR	24.14	23.00	22.53	21.42	25.17	23.09	24.40	20.69 *

Control = 0 mg/kg; Atrazine = 100 mg/kg

2-way ANOVA with Bonferroni post-hoc (* = $p < 0.05$)

Table 5: Average total number of cells per region of interest (ROI) in each adrenal cortical layer following 1, 2, 3 and 4 days of 100 mg/kg of ATR.

Average Total Number of Cells per ROI

Adrenal Layer	4 Day Treatment (mg/kg)				8 Day Treatment (mg/kg)				14 Day Treatment (mg/kg)			
	0	6.5	50	100	0	6.5	50	100	0	6.5	50	100
zG	42.33	44.77	44.76	44.94	45.67	44.43	43.63	43.57	46.88	45.50	43.60	46.03
zF	11.55	11.75	11.51	11.29	10.92	10.83	10.50	10.52	12.10	11.16	10.91	11.71
zR	24.78	23.73	23.94	22.43	24.86	21.85	23.26	21.54	25.29	24.73	22.05	23.44

2-way ANOVA with Bonferroni post-hoc (* = $p < 0.05$)

Table 6: Average total number of cells per region of interest (ROI) in each adrenal cortical layer following 4, 8, and 14 days of 6.5, 50 or 100 mg/kg of ATR.

Total Number of Ki67 Positive Cells per ROI

Adrenal Layer	4 Day Treatment			14 Day Treatment		
	Control	Atrazine	Stress	Control	Atrazine	Stress
zG	2.25	4.40	1.00	4.75	4.50	3.70
zF outer	6.75	11.60	5.50	3.00	3.50	3.00
zF inner	0.75	0.40	0.00	1.00	0.75	1.00
zR	2.25	0.40	1.50	1.70	2.00	1.00

Control = 0 mg/kg; Atrazine = 100 mg/kg; Stress = 30 minute restraint stress
 2-way ANOVA with Bonferroni post-hoc (* = $p < 0.05$)

Table 7: Total number of Ki67 positive cells per region of interest (ROI) in each adrenal cortical layer following 4 and 14 days of 100 mg/kg of ATR or restraint stress.

Chapter VI

Conclusions

With a rapidly growing population of Roundup resistant weeds across the country, ATR has quickly become one of the most commonly used herbicide in the United States. Due to its long half-life, ATR is commonly found in drinking water, and applicators, farmers and their families commonly have high levels of ATR and its metabolites in their saliva and urine. ATR has been shown to have widespread physiological effects in many mammalian species including humans, but the most common effect of ATR exposure is on reproduction. ATR has been shown to disrupt the reproductive cycle, delay the onset of puberty and increase infertility. Thus, because of its widespread use and recognized deleterious physiological effects, it is important to understand the mechanism by which ATR mediates its effects.

Recent evidence suggests the reproductive effects following ATR exposure might be mediated by ATR's disruption of normal LH pulsatility as well as its inhibition of the hormone-induced LH surge; however, these effects are transient. Following repeated exposure, ATR's inhibition of the hormone-induced LH surge is attenuated, which suggests there might be an upregulation in the metabolism of ATR or a possible adaptation or habituation after long-term exposure. Studies have shown that both phase I and phase II hepatic xenobiotic metabolism components are involved in the metabolism of ATR, but these studies were limited in scope and the regulation of these components had not been thoroughly examined after repeated exposure to ATR. Therefore,

we examined the effects of both short- and long-term ATR treatment on the expression, protein levels and activity of hepatic GST phase II xenobiotic metabolism components in the rat. In addition, we investigated the effects of ATR exposure on the expression of most known rat CYP enzymes.

We validated some previous findings but also identified possible novel players in both the short- and long-term metabolism of ATR in the rat. We reported novel findings that long-term ATR exposure differentially regulates the expression of several CYP and GST isoforms as well as GST-mediated metabolism components. Prolonged exposure to ATR leads to variations in the expression of hepatic phase I CYP and phase II GST enzymes compared to shorter-term ATR treatment, which could be due to possible liver habituation or adaptation. Further research is required to elucidate the exact role of many of the isoforms of CYP and GST that have been previously unexamined following ATR exposure. More research is also needed to elucidate the potential adaptation or habituation in the liver following ATR exposure.

Recent evidence suggests that ATR's effects on GnRH/LH release might be mediated by increased CORT secretions following ATR exposure. Alterations in the release of glucocorticoids and P disrupt both LH and GnRH secretions, and ATR has been shown to increase ACTH release from the pituitary, and subsequently, CORT and adrenal-derived P. Furthermore, subacute ATR treatment in rats increases sodium and chloride urine excretion, suggesting a possible disruption in the regulation and secretion of ALDO from the adrenal gland. However, the effects of ATR on the adrenal gland and the method by which ATR exposure leads to alterations in adrenal gland hormone secretions had not been previously examined. Therefore,

we investigated the effects of ATR treatment on adrenal gland morphology, enzymatic immunoreactivity, enzyme mRNA expression levels and CORT and ALDO secretion. In addition, we examined the effects of restraint stress on the adrenal gland in order to elucidate ATR's potential mode of action.

We found that in all measures examined, the effects of ATR treatment mimicked those of restraint stress when compared to control. ATR treatment and restraint stress led to increased CORT secretions, atrophy of the zG and reduced ALDO synthase immunoreactivity, suggesting ATR induces its effects at the level of the adrenal gland through an ACTH-mediated response similar to restraint stress. Interestingly, ATR treatment led to a significantly higher levels of CORT and ALDO compared to restraint stress, which suggests ATR might be mediating its effects on CORT and ALDO secretions via an additional mechanism. ATR has been shown to inhibit phosphodiesterase activity, leading to an increase in cAMP levels, which could potentiate the ACTH response, causing a more robust increase in CORT secretions. Furthermore, ALDO levels were significantly higher following 4 days of ATR treatment compared to 14 days, which might be due to the observed atrophy of the zG and decreased ALDO synthase expression and immunoreactivity following following long-term, ATR-induced ACTH stimulation. Increased ACTH secretion from the pituitary following ATR treatment might cause the initial increase in ALDO secretions following short-term ATR treatment, but following prolonged ATR exposure and thus ACTH stimulation, the cells of the zG become habituated and do not respond as robust to ACTH stimulation. More research is needed to determine whether ATR acts solely via an ACTH-mediated response or multiple pathways, and to elucidate the mechanism by which ATR might cause an increase in ACTH secretion. Furthermore, it will also important to determine if

the changes in adrenal gland morphology and enzyme expression following ATR exposure affect the overall function of the adrenal.

References

1. U.S. Department of Agriculture, N.A.S.S., *Agricultural chemical usage 2005 field crops summary*, USDA, Editor 2006: Washington, D.C.
2. Gysin, H. and E. Knuesli, *Chemistry and herbicidal properties of triazine derivatives*. Advances in Pest Control Research, ed. R. Metcalf. Vol. 3. 1960, New York: Wiley (Interscience).
3. Hill, R., *Oxygen Produced by Isolated Chloroplasts*. Proceedings of the Royal Society of London. Series B - Biological Sciences, 1939. **127**(847): p. 192-210.
4. Good, N.E., *Inhibitors of the Hill reaction*. Plant Physiol, 1961. **36**(6): p. 788-803.
5. Agency, U.S.E.P., *Atrazine, Chemical Summary*, U.S. EPA, Editor 2007, U.S. EPA:
6. Curwin, B.D., et al., *Urinary pesticide concentrations among children, mothers and fathers living in farm and non-farm households in iowa*. Ann Occup Hyg, 2007. **51**(1): p. 53-65.
7. Hines, C.J., et al., *Mixed-effect models for evaluating multiple measures of atrazine exposure among custom applicators*. J Occup Environ Hyg, 2006. **3**(5): p. 274-83.
8. Jowa, L. and R. Howd, *Should atrazine and related chlorotriazines be considered carcinogenic for human health risk assessment?* J Environ Sci Health C Environ Carcinog Ecotoxicol Rev, 2011. **29**(2): p. 91-144.
9. Clarke, I.J. and J.T. Cummins, *The Temporal Relationship Between Gonadotropin Releasing Hormone (GnRH) and Luteinizing Hormone (LH) Secretion in Ovariectomized Ewes*. Endocrinology, 1982. **111**(5): p. 1737-1739.
10. Levine, J.E., et al., *Amplitude and frequency modulation of pulsatile luteinizing hormone-releasing hormone release*. Cell Mol Neurobiol, 1995. **15**(1): p. 117-39.
11. Lopez, F.J., et al., *Modulating mechanisms of neuroendocrine cell activity: the LHRH pulse generator*. Cell Mol Neurobiol, 1998. **18**(1): p. 125-46.
12. Stojilkovic, S.S., et al., *Gonadotropin-releasing hormone neurons: intrinsic pulsatility and receptor-mediated regulation*. Trends Endocrinol Metab, 1994. **5**(5): p. 201-9.
13. Belchetz, P., et al., *Hypophysial responses to continuous and intermittent delivery of hypothalamic gonadotropin-releasing hormone*. Science, 1978. **202**(4368): p. 631-633.

14. Weiss, J., et al., *Divergent Responses of Gonadotropin Subunit Messenger RNAs to Continuous Versus Pulsatile Gonadotropin-Releasing Hormone in Vitro*. *Molecular Endocrinology*, 1990. **4**(4): p. 557-564.
15. WIERMAN, M.E., J.E. RIVIER, and C. WANG, *Gonadotropin-Releasing Hormone-Dependent Regulation of Gonadotropin Subunit Messenger Ribonucleic Acid Levels in the Rat*. *Endocrinology*, 1989. **124**(1): p. 272-278.
16. FERIN, M., et al., *Effect of Antibodies to 17 β -Estradiol and Progesterone on the Estrous Cycle of the Rat*. *Endocrinology*, 1969. **85**(6): p. 1070-1078.
17. FREEMAN, M.C., K.C. DUPKE, and C.M. CROTEAU, *Extinction of the Estrogen-Induced Daily Signal for LH Release in the Rat: A Role for the Proestrous Surge of Progesterone*. *Endocrinology*, 1976. **99**(1): p. 223-229.
18. Moenter, S.M., A. Caraty, and F.J. Karsch, *The estradiol-induced surge of gonadotropin-releasing hormone in the ewe*. *Endocrinology*, 1990. **127**(3): p. 1375-84.
19. Foradori, C.D., et al., *Effects of atrazine and its withdrawal on gonadotropin-releasing hormone neuroendocrine function in the adult female Wistar rat*. *Biol Reprod*, 2009. **81**(6): p. 1099-105.
20. Lee, W.S., M.S. Smith, and G.E. Hoffman, *Luteinizing hormone-releasing hormone neurons express Fos protein during the proestrous surge of luteinizing hormone*. *Proceedings of the National Academy of Sciences*, 1990. **87**(13): p. 5163-5167.
21. McMullin, T.S., et al., *Evidence That Atrazine and Diaminochlorotriazine Inhibit the Estrogen/Progesterone Induced Surge of Luteinizing Hormone in Female Sprague-Dawley Rats Without Changing Estrogen Receptor Action*. *Toxicological Sciences*, 2004. **79**(2): p. 278-286.
22. Eldridge, J.C., et al., *Factors affecting mammary tumor incidence in chlorotriazine-treated female rats: hormonal properties, dosage, and animal strain*. *Environ Health Perspect*, 1994. **102 Suppl 11**: p. 29-36.
23. Wetzel, L.T., et al., *Chronic effects of atrazine on estrus and mammary tumor formation in female Sprague-Dawley and Fischer 344 rats*. *J Toxicol Environ Health*, 1994. **43**(2): p. 169-82.
24. Eldridge, J.C., et al., *The mammary tumor response in triazine-treated female rats: a threshold-mediated interaction with strain and species-specific reproductive senescence*. *Steroids*, 1999. **64**(9): p. 672-8.
25. Eldridge, J.C., L.T. Wetzel, and L. Tyrey, *Estrous cycle patterns of Sprague-Dawley rats during acute and chronic atrazine administration*. *Reprod Toxicol*, 1999. **13**(6): p. 491-9.
26. Cooper, R.L., et al., *Atrazine and reproductive function: mode and mechanism of action studies*. *Birth Defects Res B Dev Reprod Toxicol*, 2007. **80**(2): p. 98-112.

27. Friedmann, A.S., *Atrazine inhibition of testosterone production in rat males following peripubertal exposure*. *Reprod Toxicol*, 2002. **16**(3): p. 275-9.
28. Laws, S.C., et al., *Pubertal development in female Wistar rats following exposure to propazine and atrazine biotransformation by-products, diamino-S-chlorotriazine and hydroxyatrazine*. *Toxicol Sci*, 2003. **76**(1): p. 190-200.
29. Trentacoste, S.V., et al., *Atrazine effects on testosterone levels and androgen-dependent reproductive organs in peripubertal male rats*. *J Androl*, 2001. **22**(1): p. 142-8.
30. Stoker, T.E., et al., *The effects of atrazine metabolites on puberty and thyroid function in the male Wistar rat*. *Toxicol Sci*, 2002. **67**(2): p. 198-206.
31. Stoker, T.E., et al., *The effect of atrazine on puberty in male wistar rats: an evaluation in the protocol for the assessment of pubertal development and thyroid function*. *Toxicol Sci*, 2000. **58**(1): p. 50-9.
32. Foradori, C.D., et al., *Atrazine inhibits pulsatile luteinizing hormone release without altering pituitary sensitivity to a gonadotropin-releasing hormone receptor agonist in female Wistar rats*. *Biol Reprod*, 2009. **81**(1): p. 40-5.
33. Beck, W. and W. Wuttke, *Diurnal Variations of Plasma Luteinizing Hormone, Follicle-Stimulating Hormone, and Prolactin in Boys and Girls from Birth to Puberty*. *Journal of Clinical Endocrinology & Metabolism*, 1980. **50**(4): p. 635-639.
34. Boyar, R., et al., *Synchronization of augmented luteinizing hormone secretion with sleep during puberty*. *N Engl J Med*, 1972. **287**(12): p. 582-6.
35. KULIN, H.E., R.G. MOORE, and S.J. SANTNER, *Circadian Rhythms in Gonadotropin Excretion in Prepubertal and Pubertal Children*. *Journal of Clinical Endocrinology & Metabolism*, 1976. **42**(4): p. 770-773.
36. PARKER, D.C., et al., *Pubertal Sleep-Wake Patterns of Episodic LH, FSH and Testosterone Release in Twin Boys*. *Journal of Clinical Endocrinology & Metabolism*, 1975. **40**(6): p. 1099-1109.
37. Coquelin, A. and C. Desjardins, *Luteinizing hormone and testosterone secretion in young and old male mice*. *Am J Physiol*, 1982. **243**(3): p. E257-63.
38. Dufau, M.L., et al., *Mode of secretion of bioactive luteinizing hormone in man*. *J Clin Endocrinol Metab*, 1983. **57**(5): p. 993-1000.
39. Ching, M., *Differential effect of althesin versus chloralose-urethane anesthesia on in vivo LHRH and LH release in the proestrous rat*. *Endocr Res Commun*, 1982. **9**(1): p. 37-46.
40. Wildt, L., et al., *Frequency and amplitude of gonadotropin-releasing hormone stimulation and gonadotropin secretion in the rhesus monkey*. *Endocrinology*, 1981. **109**(2): p. 376-85.

41. Wu, F.C., et al., *Effects of gonadotropin-releasing hormone pulse-frequency modulation on luteinizing hormone, follicle-stimulating hormone and testosterone secretion in hypothalamo/pituitary-disconnected rams*. Biol Reprod, 1987. **37**(3): p. 501-10.
42. Hoffman, G.E., et al., *Luteinizing hormone-releasing hormone neurons express c-fos antigen after steroid activation*. Endocrinology, 1990. **126**(3): p. 1736-41.
43. Lee, W.S., M.S. Smith, and G.E. Hoffman, *Luteinizing hormone-releasing hormone neurons express Fos protein during the proestrous surge of luteinizing hormone*. Proc Natl Acad Sci U S A, 1990. **87**(13): p. 5163-7.
44. Foradori, C.D., et al., *Atrazine inhibits pulsatile gonadotropin-releasing hormone (GnRH) release without altering GnRH messenger RNA or protein levels in the female rat*. Biol Reprod, 2013. **88**(1): p. 9.
45. Agency, U.S.E.P., *Drinking Water Health Advisory: Pesticides*. , 1991, Lewis Publishers, Chelsea.
46. Bakke, J., J. Larson, and C. Price, *Metabolism of atrazine and 2-hydroxyatrazine by the rat*. J. Agric. Food Chem., 1972(20): p. 602-607.
47. Bakke, J., J. Robbins, and V. Feil, *Metabolism of 2-chloro-4,6-bis(isopropylamine)-s-triazine (propazine) and 2-methoxy-4,6-bis(isopropylamino)-s-triazine (prometone) in the rat: Balance study and urinary metabolite separation*. J. Agric. Food Chem., 1967(15): p. 628-631.
48. Williams, R., *The Metabolism and Detoxication of Drugs, Toxic Substances and Other Organic Compounds*, in *Detoxication Mechanisms* 1959, Wiley: New York, NY.
49. Klingenberg, M., *Pigments of rat liver microsomes*. Arch Biochem Biophys, 1958. **75**(2): p. 376-86.
50. Omura, T. and R. Sato, *A new cytochrome in liver microsomes*. J Biol Chem, 1962. **237**: p. 1375-6.
51. Omiecinski, C.J., et al., *Xenobiotic Metabolism, Disposition, and Regulation by Receptors: From Biochemical Phenomenon to Predictors of Major Toxicities*. Toxicological Sciences, 2011. **120**(suppl 1): p. S49-S75.
52. Meyer, J. and K. Rodvold, *Drug biotransformation by the cytochrome P-450 enzyme system*. Infect Med, 1996. **13**(6): p. 452, 459, 463-464, 523.
53. Eichelbaum, M., et al., *Defective N-oxidation of sparteine in man: a new pharmacogenetic defect*. Eur J Clin Pharmacol, 1979. **16**(3): p. 183-7.
54. Brosen, K. and L.F. Gram, *Clinical significance of the sparteine/debrisoquine oxidation polymorphism*. Eur J Clin Pharmacol, 1989. **36**(6): p. 537-47.

55. Eichelbaum, M. and A.S. Gross, *The genetic polymorphism of debrisoquine/sparteine metabolism--clinical aspects*. Pharmacol Ther, 1990. **46**(3): p. 377-94.
56. Gillum, J.G., D.S. Israel, and R.E. Polk, *Pharmacokinetic drug interactions with antimicrobial agents*. Clin Pharmacokinet, 1993. **25**(6): p. 450-82.
57. *Animal Models in Toxicology*. Second Edition ed2007, Boca Raton, FL: CRC Press.
58. Payne, A.H. and D.B. Hales, *Overview of steroidogenic enzymes in the pathway from cholesterol to active steroid hormones*. Endocr Rev, 2004. **25**(6): p. 947-70.
59. Topletz, A.R., et al., *Comparison of the function and expression of CYP26A1 and CYP26B1, the two retinoic acid hydroxylases*. Biochem Pharmacol, 2012. **83**(1): p. 149-63.
60. Mast, N., et al., *Cholesterol binding to cytochrome P450 7A1, a key enzyme in bile acid biosynthesis*. Biochemistry, 2005. **44**(9): p. 3259-71.
61. Myant, N.B. and K.A. Mitropoulos, *Cholesterol 7 alpha-hydroxylase*. J Lipid Res, 1977. **18**(2): p. 135-53.
62. Stiles, A.R., et al., *CYP7B1: one cytochrome P450, two human genetic diseases, and multiple physiological functions*. J Biol Chem, 2009. **284**(42): p. 28485-9.
63. Okuda, K., T. Ogishima, and M. Noshiro, *Cholesterol 7 α -hydroxylase and 12 α -hydroxylase in Cytochrome P450*, J. Schenkman and H. Greim, Editors. 1993, Springer Verlag: Berlin, Germany. p. 599-610.
64. Martin, C., et al., *cyp7b1 catalyses the 7 α -hydroxylation of dehydroepiandrosterone and 25-hydroxycholesterol in rat prostate*. Biochem J, 2001. **355**(Pt 2): p. 509-15.
65. Pettersson, H., et al., *CYP7B1-mediated metabolism of dehydroepiandrosterone and 5 α -androstane-3 β ,17 β -diol--potential role(s) for estrogen signaling*. FEBS J, 2008. **275**(8): p. 1778-89.
66. Jellinck, P.H., S.J. Lee, and B.S. McEwen, *Metabolism of dehydroepiandrosterone by rat hippocampal cells in culture: possible role of aromatization and 7-hydroxylation in neuroprotection*. J Steroid Biochem Mol Biol, 2001. **78**(4): p. 313-7.
67. Rose, K.A., et al., *Cyp7b, a novel brain cytochrome P450, catalyzes the synthesis of neurosteroids 7 α -hydroxy dehydroepiandrosterone and 7 α -hydroxy pregnenolone*. Proc Natl Acad Sci U S A, 1997. **94**(10): p. 4925-30.
68. Caldwell, J. *Xenobiotic metabolism: mammalian aspects*. in ACS Symp. Ser. Am. Chem. Soc. 1986.

69. Smith, R. and R. Williams, *History of the discovery of the conjugation mechanisms*, in *Metabolic Conjugation and Metabolic Hydrolysis*, W.H. Fishman, Editor 1970, Academic Press: New York, NY. p. 1-19.
70. Sherratt, P. and J. Hayes, *Glutathione S-transferases*, in *Enzyme Systems that Metabolise Drugs and Other Xenobiotics*, C. Ioannides, Editor 2001, John Wiley & Sons Ltd.
71. Hayes, J.D. and D.J. Pulford, *The glutathione S-transferase supergene family: regulation of GST and the contribution of the isoenzymes to cancer chemoprotection and drug resistance*. Crit Rev Biochem Mol Biol, 1995. **30**(6): p. 445-600.
72. Boyer, T.D., *The glutathione S-transferases: an update*. Hepatology, 1989. **9**(3): p. 486-96.
73. Wilce, M. and M. Parker, *Structure and fuction of glutathione S-transferases*. Biochem. Biophys. Acta, 1994(1205): p. 1-18.
74. Chasseaud, L.F., *The role of glutathione and glutathione S-transferases in the metabolism of chemical carcinogens and other electrophilic agents*. Adv Cancer Res, 1979. **29**: p. 175-274.
75. Hayes, J. and L. McLellan, *Glutathione and glutathione-dependent enzymes represent a co-ordinately regulated defence against oxidative stress*. Free Radical Research, 1999(31): p. 273-300.
76. Ketterer, B., G. Fraser, and D.J. Meyer, *Nuclear glutathione transferases which detoxify irradiated DNA*. Adv Exp Med Biol, 1990. **264**: p. 301-10.
77. Adler, V., et al., *Regulation of JNK signaling by GSTp*. EMBO J, 1999. **18**(5): p. 1321-34.
78. Cho, S.G., et al., *Glutathione S-transferase mu modulates the stress-activated signals by suppressing apoptosis signal-regulating kinase 1*. J Biol Chem, 2001. **276**(16): p. 12749-55.
79. Listowsky, I., *High capacity binding by glutathione S-transferases and glucocorticoid resistance*, in *Structure and Function of Glutathione Transferases*, T. KD, et al., Editors. 1993, CRC Press: Boca Raton, FL. p. 199-209.
80. Boyland, E. and L.F. Chasseaud, *The role of glutathione and glutathione S-transferases in mercapturic acid biosynthesis*. Adv Enzymol Relat Areas Mol Biol, 1969. **32**: p. 173-219.
81. Mannervik, B., *The isoenzymes of glutathione transferase*. Adv Enzymol Relat Areas Mol Biol, 1985. **57**: p. 357-417.
82. Meyer, D.J., et al., *Theta, a new class of glutathione transferases purified from rat and man*. Biochem J, 1991. **274** (Pt 2): p. 409-14.

83. Meyer, D.J. and M. Thomas, *Characterization of rat spleen prostaglandin H D-isomerase as a sigma-class GSH transferase*. *Biochem J*, 1995. **311 (Pt 3)**: p. 739-42.
84. Jakobsson, P.J., et al., *Common structural features of MAPEG -- a widespread superfamily of membrane associated proteins with highly divergent functions in eicosanoid and glutathione metabolism*. *Protein Sci*, 1999. **8(3)**: p. 689-92.
85. Sato, K., *Glutathione transferases as markers of preneoplasia and neoplasia*. *Adv Cancer Res*, 1989. **52**: p. 205-55.
86. Staffas, L., et al., *Growth hormone- and testosterone-dependent regulation of glutathione transferase subunit A5 in rat liver*. *Biochem J*, 1998. **332 (Pt 3)**: p. 763-8.
87. Koskinen, W.C. and S.A. Clay, *Factors affecting atrazine fate in north central U.S. soils*. *Rev Environ Contam Toxicol*, 1997. **151**: p. 117-65.
88. Lamoureux Gerald, L., B. Simoneaux, and J. Larson, *The Metabolism of Atrazine and Related 2-Chloro-4,6-bis(alkylamino)-<italic>s</italic>-triazines in Plants*, in *Triazine Herbicides: Risk Assessment* 1998, American Chemical Society. p. 60-81.
89. Sorenson, B., et al., *Formation and movement of 14C-atrazine degradation products in sandy loam soil under field conditions*. *Weed Sci.*, 1993(41): p. 239-245.
90. Barr, D.B., et al., *Assessing exposure to atrazine and its metabolites using biomonitoring*. *Environ Health Perspect*, 2007. **115(10)**: p. 1474-8.
91. Catenacci, G., et al., *Assessment of human exposure to atrazine through the determination of free atrazine in urine*. *Bull Environ Contam Toxicol*, 1990. **44(1)**: p. 1-7.
92. Ikonen, R., J. Kangas, and H. Savolainen, *Urinary atrazine metabolites as indicators for rat and human exposure to atrazine*. *Toxicol Lett*, 1988. **44(1-2)**: p. 109-12.
93. McMullin, T.S., et al., *Pharmacokinetic modeling of disposition and time-course studies with [14C]atrazine*. *J Toxicol Environ Health A*, 2003. **66(10)**: p. 941-64.
94. McMullin, T.S., et al., *Oral absorption and oxidative metabolism of atrazine in rats evaluated by physiological modeling approaches*. *Toxicology*, 2007. **240(1-2)**: p. 1-14.
95. Fraites, M.J., et al., *Gestational atrazine exposure: effects on male reproductive development and metabolite distribution in the dam, fetus, and neonate*. *Reprod Toxicol*, 2011. **32(1)**: p. 52-63.
96. Laws, S.C., et al., *Chlorotriazine herbicides and metabolites activate an ACTH-dependent release of corticosterone in male Wistar rats*. *Toxicol Sci*, 2009. **112(1)**: p. 78-87.

97. Adams, N., P. Levi, and E. Hodgson, *In vitro studies of the metabolism of atrazine, simazine, and terbutryn in several vertebrate species*. Journal of Agricultural and Food Chemistry, 1990(38): p. 1411-1417.
98. Lang, D., et al., *In vitro metabolism of atrazine, terbuthylazine, ametryne, and terbutryne in rats, pigs, and humans*. Drug Metab Dispos, 1996. **24**(8): p. 859-65.
99. Hanioka, N., et al., *In vitro metabolism of chlorotriazines: characterization of simazine, atrazine, and propazine metabolism using liver microsomes from rats treated with various cytochrome P450 inducers*. Toxicol Appl Pharmacol, 1999. **156**(3): p. 195-205.
100. Hanioka, N., et al., *In vitro biotransformation of atrazine by rat liver microsomal cytochrome P450 enzymes*. Chem Biol Interact, 1998. **116**(3): p. 181-98.
101. Hanioka, N., et al., *Changes in rat liver cytochrome P450 enzymes by atrazine and simazine treatment*. Xenobiotica, 1998. **28**(7): p. 683-98.
102. Islam, M.O., M. Hara, and J. Miyake, *Induction of P-glycoprotein, glutathione-S-transferase and cytochrome P450 in rat liver by atrazine*. Environ Toxicol Pharmacol, 2002. **12**(1): p. 1-6.
103. Pogrmic-Majkic, K., et al., *Atrazine effects on antioxidant status and xenobiotic metabolizing enzymes after oral administration in peripubertal male rat*. Environ Toxicol Pharmacol, 2012. **34**(2): p. 495-501.
104. Schulz, T.G., et al., *Assessment of P450 induction in the marmoset monkey using targeted anti-peptide antibodies*. Biochimica et Biophysica Acta (BBA) - Protein Structure and Molecular Enzymology, 2001. **1546**(1): p. 143-155.
105. Sanderson, J.T., et al., *2-Chloro-s-triazine herbicides induce aromatase (CYP19) activity in H295R human adrenocortical carcinoma cells: a novel mechanism for estrogenicity?* Toxicol Sci, 2000. **54**(1): p. 121-7.
106. Quignot, N., et al., *Characterization of endocrine-disrupting chemicals based on hormonal balance disruption in male and female adult rats*. Reprod Toxicol, 2012. **33**(3): p. 339-52.
107. Egaas, E., et al., *A comparative study of effects of atrazine on xenobiotic metabolizing enzymes in fish and insect, and of the in vitro phase II atrazine metabolism in some fish, insects, mammals and one plant species*. Comp Biochem Physiol C, 1993. **106**(1): p. 141-9.
108. Buchholz, B.A., et al., *HPLC-accelerator MS measurement of atrazine metabolites in human urine after dermal exposure*. Anal Chem, 1999. **71**(16): p. 3519-25.
109. Jaeger, L.L., A.D. Jones, and B.D. Hammock, *Development of an enzyme-linked immunosorbent assay for atrazine mercapturic acid in human urine*. Chem Res Toxicol, 1998. **11**(4): p. 342-52.

110. Lucas, A.D., et al., *Determination of atrazine metabolites in human urine: development of a biomarker of exposure*. Chem Res Toxicol, 1993. **6**(1): p. 107-16.
111. Egaas, E., J.G. Falls, and W.C. Dauterman, *A study of gender, strain and age differences in mouse liver glutathione-S-transferase*. Comp Biochem Physiol C Pharmacol Toxicol Endocrinol, 1995. **110**(1): p. 35-40.
112. Abel, E.L., et al., *Characterization of atrazine biotransformation by human and murine glutathione S-transferases*. Toxicol Sci, 2004. **80**(2): p. 230-8.
113. Courtois, A., et al., *Differential regulation of canalicular multispecific organic anion transporter (cMOAT) expression by the chemopreventive agent oltipraz in primary rat hepatocytes and in rat liver*. Carcinogenesis, 1999. **20**(12): p. 2327-30.
114. Santa Maria, C., J. Moreno, and J.L. Lopez-Campos, *Hepatotoxicity induced by the herbicide atrazine in the rat*. J Appl Toxicol, 1987. **7**(6): p. 373-8.
115. Campos-Pereira, F.D., et al., *Early cytotoxic and genotoxic effects of atrazine on Wistar rat liver: a morphological, immunohistochemical, biochemical, and molecular study*. Ecotoxicol Environ Saf, 2012. **78**: p. 170-7.
116. Liu, X.M., et al., *Cytotoxic effects and apoptosis induction of atrazine in a grass carp (Ctenopharyngodon idellus) cell line*. Environ Toxicol, 2006. **21**(1): p. 80-9.
117. Bradford, M.M., *A rapid and sensitive method for the quantitation of microgram quantities of protein utilizing the principle of protein-dye binding*. Anal Biochem, 1976. **72**: p. 248-54.
118. Pogrmic-Majkic, K., et al., *Upregulation of peripubertal rat Leydig cell steroidogenesis following 24 h in vitro and in vivo exposure to atrazine*. Toxicol Sci, 2010. **118**(1): p. 52-60.
119. Choi, S.Y., et al., *Isoform-specific regulation of cytochrome P450 expression and activity by estradiol in female rats*. Biochem Pharmacol, 2011. **81**(6): p. 777-82.
120. Hanioka, N., et al., *In vitro metabolism of simazine, atrazine and propazine by hepatic cytochrome P450 enzymes of rat, mouse and guinea pig, and oestrogenic activity of chlorotriazines and their main metabolites*. Xenobiotica, 1999. **29**(12): p. 1213-26.
121. Abarikwu, S.O., et al., *Changes in sperm characteristics and induction of oxidative stress in the testis and epididymis of experimental rats by a herbicide, atrazine*. Arch Environ Contam Toxicol, 2010. **58**(3): p. 874-82.
122. Singh, M., R. Sandhir, and R. Kiran, *Oxidative stress induced by atrazine in rat erythrocytes: mitigating effect of vitamin E*. Toxicol Mech Methods, 2010. **20**(3): p. 119-26.

123. Orth, D., W. Kavaacs, and D. Rowan, *The Adrenal Cortex*, in *William's Textbook of Endocrinology* J. Wilson and D. Foster, Editors. 1992, Saunders: Philadelphia, PA. p. 489-619.
124. Nonaka, Y. and M. Okamoto, *Functional expression of cDNAs encoding rat 11 β -hydroxylase [cytochrome P-450(11 β)] and aldosterone synthase [cytochrome P-450(11 β ,ald0)].* Eur J Biochem, 1991. **202**: p. 897-902.
125. Lauber, M. and J. Muller, *Purification and characterization of two distinct forms of rat adrenal cytochrome P-45011 β -functional and structural aspects.* Arch Biochem Biophys, 1989. **274**: p. 109-119.
126. Ogishima, T., et al., *Zone-specific expression of aldosterone synthase cytochrome P-450 and cytochrome P-45011 beta in rat adrenal cortex: histochemical basis for the functional zonation.* Endocrinology, 1992. **130**(5): p. 2971-7.
127. Boon, W.C., et al., *Aldosterone secretion: a molecular perspective.* Trends Endocrinol Metab, 1997. **8**(9): p. 346-54.
128. Peart, W.S., *C. The renin-angiotensin system. A history and review of the renin-angiotensin system.* Proc R Soc Lond B Biol Sci, 1969. **173**(32): p. 317-25.
129. Kurtz, A., *Cellular control of renin secretion.* Rev Physiol Biochem Pharmacol, 1989. **113**: p. 1-40.
130. Ganguly, A. and J.S. Davis, *Role of calcium and other mediators in aldosterone secretion from the adrenal glomerulosa cells.* Pharmacol Rev, 1994. **46**(4): p. 417-47.
131. Viard, I., et al., *Ovine adrenal fasciculata cells contain angiotensin-II receptors coupled to intracellular effectors but are resistant to the steroidogenic effects of this hormone.* Endocrinology, 1990. **127**(5): p. 2071-8.
132. Whitley, G.S., P.J. Hyatt, and J.F. Tait, *Angiotensin II-induced inositol phosphate production in isolated rat zona glomerulosa and fasciculata/reticularis cells.* Steroids, 1987. **49**(4-5): p. 271-86.
133. Szabadkai, G., et al., *Expression of inositol 1,4,5-trisphosphate receptors in rat adrenocortical zones.* J Steroid Biochem Mol Biol, 1996. **57**(1-2): p. 13-7.
134. McDougall, J.G., et al., *Biosynthetic and morphological evidence for inhibition of aldosterone production following administration of ACTH to sheep.* Acta Endocrinol (Copenh), 1980. **94**(4): p. 559-70.
135. Ulrich-Lai, Y.M., et al., *Chronic stress induces adrenal hyperplasia and hypertrophy in a subregion-specific manner.* Am J Physiol Endocrinol Metab, 2006. **291**(5): p. E965-73.
136. Engeland, W.C. and B.K. Levay-Young, *Changes in the glomerulosa cell phenotype during adrenal regeneration in rats.* Am J Physiol, 1999. **276**(5 Pt 2): p. R1374-82.

137. Bassett, M.H., P.C. White, and W.E. Rainey, *The regulation of aldosterone synthase expression*. Mol Cell Endocrinol, 2004. **217**(1-2): p. 67-74.
138. Denner, K., et al., *Differential regulation of 11 beta-hydroxylase and aldosterone synthase in human adrenocortical H295R cells*. Mol Cell Endocrinol, 1996. **121**(1): p. 87-91.
139. Curnow, K.M., et al., *The product of the CYP11B2 gene is required for aldosterone biosynthesis in the human adrenal cortex*. Mol Endocrinol, 1991. **5**(10): p. 1513-22.
140. Yoshida, A., et al., *ACTH-induced inhibition of the action of angiotensin II in bovine zona glomerulosa cells. A modulatory effect of cyclic AMP on the angiotensin II receptor*. J Biol Chem, 1991. **266**(7): p. 4288-94.
141. Andoka, G., et al., *Adrenocorticotropin regulates angiotensin II receptors in bovine adrenal cells in vitro*. Biochem Biophys Res Commun, 1984. **121**(2): p. 441-7.
142. Hausdorff, W.P., et al., *Control of aldosterone production by angiotensin II is mediated by two guanine nucleotide regulatory proteins*. Endocrinology, 1987. **120**(4): p. 1668-78.
143. Begeot, M., et al., *Variations in guanine-binding proteins (Gs, Gi) in cultured bovine adrenal cells. Consequences on the effects of phorbol ester and angiotensin II on adrenocorticotropin-induced and cholera-toxin-induced cAMP production*. Eur J Biochem, 1988. **174**(2): p. 317-21.
144. Shen, T., et al., *Localization and differential expression of adenylyl cyclase messenger ribonucleic acids in rat adrenal gland determined by in situ hybridization*. Endocrinology, 1997. **138**(11): p. 4591-8.
145. Rosol, T.J., et al., *Adrenal gland: structure, function, and mechanisms of toxicity*. Toxicol Pathol, 2001. **29**(1): p. 41-8.
146. Pruetz, S.B., et al., *Modeling and predicting immunological effects of chemical stressors: characterization of a quantitative biomarker for immunological changes caused by atrazine and ethanol*. Toxicol Sci, 2003. **75**(2): p. 343-54.
147. Fraites, M.J.P., et al., *Characterization of the Hypothalamic-Pituitary-Adrenal Axis Response to Atrazine and Metabolites in the Female Rat*. Toxicological Sciences, 2009. **112**(1): p. 88-99.
148. Modic, M., *The role of testicular aromatase in the atrazine mediated changes of estrone and estradiol in the male wistar rat*, 2004, North Carolina State University.
149. Resko, J.A., *Endocrine control of adrenal progesterone secretion in the ovariectomized rat*. Science, 1969. **164**(3875): p. 70-1.

150. Tinfo, N.S., et al., *Understanding the effects of atrazine on steroidogenesis in rat granulosa and H295R adrenal cortical carcinoma cells*. *Reproductive Toxicology*, 2011. **31**(2): p. 184-193.
151. Wagenmaker, E.R., et al., *Cortisol interferes with the estradiol-induced surge of luteinizing hormone in the ewe*. *Biol Reprod*, 2009. **80**(3): p. 458-63.
152. Suter, D.E., N.B. Schwartz, and S.J. Ringstrom, *Dual role of glucocorticoids in regulation of pituitary content and secretion of gonadotropins*. *Am J Physiol*, 1988. **254**(5 Pt 1): p. E595-600.
153. Ringstrom, S.J. and N.B. Schwartz, *Cortisol suppresses the LH, but not the FSH, response to gonadotropin-releasing hormone after orchidectomy*. *Endocrinology*, 1985. **116**(1): p. 472-4.
154. Li, X.F., A.M. Knox, and K.T. O'Byrne, *Corticotrophin-releasing factor and stress-induced inhibition of the gonadotrophin-releasing hormone pulse generator in the female*. *Brain Res*, 2010. **1364**: p. 153-63.
155. Breen, K.M. and F.J. Karsch, *Does cortisol inhibit pulsatile luteinizing hormone secretion at the hypothalamic or pituitary level?* *Endocrinology*, 2004. **145**(2): p. 692-8.
156. Rabin, D., et al., *Stress and reproduction: physiologic and pathophysiologic interactions between the stress and reproductive axes*. *Adv Exp Med Biol*, 1988. **245**: p. 377-87.
157. Rivest, S. and C. Rivier, *The role of corticotropin-releasing factor and interleukin-1 in the regulation of neurons controlling reproductive functions*. *Endocr Rev*, 1995. **16**(2): p. 177-99.
158. Schwab, C.L., et al., *Modeling and predicting stress-induced immunosuppression in mice using blood parameters*. *Toxicol Sci*, 2005. **83**(1): p. 101-13.
159. Suter, D.E. and N.B. Schwartz, *Effects of glucocorticoids on responsiveness of luteinizing hormone and follicle-stimulating hormone to gonadotropin-releasing hormone by male rat pituitary cells in vitro*. *Endocrinology*, 1985. **117**(3): p. 855-9.
160. Kamel, F. and C.L. Kubajak, *Modulation of gonadotropin secretion by corticosterone: interaction with gonadal steroids and mechanism of action*. *Endocrinology*, 1987. **121**(2): p. 561-8.
161. Briski, K.P. and P.W. Sylvester, *Acute inhibition of pituitary LH release in the male rat by the glucocorticoid agonist decadron phosphate*. *Neuroendocrinology*, 1991. **54**(4): p. 313-20.
162. Schultz, R., et al., *Localization of the glucocorticoid receptor in testis and accessory sexual organs of male rat*. *Mol Cell Endocrinol*, 1993. **95**(1-2): p. 115-20.

163. Tetsuka, M., et al., *Expression of 11beta-hydroxysteroid dehydrogenase, glucocorticoid receptor, and mineralocorticoid receptor genes in rat ovary*. Biol Reprod, 1999. **60**(2): p. 330-5.
164. Foradori, C.D., et al., *The differential effect of atrazine on luteinizing hormone release in adrenalectomized adult female Wistar rats*. Biol Reprod, 2011. **85**(4): p. 684-9.
165. Skinner, D.C., A. Caraty, and R. Allingham, *Unmasking the progesterone receptor in the preoptic area and hypothalamus of the ewe: no colocalization with gonadotropin-releasing neurons*. Endocrinology, 2001. **142**(2): p. 573-9.
166. Dufourny, L. and D.C. Skinner, *Type II glucocorticoid receptors in the ovine hypothalamus: distribution, influence of estrogen and absence of co-localization with GnRH*. Brain Res, 2002. **946**(1): p. 79-86.
167. Kalra, S.P., *Mandatory neuropeptide-steroid signaling for the preovulatory luteinizing hormone-releasing hormone discharge*. Endocr Rev, 1993. **14**(5): p. 507-38.
168. Ferin, M. and R. Vande Wiele, *Endogenous opioid peptides and the control of the menstrual cycle*. Eur J Obstet Gynecol Reprod Biol, 1984. **18**(5-6): p. 365-73.
169. Whisnant, C.S. and R.L. Goodman, *Effects of an opioid antagonist on pulsatile luteinizing hormone secretion in the ewe vary with changes in steroid negative feedback*. Biol Reprod, 1988. **39**(5): p. 1032-8.
170. Van Vugt, D.A., N.Y. Lam, and M. Ferin, *Reduced frequency of pulsatile luteinizing hormone secretion in the luteal phase of the rhesus monkey. Involvement of endogenous opiates*. Endocrinology, 1984. **115**(3): p. 1095-101.
171. Foradori, C.D., et al., *Colocalization of progesterone receptors in parvicellular dynorphin neurons of the ovine preoptic area and hypothalamus*. Endocrinology, 2002. **143**(11): p. 4366-74.
172. Dufourny, L. and D.C. Skinner, *Progesterone receptor, estrogen receptor alpha, and the type II glucocorticoid receptor are coexpressed in the same neurons of the ovine preoptic area and arcuate nucleus: a triple immunolabeling study*. Biol Reprod, 2002. **67**(5): p. 1605-12.
173. Dufourny, L., et al., *Progesterone-receptive dopaminergic and neuropeptide Y neurons project from the arcuate nucleus to gonadotropin-releasing hormone-rich regions of the ovine preoptic area*. Neuroendocrinology, 2005. **82**(1): p. 21-31.
174. Tomaszewska, D., K. Mateusiak, and F. Przekop, *Changes in extracellular LHRH and beta-endorphin-like immunoreactivity in the nucleus infundibularis-median eminence of anestrus ewes under stress condition*. J Neural Transm, 1999. **106**(3-4): p. 265-74.
175. Petraglia, F., W. Vale, and C. Rivier, *Opioids act centrally to modulate stress-induced decrease in luteinizing hormone in the rat*. Endocrinology, 1986. **119**(6): p. 2445-50.

176. Cagampang, F.R., et al., *Hypoglycaemia-induced inhibition of pulsatile luteinizing hormone secretion in female rats: role of oestradiol, endogenous opioids and the adrenal medulla*. J Neuroendocrinol, 1997. **9**(11): p. 867-72.
177. Bibeau, K., et al., *Differential responses to salt supplementation in adult male and female rat adrenal glands following intrauterine growth restriction*. J Endocrinol, 2011. **209**(1): p. 85-94.
178. Lorente, M., et al., *Chronic hypoxia induced ultrastructural changes in the rat adrenal zona glomerulosa*. Histol Histopathol, 2002. **17**(1): p. 185-90.
179. Wolman, M., et al., *Pathological changes in organs of rats chronically exposed to hypoxia. Development of pulmonary lipidosis*. Histol Histopathol, 1993. **8**(2): p. 247-55.
180. Alario, P., et al., *Body weight gain, food intake and adrenal development in chronic noise stressed rats*. Physiol Behav, 1987. **40**(1): p. 29-32.
181. Dallman, M.F., et al., *Adrenocorticotropin inhibits compensatory adrenal growth after unilateral adrenalectomy*. Endocrinology, 1980. **107**(5): p. 1397-404.
182. Farese, R.V. and W.J. Reddy, *Effect of Adrenocorticotrophin on Adrenal Protein Synthesis*. Endocrinology, 1963. **73**: p. 294-303.
183. Imrie, R.C., et al., *The Effect of Adrenocorticotrophin on the Nucleic Acid Metabolism of the Rat Adrenal Gland*. J Endocrinol, 1965. **32**: p. 303-12.
184. Mukai, S., et al., *Cholesterol accumulation in adrenocortical mitochondria after ACTH-stimulation*. Endocrinol Jpn, 1984. **31**(2): p. 177-84.
185. Mahaffee, D., R.C. Reitz, and R.L. Ney, *The mechanism of action of adrenocorticotrophic hormone. The role of mitochondrial cholesterol accumulation in the regulation of steroidogenesis*. J Biol Chem, 1974. **249**(1): p. 227-33.
186. Aguilera, G., et al., *Regulation of adrenal steroidogenesis during chronic stress*. Endocr Res, 1996. **22**(4): p. 433-43.
187. Sowers, J., et al., *Plasma aldosterone and corticosterone responses to adrenocorticotropin, angiotensin, potassium, and stress in spontaneously hypertensive rats*. Endocrinology, 1981. **108**(4): p. 1216-21.
188. Hayashi, M., W. Kitajima, and T. Saruta, *Aldosterone responses to angiotensin II, adrenocorticotropin and potassium in chronic experimental diabetes mellitus in rats*. Endocrinology, 1984. **115**: p. 2205-2209.
189. Chartier, L. and E.L. Schiffrin, *Atrial natriuretic peptide inhibits the stimulation of aldosterone secretion by ACTH in vitro and in vivo*. Proc Soc Exp Biol Med, 1986. **182**(1): p. 132-6.

190. Chartier, L., et al., *Atrial natriuretic factor inhibits the stimulation of aldosterone secretion by angiotensin II, ACTH and potassium in vitro and angiotensin II-induced steroidogenesis in vivo*. *Endocrinology*, 1984. **115**(5): p. 2026-8.
191. Roberge, M., H. Hakk, and G. Larsen, *Atrazine is a competitive inhibitor of phosphodiesterase but does not affect the estrogen receptor*. *Toxicol Lett*, 2004. **154**(1-2): p. 61-8.
192. Sanderson, J.T., et al., *Effects of chloro-s-triazine herbicides and metabolites on aromatase activity in various human cell lines and on vitellogenin production in male carp hepatocytes*. *Environ Health Perspect*, 2001. **109**(10): p. 1027-31.
193. Sewer, M.B. and M.R. Waterman, *ACTH modulation of transcription factors responsible for steroid hydroxylase gene expression in the adrenal cortex*. *Microsc Res Tech*, 2003. **61**(3): p. 300-7.
194. Aguilera, G., A. Kiss, and B. Sunar-Akbasak, *Hyperreninemic hypoaldosteronism after chronic stress in the rat*. *J Clin Invest*, 1995. **96**(3): p. 1512-9.
195. Engeland, W.C., et al., *Differential gene expression of cytochrome P450 11beta-hydroxylase in rat adrenal cortex after in vivo activation*. *Endocrinology*, 1997. **138**(6): p. 2338-46.
196. Mazzocchi, G., et al., *Short- and long-term effects of ACTH on the adrenal zona glomerulosa of the rat. A coupled stereological and enzymological study*. *Cell Tissue Res*, 1986. **243**(2): p. 303-10.
197. Kitamura, Y., et al., *Effects of ACTH on adrenal angiotensin II receptor subtype expression in vivo*. *Mol Cell Endocrinol*, 1998. **146**(1-2): p. 187-95.
198. Leong, D.S., et al., *Restraint stress modulates brain, pituitary and adrenal expression of angiotensin II AT(1A), AT(1B) and AT(2) receptors*. *Neuroendocrinology*, 2002. **75**(4): p. 227-40.
199. Santa Maria, C., et al., *Subacute Atrazine Treatment Effects on Rat Renal Functions*. *Environ. Contam. Toxicol.*, 1986. **36**: p. 325-331.
200. Morgan, D.P. and C.C. Roan, *Renal function in persons occupationally exposure to pesticides*. *Arch Environ Health*, 1969. **19**: p. 633-639.